Supporting Information

Iron vs Ruthenium: Syntheses, structures and IR spectroelectrochemical characterisation of half-sandwich Group 8 acetylide complexes†

Daniel P. Harrison, Varshini Jayantha Kumar, Johanna N. Noppers, Josef B.G. Gluyas, Alexandre N. Sobolev, Stephen A. Moggach, Paul J. Low

School of Molecular Sciences, University of Western Australia, 35 Stirling Highway, Crawley, Western Australia, 6009, Australia

Table of Contents

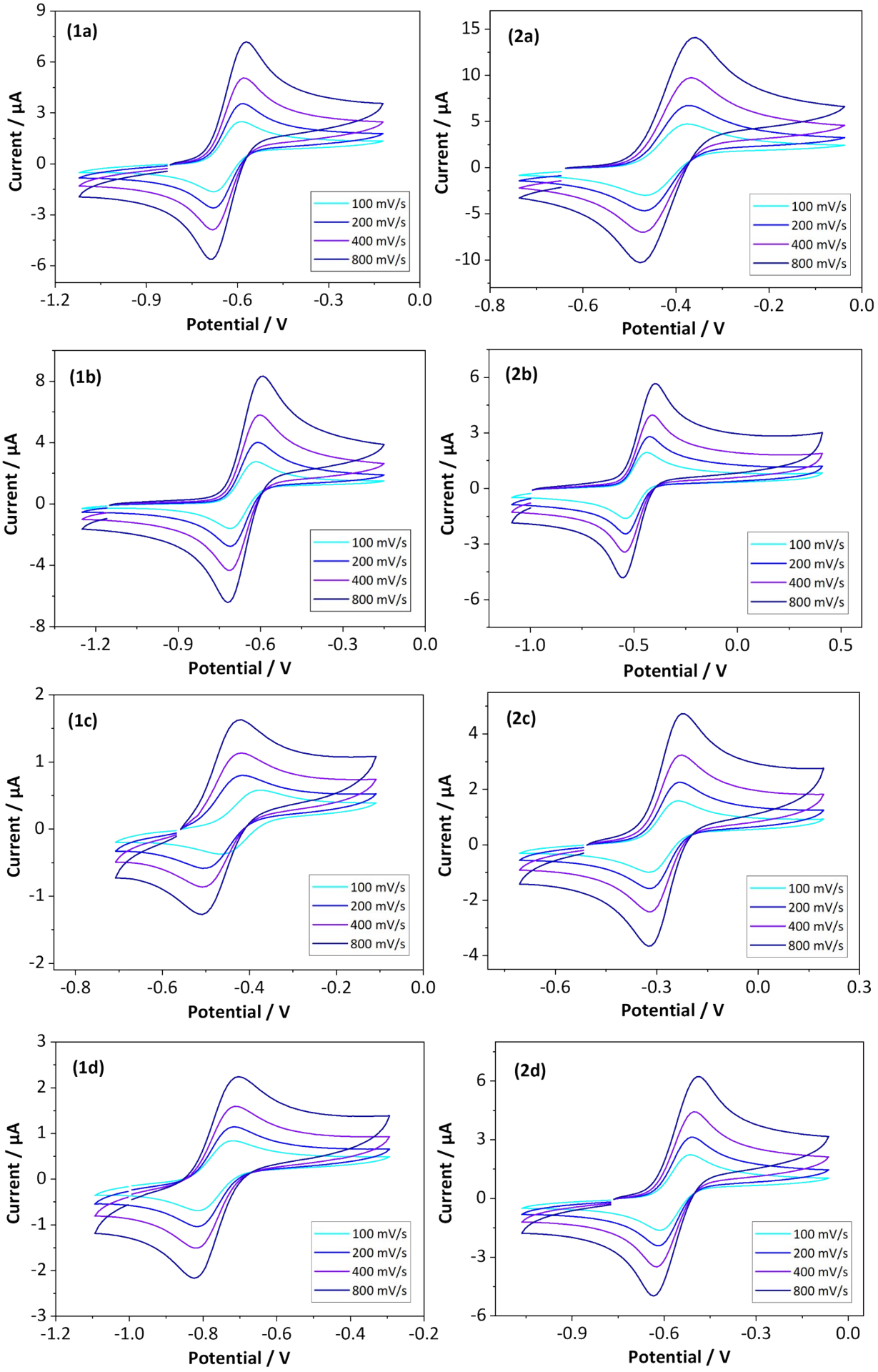
(1a)
(2a)
(1b)
(2b)
(1c)
(2c)
(1d)
(2d)
Current / µA
Potential / V
100 mV/s
200 mV/s
400 mV/s
800 mV/s

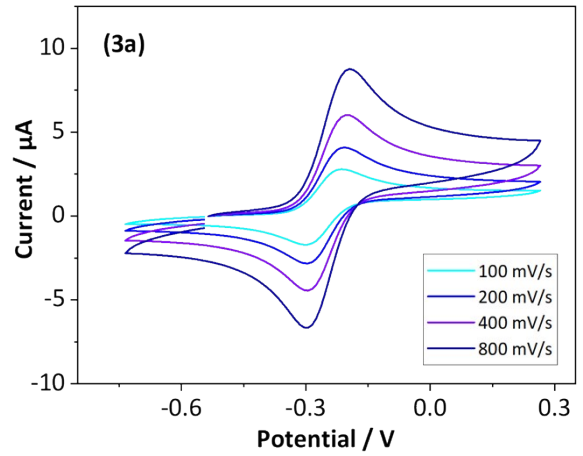
(3a)
Current / µA
Potential / V
100 mV/s
200 mV/s
400 mV/s
800 mV/s

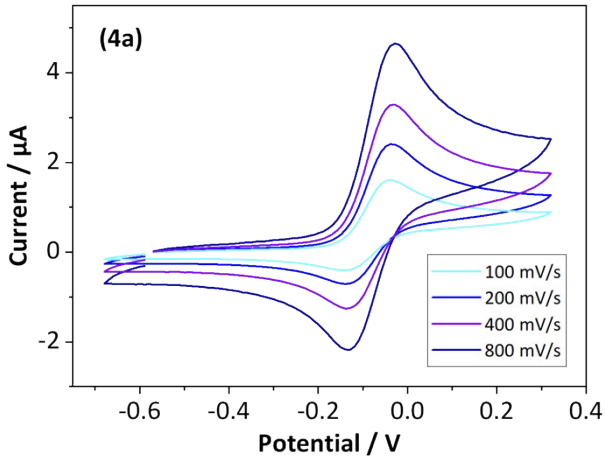
(4a)
Current / µA
Potential / V
100 mV/s
200 mV/s
400 mV/s
800 mV/s

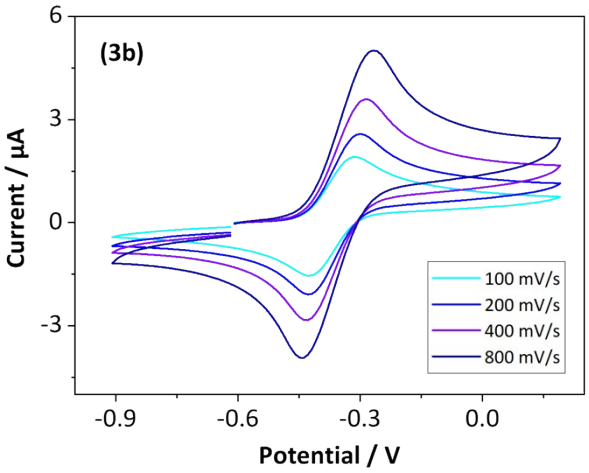
(3b)
Current / µA
Potential / V
100 mV/s
200 mV/s
400 mV/s
800 mV/s

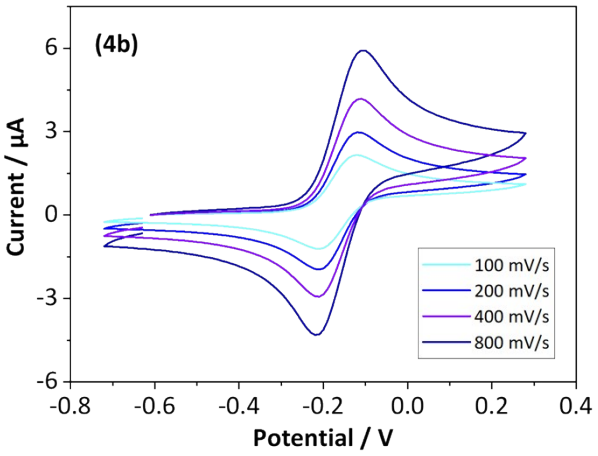
(4b)
Current / µA
Potential / V
100 mV/s
200 mV/s
400 mV/s
800 mV/s

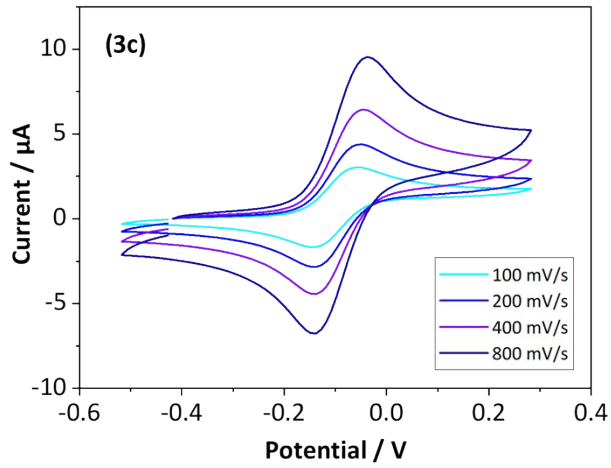
(3c)
Current / µA
Potential / V
100 mV/s
200 mV/s
400 mV/s
800 mV/s

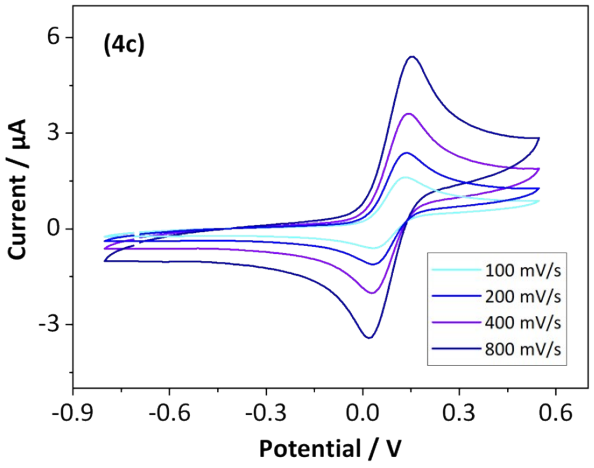
(4c)
Current / µA
Potential / V
100 mV/s
200 mV/s
400 mV/s
800 mV/s

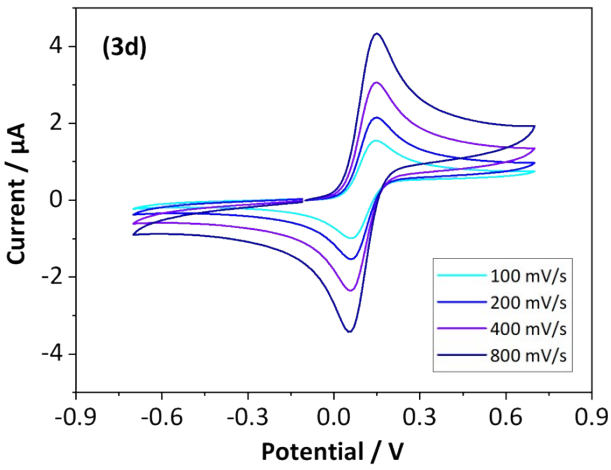
(3d)
Current / µA
Potential / V
100 mV/s
200 mV/s
400 mV/s
800 mV/s

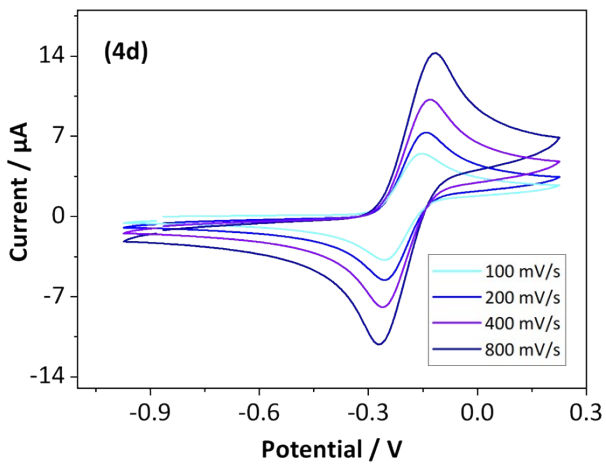
(4d)
Current / µA
Potential / V
100 mV/s
200 mV/s
400 mV/s
800 mV/s

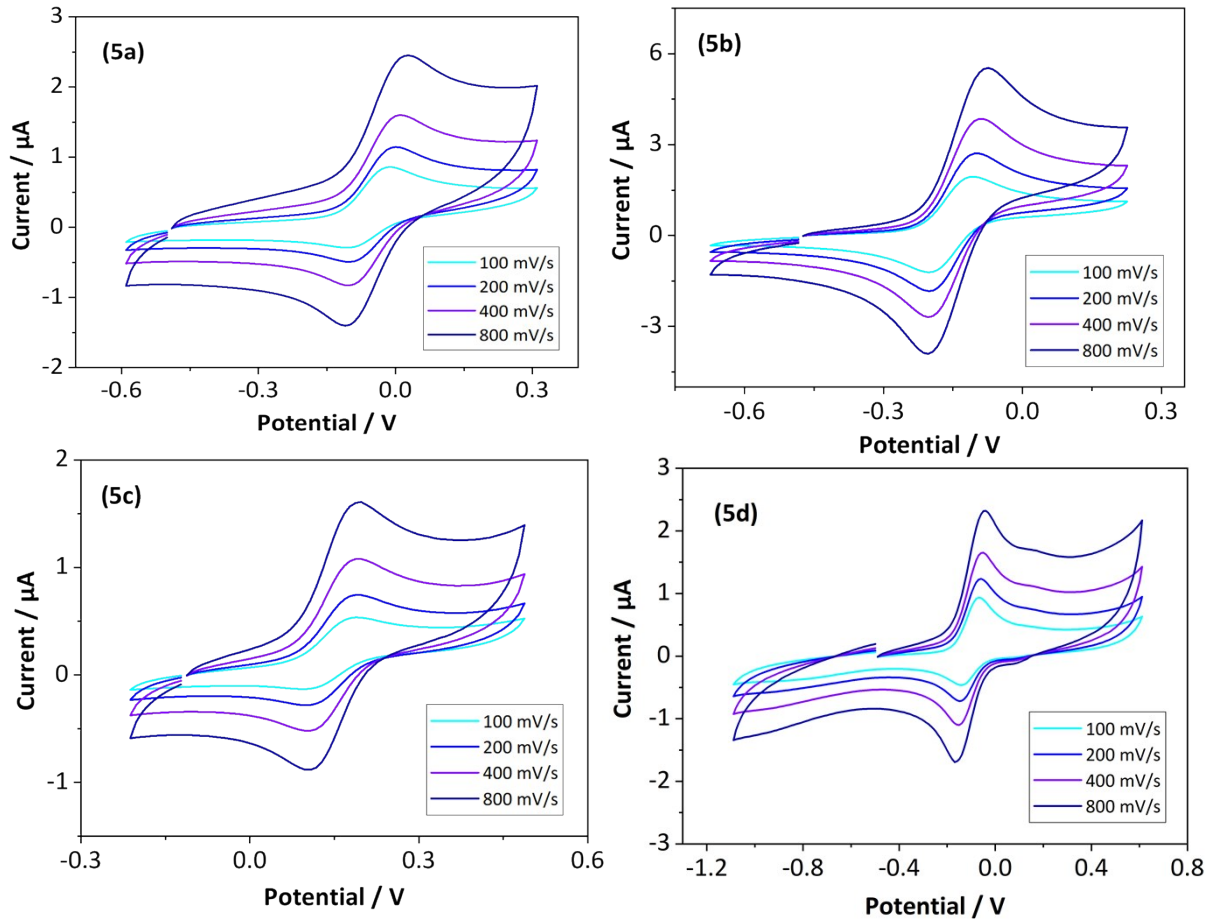

Figure S1 Plots of the cyclic voltammograms (CV) data for complexes [**1a-d**] - [**5a-d**] (CH_2Cl_2, 0.1 M NBu_4PF_6, room temperature) vs ferrocene/ferricenium [$E_{1/2}(Fc/Fc^+) = 0$ V] at a platinum working electrode.

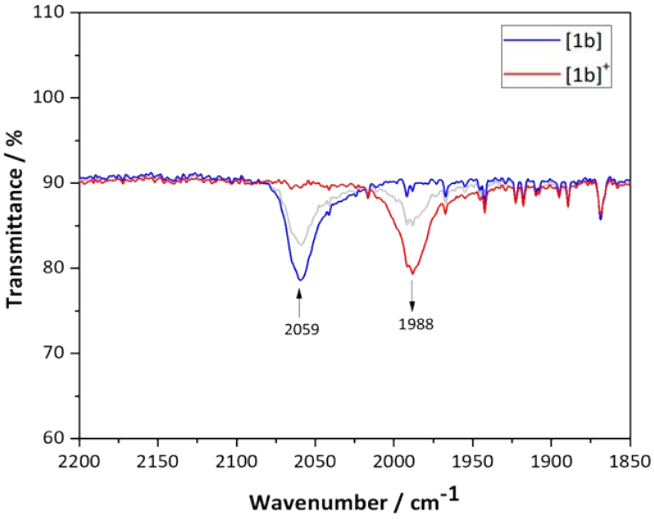
[1b]
[1b]+
Transmittance / %
Wavenumber / cm-1
2059
1988

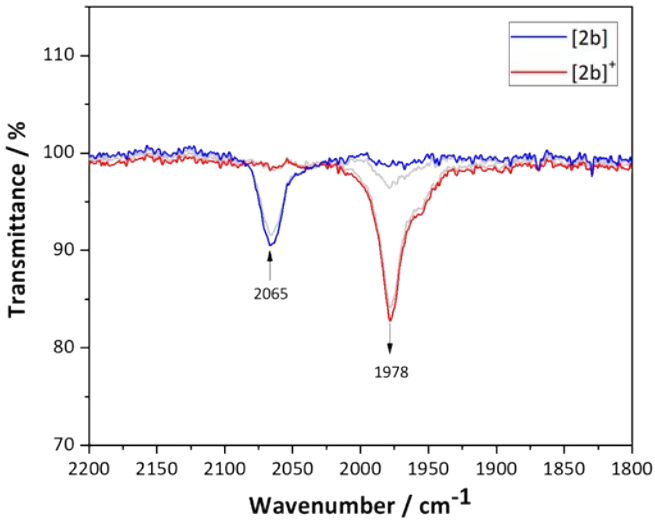
[2b]
[2b]+
Transmittance / %
Wavenumber / cm-1
2065
1978

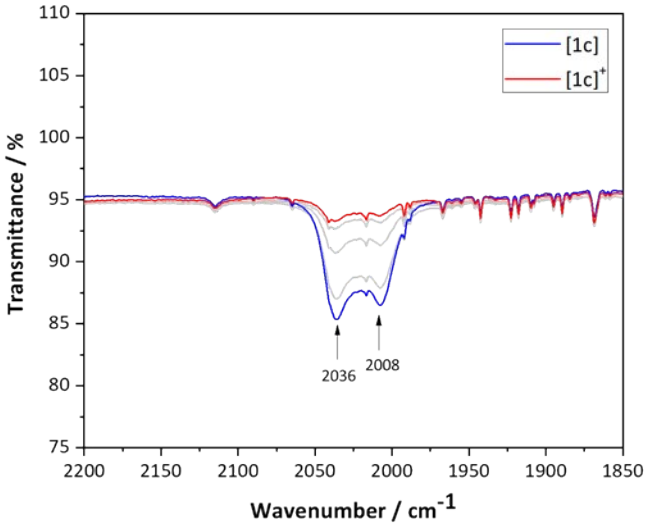
[1c]
[1c]+
Transmittance / %
Wavenumber / cm-1
2036
2008

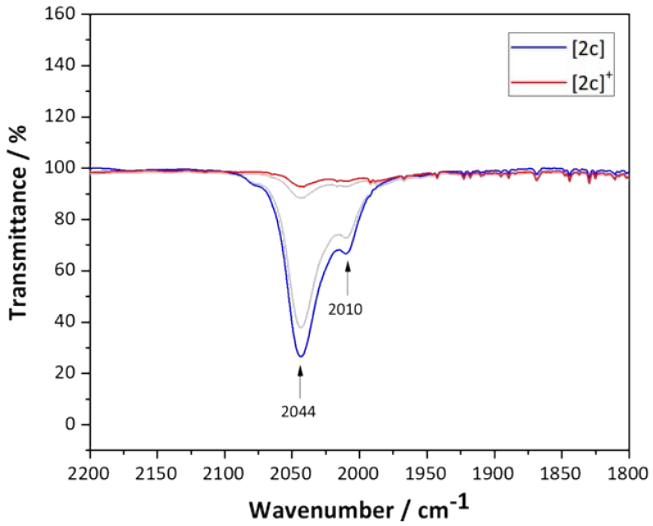
[2c]
[2c]+
Transmittance / %
Wavenumber / cm-1
2044
2010

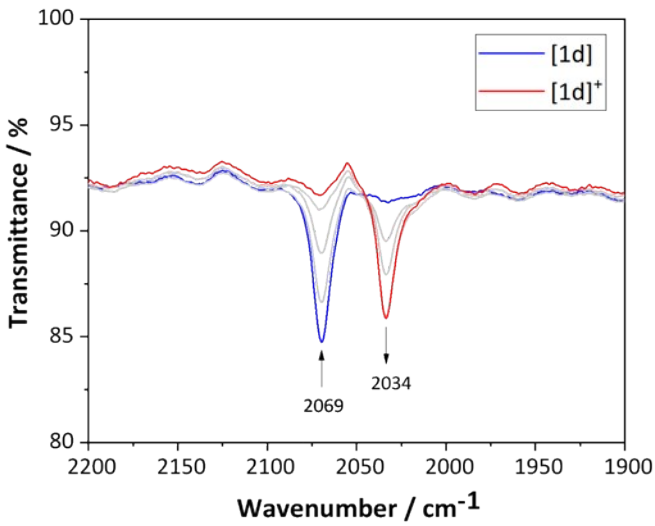
[1d]
[1d]+
Transmittance / %
Wavenumber / cm-1
2069
2034

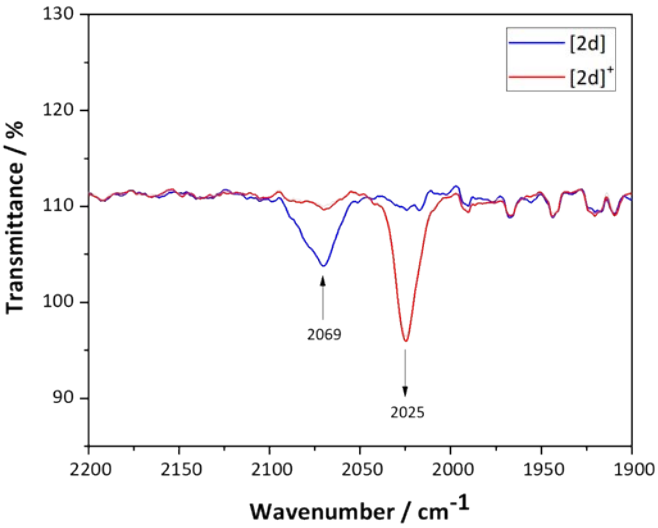
[2d]
[2d]+
Transmittance / %
Wavenumber / cm-1
2069
2025

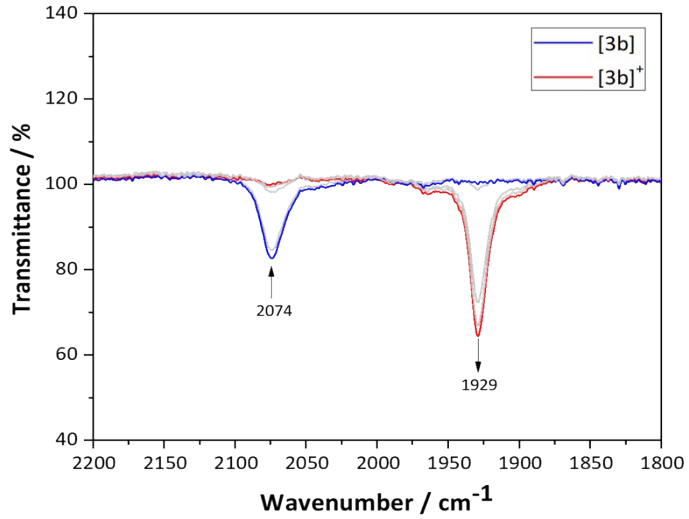
[3b]
[3b]+
Transmittance / %
Wavenumber / cm-1
2074
1929

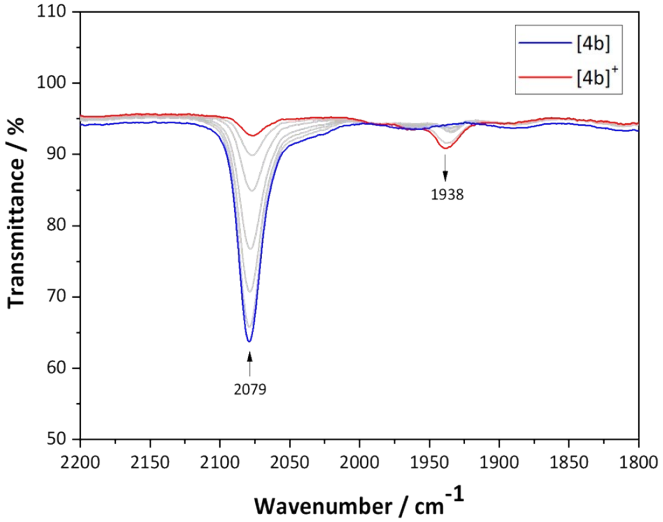
[4b]
[4b]+
Transmittance / %
Wavenumber / cm-1
1938
2079

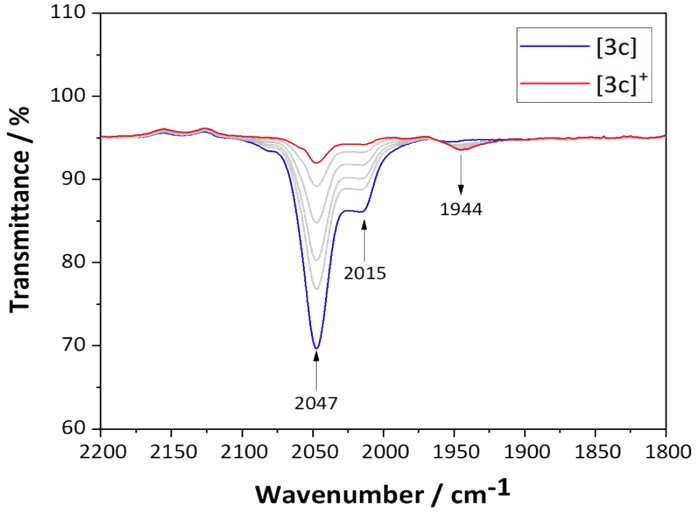
[3c]
[3c]+
Transmittance / %
Wavenumber / cm-1
1944
2015
2047

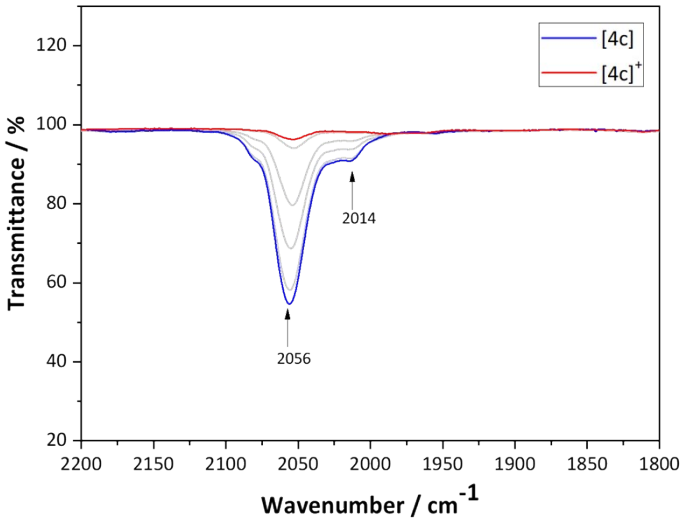
[4c]
[4c]+
Transmittance / %
Wavenumber / cm-1
2014
2056

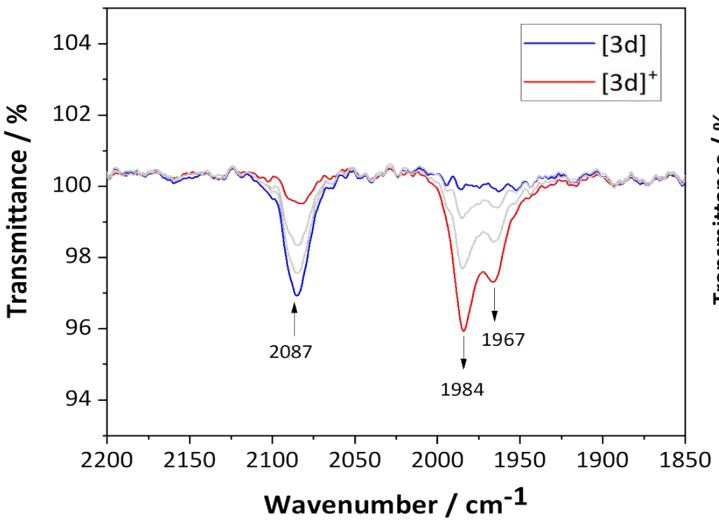
[3d]
[3d]+
Transmittance / %
Wavenumber / cm-1
2087
1967
1984

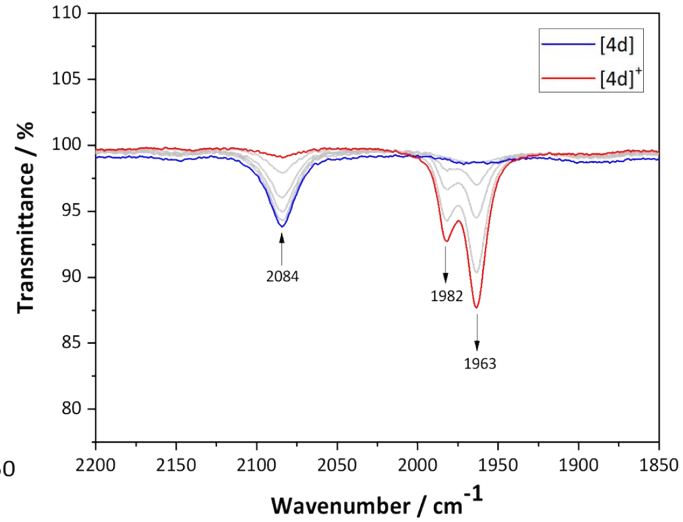
[4d]
[4d]+
Transmittance / %
Wavenumber / cm-1
2084
1982
1963

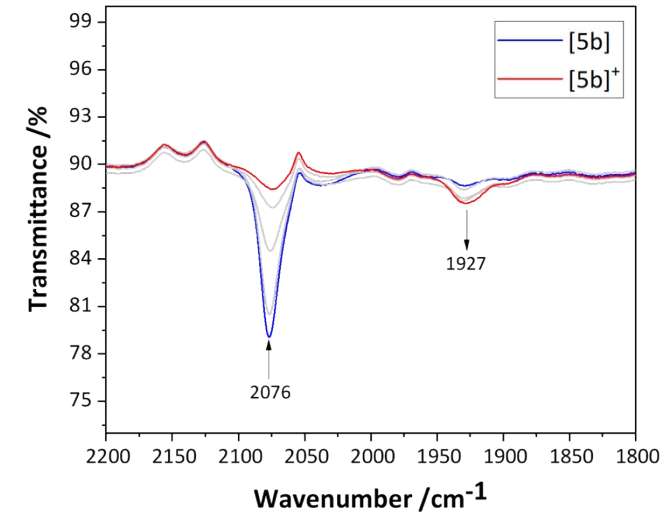

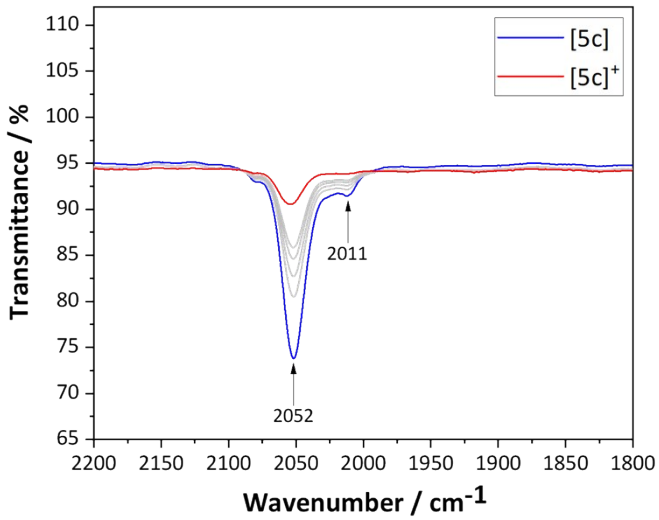

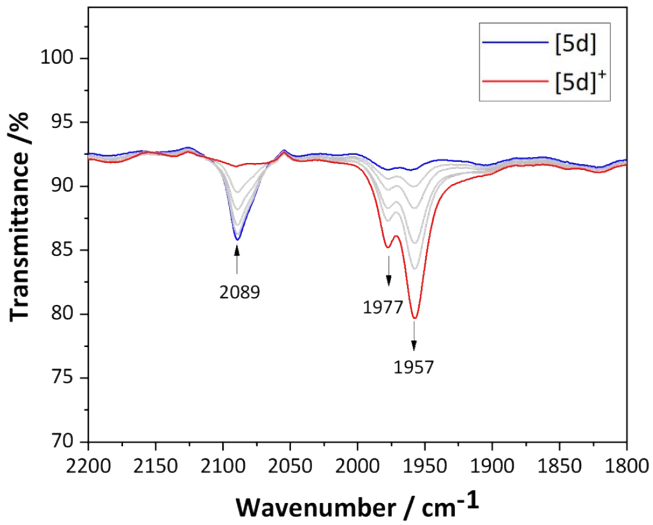

Figure S2 Plots of the IR spectroelectrochemical results (from 0.1 M NBu_4PF_6 / CH_2Cl_2 solutions) for compounds [**1b-d**]$^{n+}$ – [**5b-d**]$^{n+}$ (n= 0, 1).

Table S1. Summary of the $^{13}C\{^{1}H\}$ NMR data (δ / ppm) from complexes [**1a-d**] – [**5a-d**].

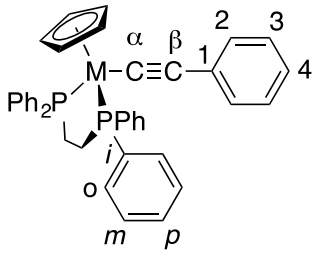

	α (J_{CP})	β	1	2	3	4	*i*	o (J_{CP})	*m*	*p*	dppe	Cp	Me	OMe	CMe_3	CMe_3	Ref
1a	137.4 (t, *40*Hz)	120.3	130.6	131.7	127.5	123.2	139.8, 137.8	134.7, 134.0	127.4, 127.2	129.2, 129.0	31.1	87.8	10.5				1
1b	132.0 (m)	119.3	124.8	131.5	114.1	156.7	140.0, 138.2	134.7, 134.4	127.4, 127.2	129.2, 128.9	31.2	87.7	10.5	54.9			2
1c	165.9 (t, *40*Hz)	125.1	137.7	129.7	124.0	141.8	138.3, 136.8	134.0, 133.9	127.6, 127.4	129.4, 129.3	30.8	88.8	10.2				2
1d	107.7 (m)	124.8					140.4, 138.7	134.9, 134.3	127.3, 127.2	128.9, 128.7	30.4	87.0	10.5		31.1	33.0	2
2a	125.0 (t, *41*Hz)	120.6	130.0	130.4	127.5	123.0	142.5, 138.2	133.9, 131.9	128.7, 128.0	129.3, 128.9	28.6	79.2					3
2b	132.9 (m)	119.7	123.1	131.3	113.1	155.9	142.6, 138.3	133.9, 131.9	128.0, 127.7	129.2, 128.8	28.5	79.1		55.3			
2c	146.4 (m)	124.0	136.8	130.3	123.7	143.3	142.0, 137.9	133.8, 132.1	128.2, 127.9	129.7, 129.1	28.7	80.1					4
2d	95.0 (t, *43*Hz)	-					144.0 139.2	134.7, 132.0	127.9, 127.4	129.2, 128.5	28.6	79.3			30.2	32.8	5

3a	128.9 (m)	109.8	131.5	130.3	127.6	122.6	139.1, 137.1	133.9, 133.4 (t, *4.3* Hz)	127.5, 127.3	129.0, 128.9	29.6	92.7	10.2				6
3b	124.3 (t, *25*Hz)	108.5	124.5	131.2	113.3	155.7	139.3, 137.2	133.9, 133.4 (t, *4.5* Hz)	127.5, 127.2 (t, *4.5* Hz)	128.9, 128.8	29.6	92.6	10.2	55.4			6
3c	152.8 (t, *24*Hz)	114.3	138.5	130.0	123.6	142.1	138.2, 136.4	133.5, 133.2 (t, *5.3* Hz)	127.8, 127.5 (t, *4.5*Hz)	129.4, 129.3	29.5	93.4	10.1				6
3d	100.5 (t, *26*Hz)	116.4					139.7, 137.8	134.2, 133.3 (t, *4.5* Hz)	127.4, 127.0 (t, *4.5* Hz)	128.6	29.6	91.9	10.1		29.4	32.8	5
4a	116.1	111.7	129.9	130.5	127.1	122.9	142.4, 137.0	133.9, 131.5	127.8, 127.6	129.2, 128.8	28.0	82.4					7
4b	112.0 (t, *25*Hz)	110.9	123.1	131.7	113.0	156.0	142.7, 137.4	134.1, 131.8 (t, *5.2* Hz)	128.0, 127.8 (t, *5.0* Hz)	129.4, 129.0	28.2	82.5		55.3			
4c	138.4 (t, *25*Hz)	114.7	137.4	130.5	123.3	142.7	141.8, 136.4	131.6, 133.9 (t, *5.2* Hz)	128.3, 128.0 (t, *4.6* Hz)	129.8, 129.3	28.3	83.1					8
4d	88.3 (t, *25*Hz)	119.0					143.6, 137.4	134.5, 131.5 (t, *5.2* Hz)	127.8, 127.4 (t, *4.6* Hz)	129.0, 128.5	28.2	82.2			29.4	32.3	
5a	116.3 (t, *25*Hz)	114.5	130.7	130.6	127.8	123.1	139.1 (t, *20.4* Hz)	134.0 (t, *5.3* Hz)	127.3 (t, *4.5* Hz)	128.5		85.3					9
5b	111.8 (t, *25*Hz)	113.3	123.8	131.5	113.4	156.0	139.1 (t, *20.8* Hz)	134.01 (t, *4.9* Hz)	127.3 (t, *4.5* Hz)	128.5		85.2		55.4			10
5c	139.1 (t, *25*Hz)	117.6	137.7	130.5	123.8	142.8	138.6	133.8 (t, *4.5* Hz)	127.5 (t, *4.5* Hz)	128.8		85.8					11
5d	86.4 (t, *25*Hz)	120.3					139.6	134.1 (t, *4.5* Hz)	127.0 (t, *4.5* Hz)	128.2		85.2			30.2	33.1	5

^{1}H NMR, ^{31}P, ^{13}C{^{1}H} and MS Spectra of complexes [1a-d] – [5a-d].

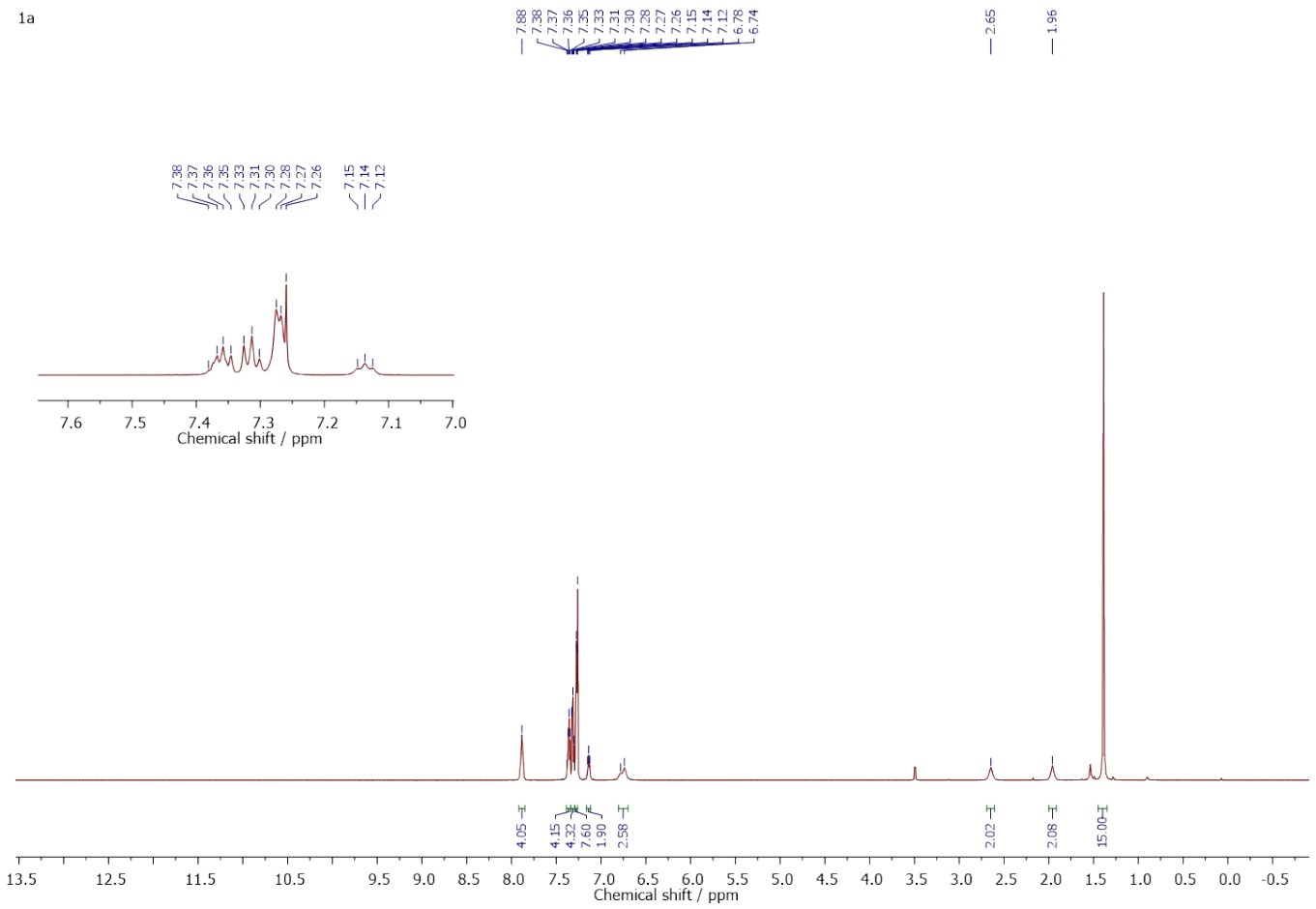

Figure S3. The ^{1}H NMR spectrum of [**1a**]. The inset shows an expansion of the aromatic region for clarity.

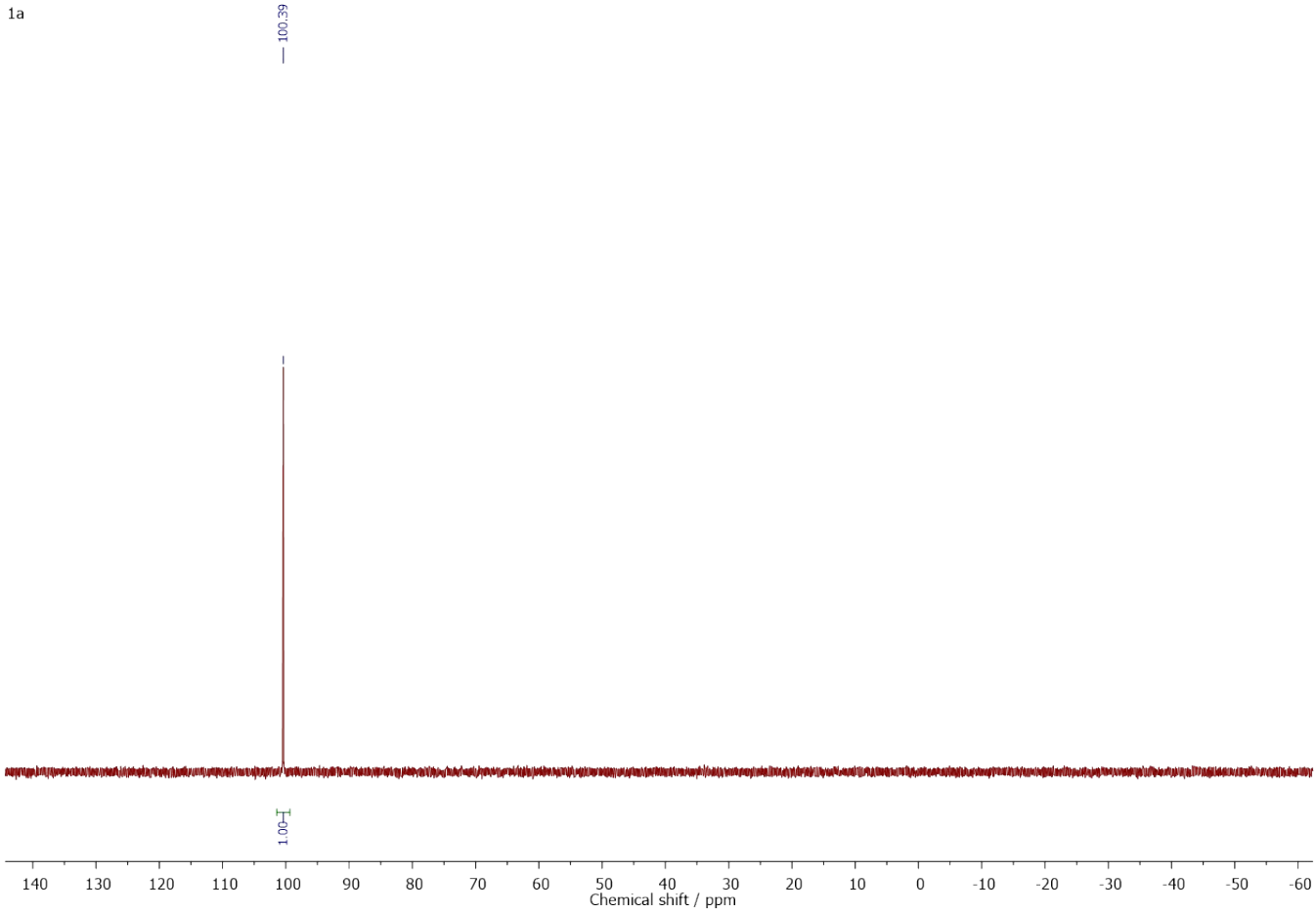

Figure S4. The ^{31}P NMR spectrum of [**1a**].

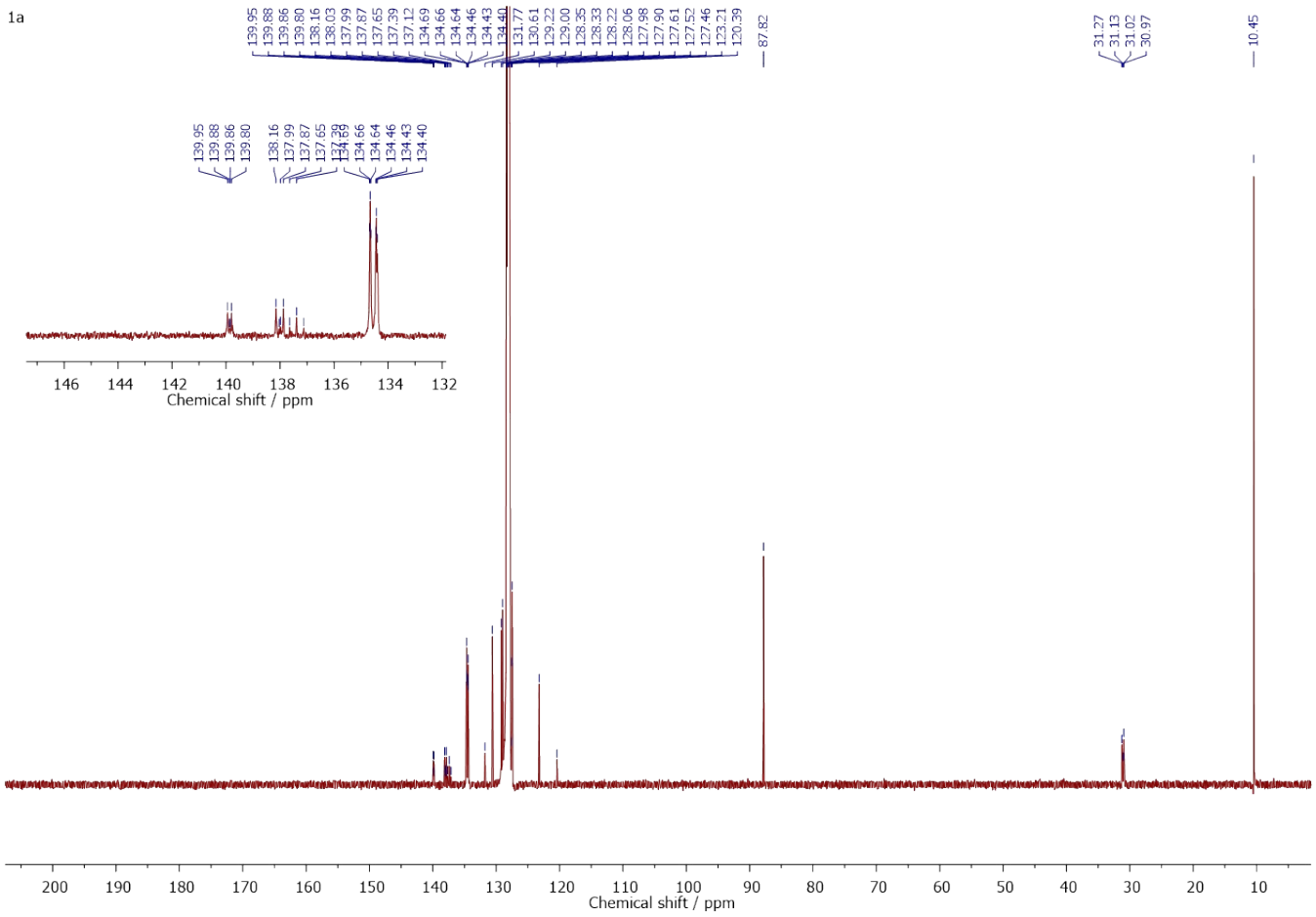

Figure S5. The $^{13}C\{^{1}H\}$ NMR spectrum of [**1a**]. The inset shows an expansion of the aromatic region for clarity.

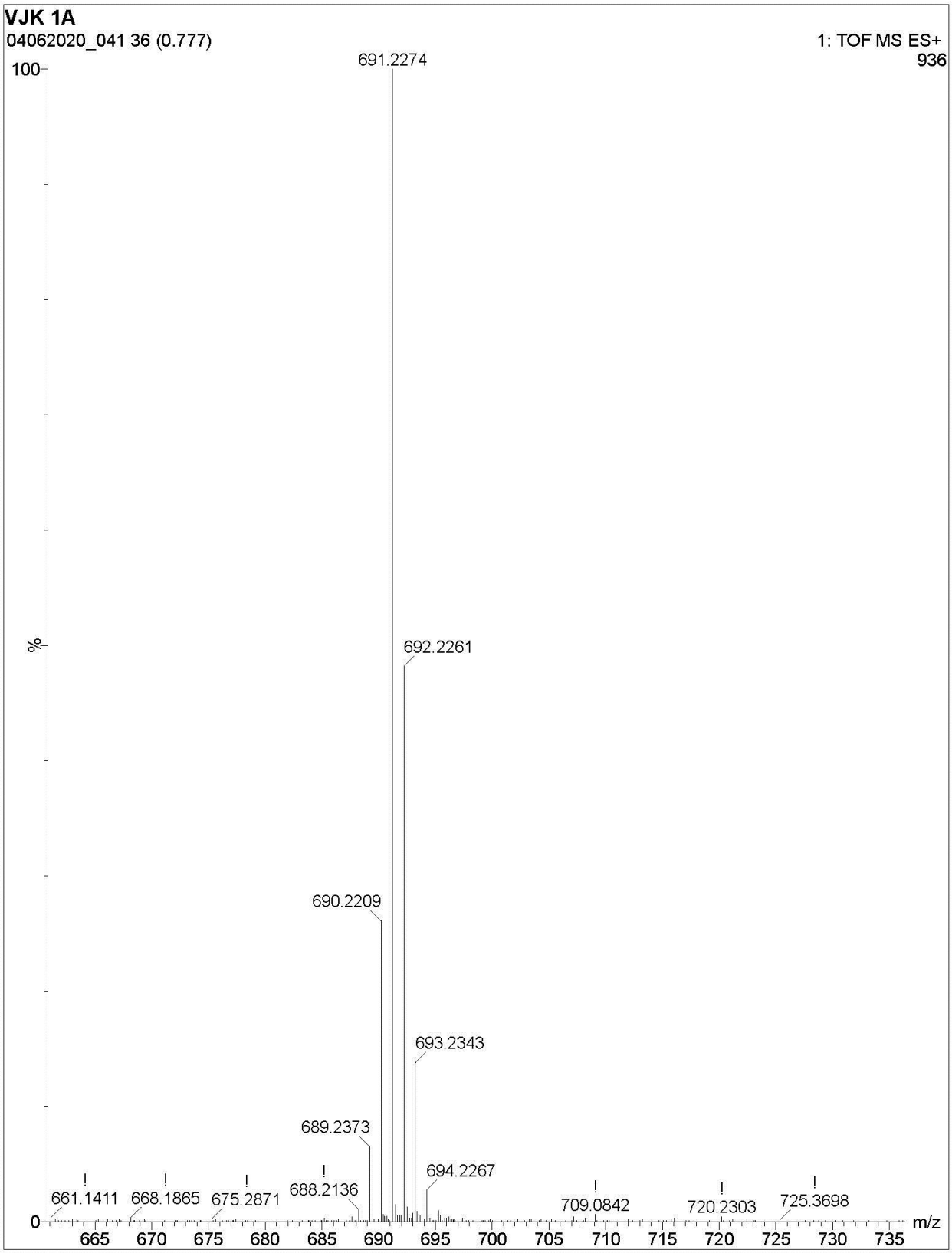

Figure S6. The ESI(+) mass spectrum of [**1a**].

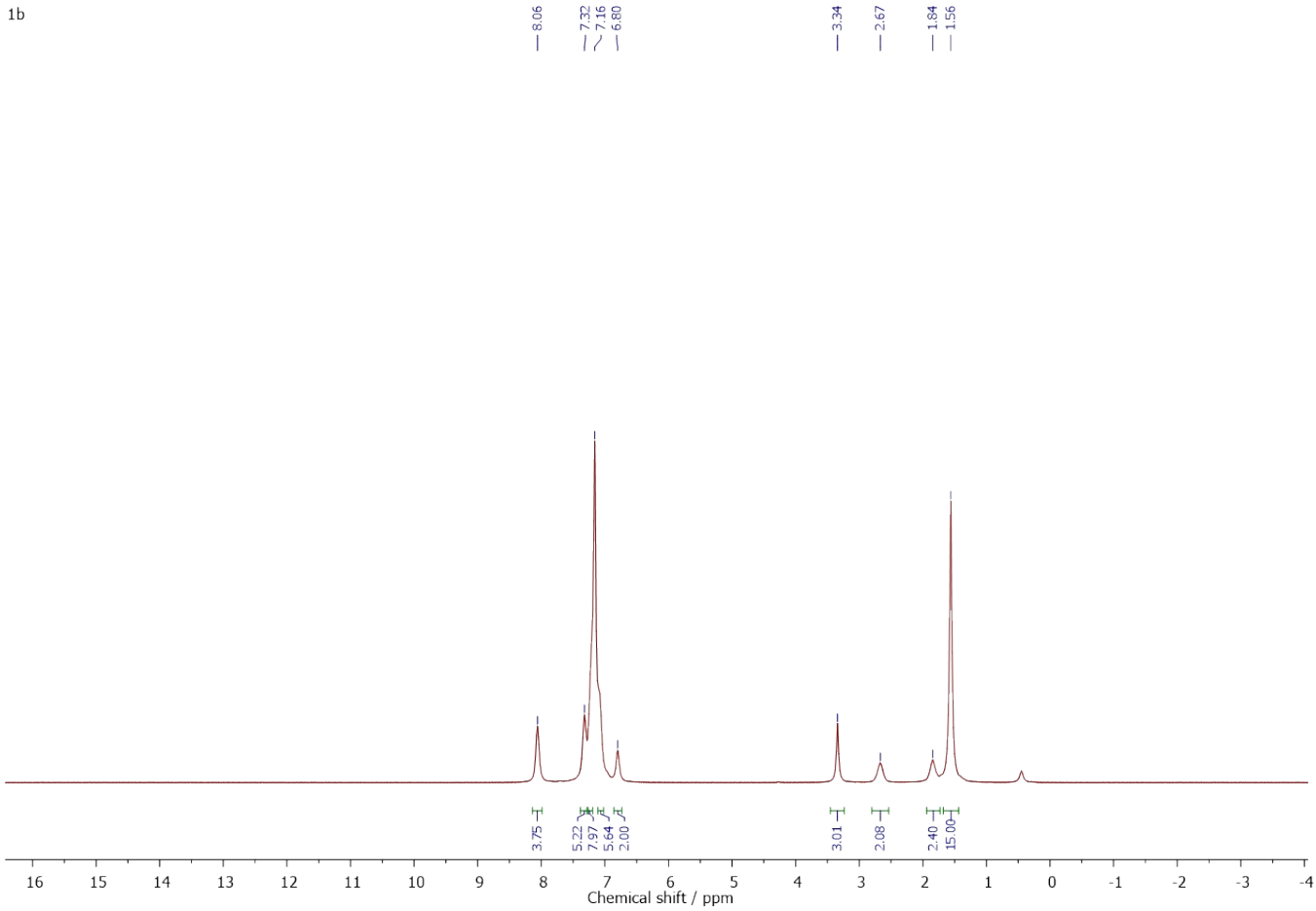

Figure S7. The ^{1}H NMR spectrum of [**1b**].

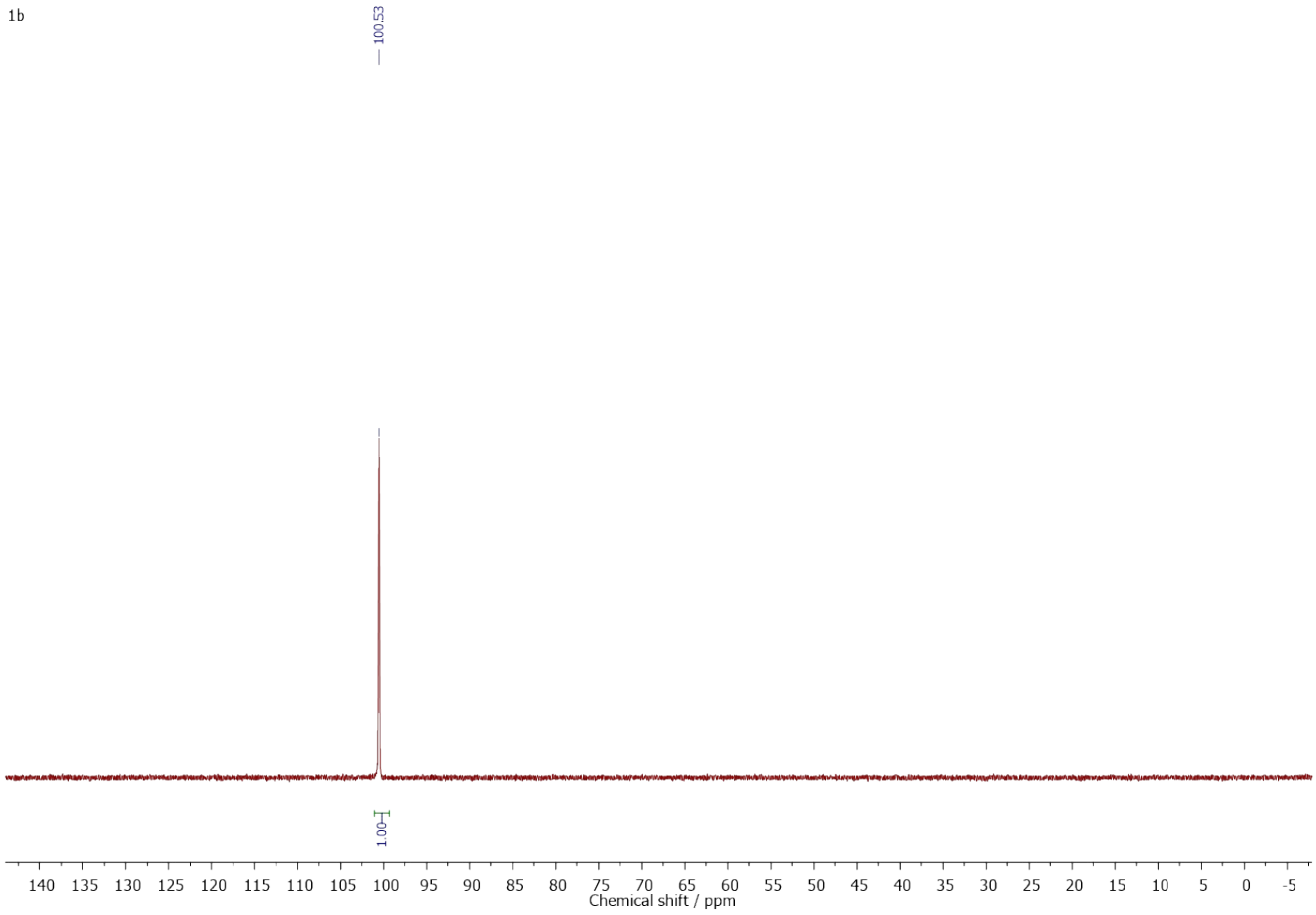

Figure S8. The ^{31}P NMR spectrum of [**1b**].

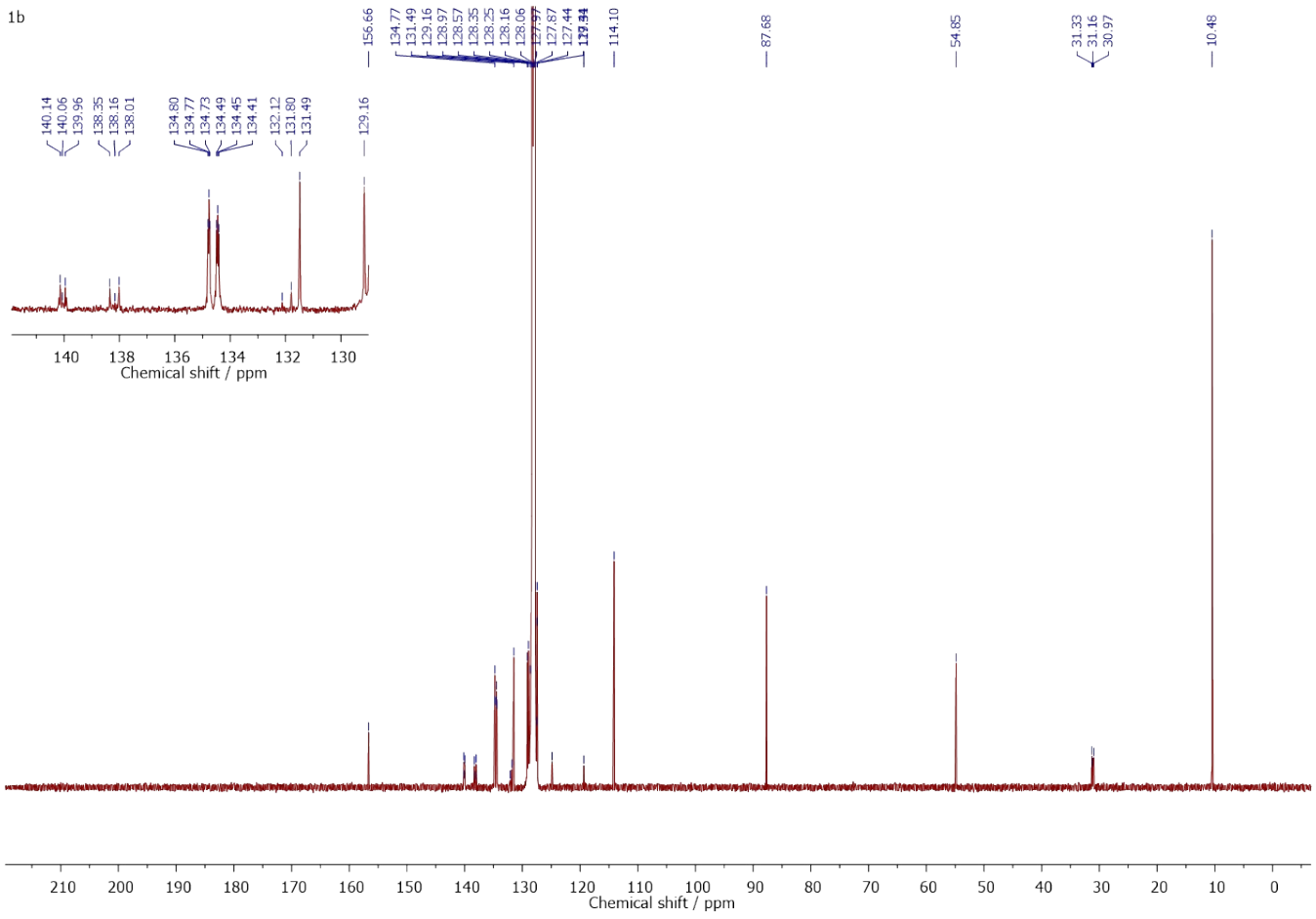

Figure S9. The $^{13}C\{^{1}H\}$ NMR spectrum of [**1b**]. The inset shows an expansion of the aromatic region for clarity.

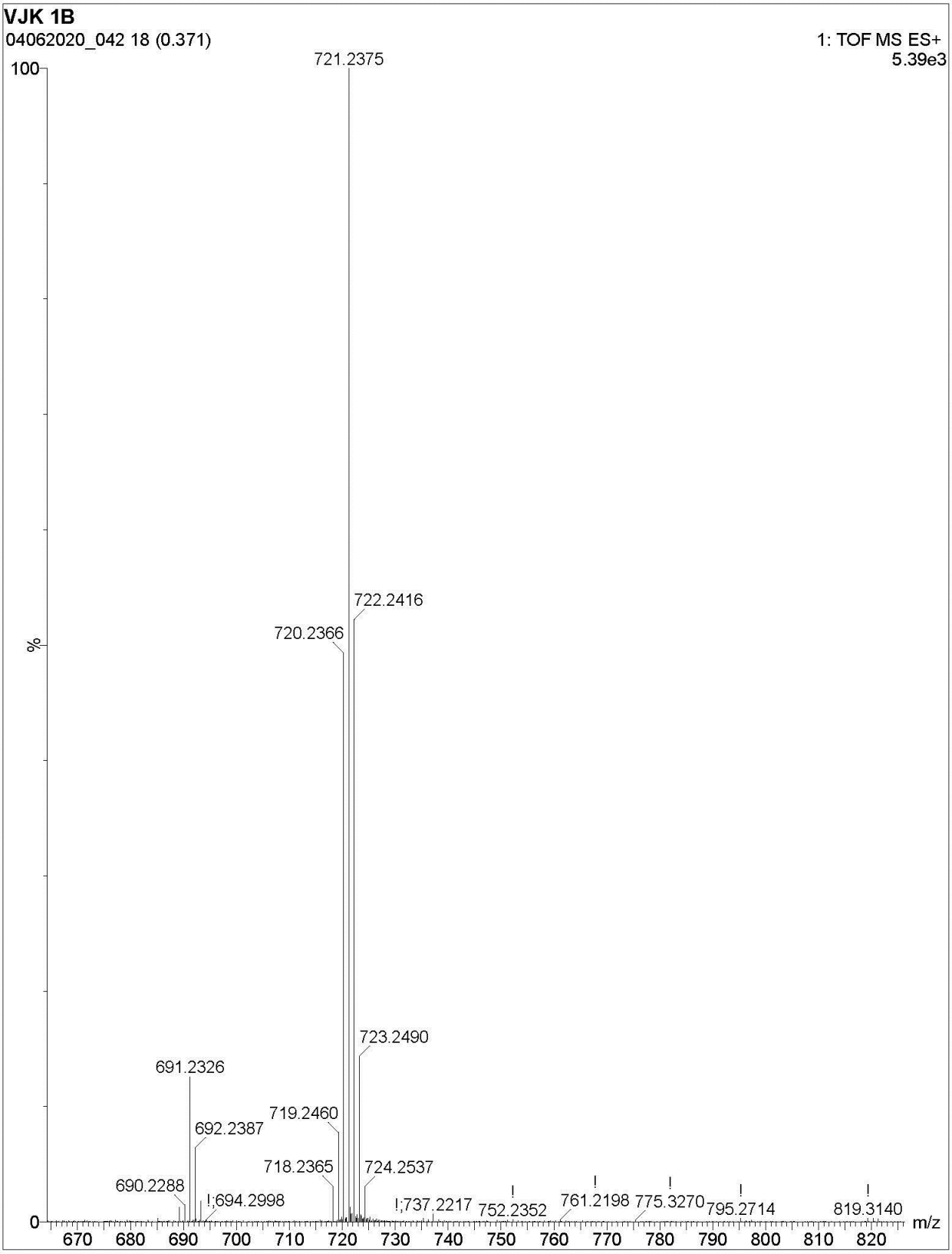

Figure S10. The ESI(+) mass spectrum of [**1b**].

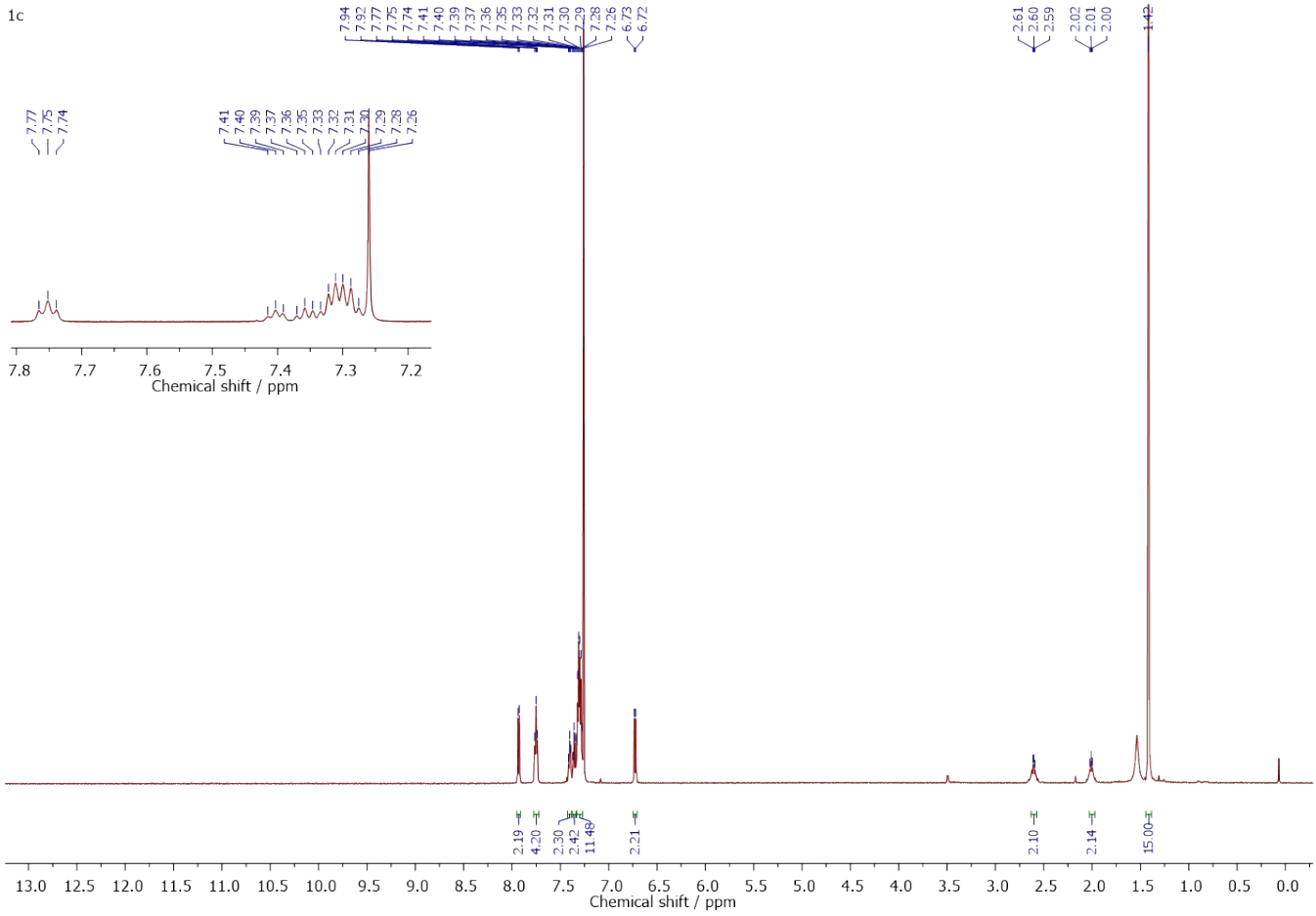

Figure S11. The ^{1}H NMR spectrum of [**1c**]. The inset shows an expansion of the aromatic region for clarity.

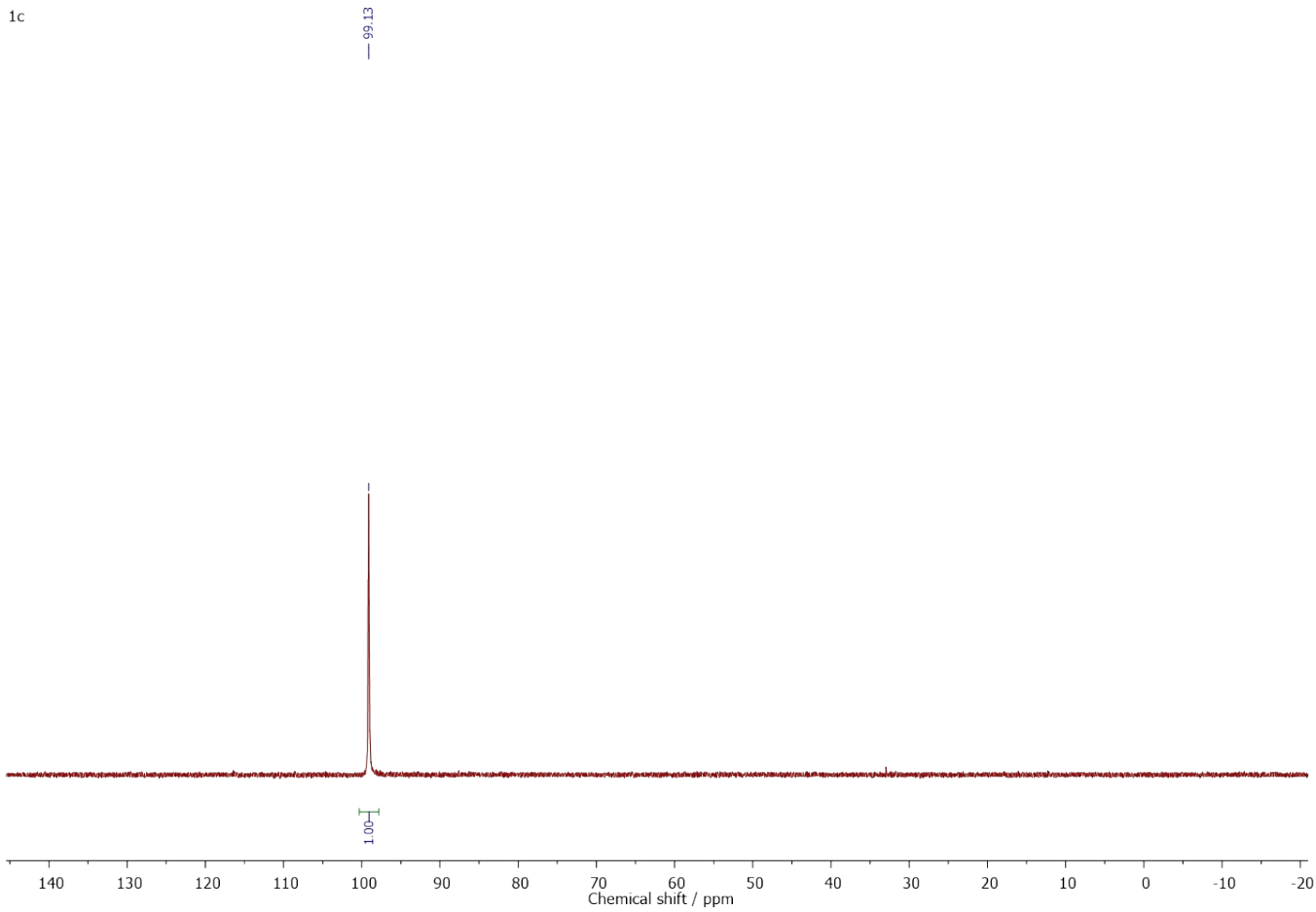

Figure S12. The ^{31}P NMR spectrum of [**1c**].

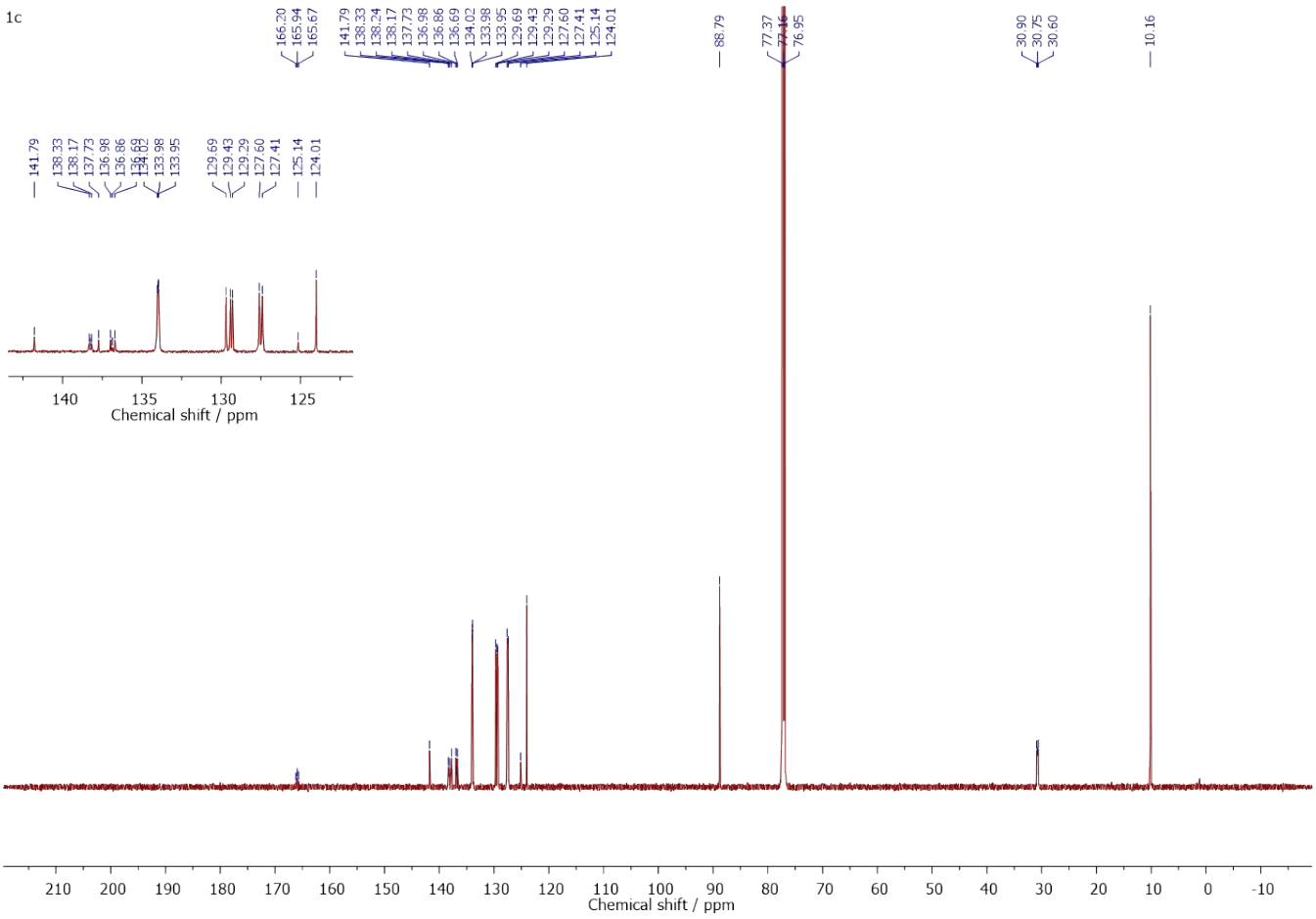

Figure S13. The $^{13}C\{^{1}H\}$ NMR spectrum of [**1c**]. The inset shows an expansion of the aromatic region for clarity.

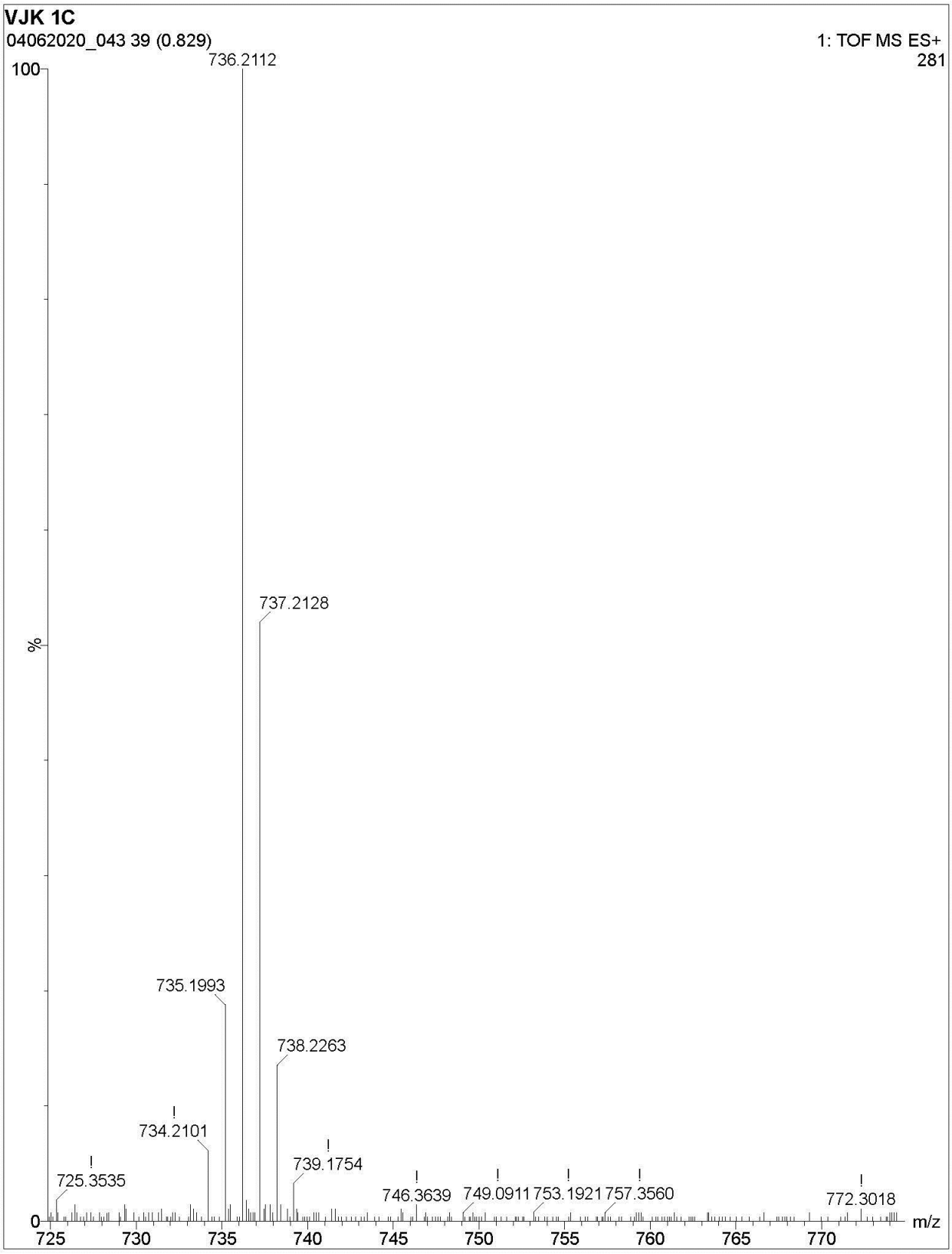

Figure S14. The ESI(+) mass spectrum of [**1c**].

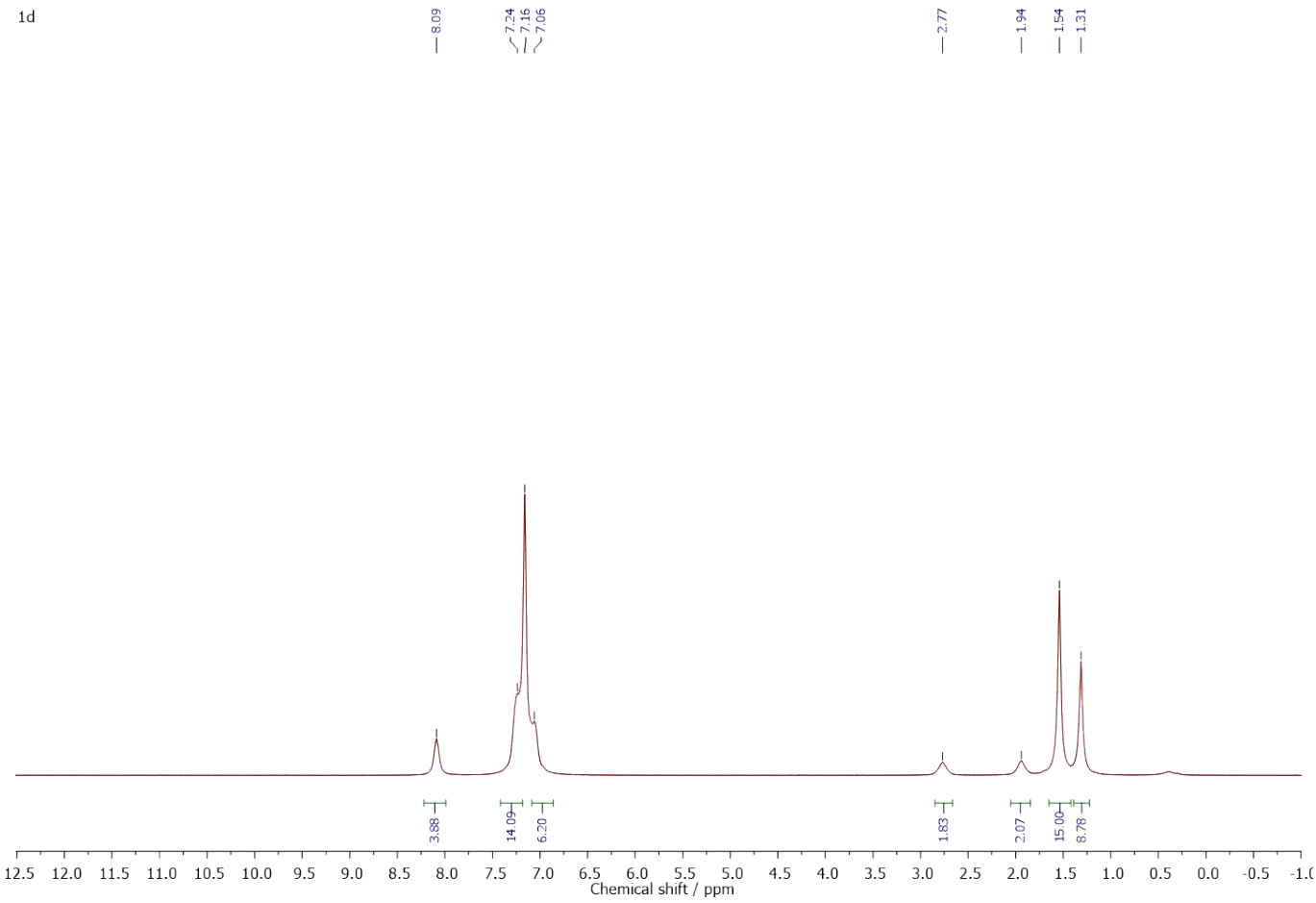

Figure S15. The ^{1}H NMR spectrum of [**1d**].

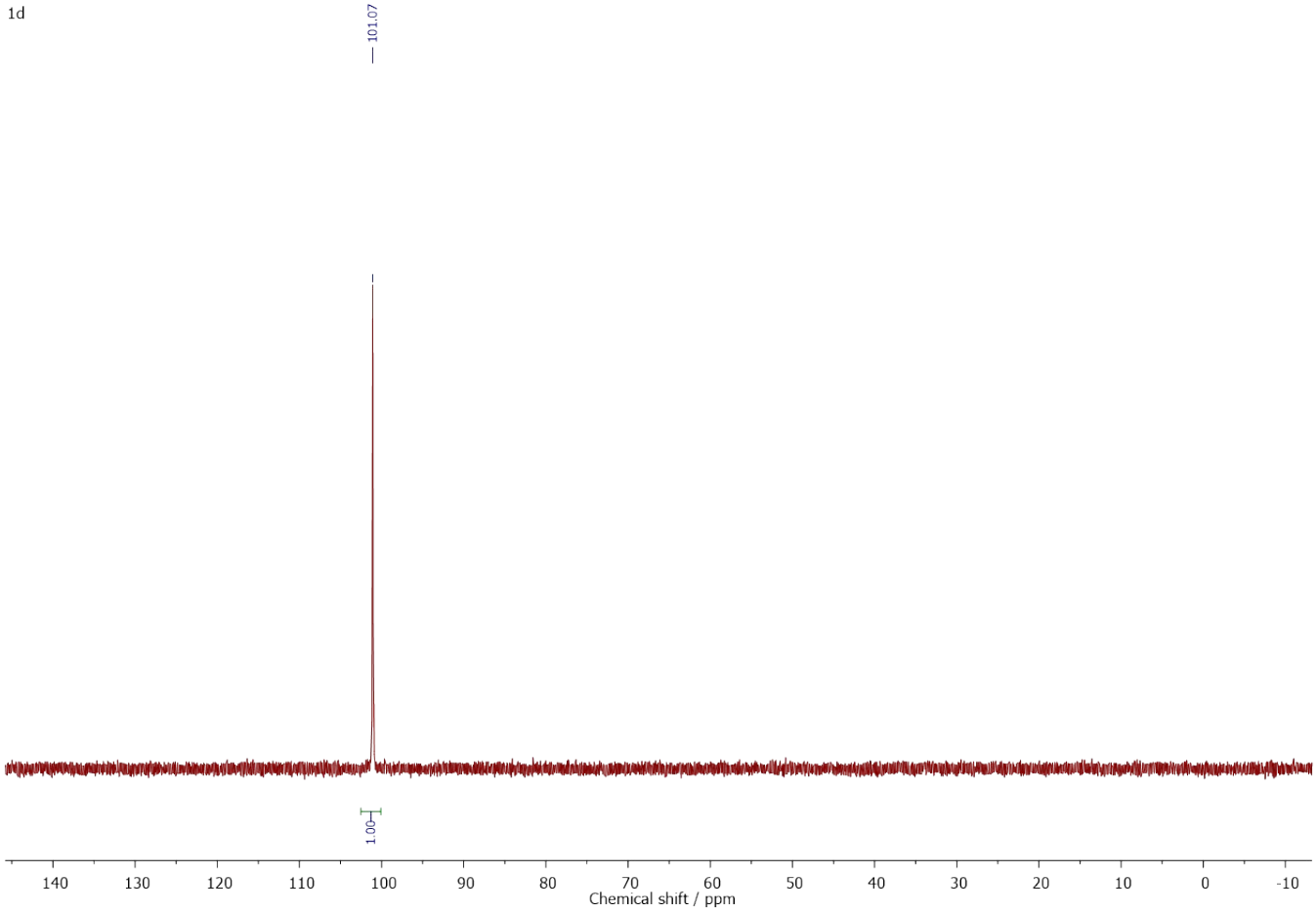

Figure S16. The ^{31}P NMR spectrum of [**1d**].

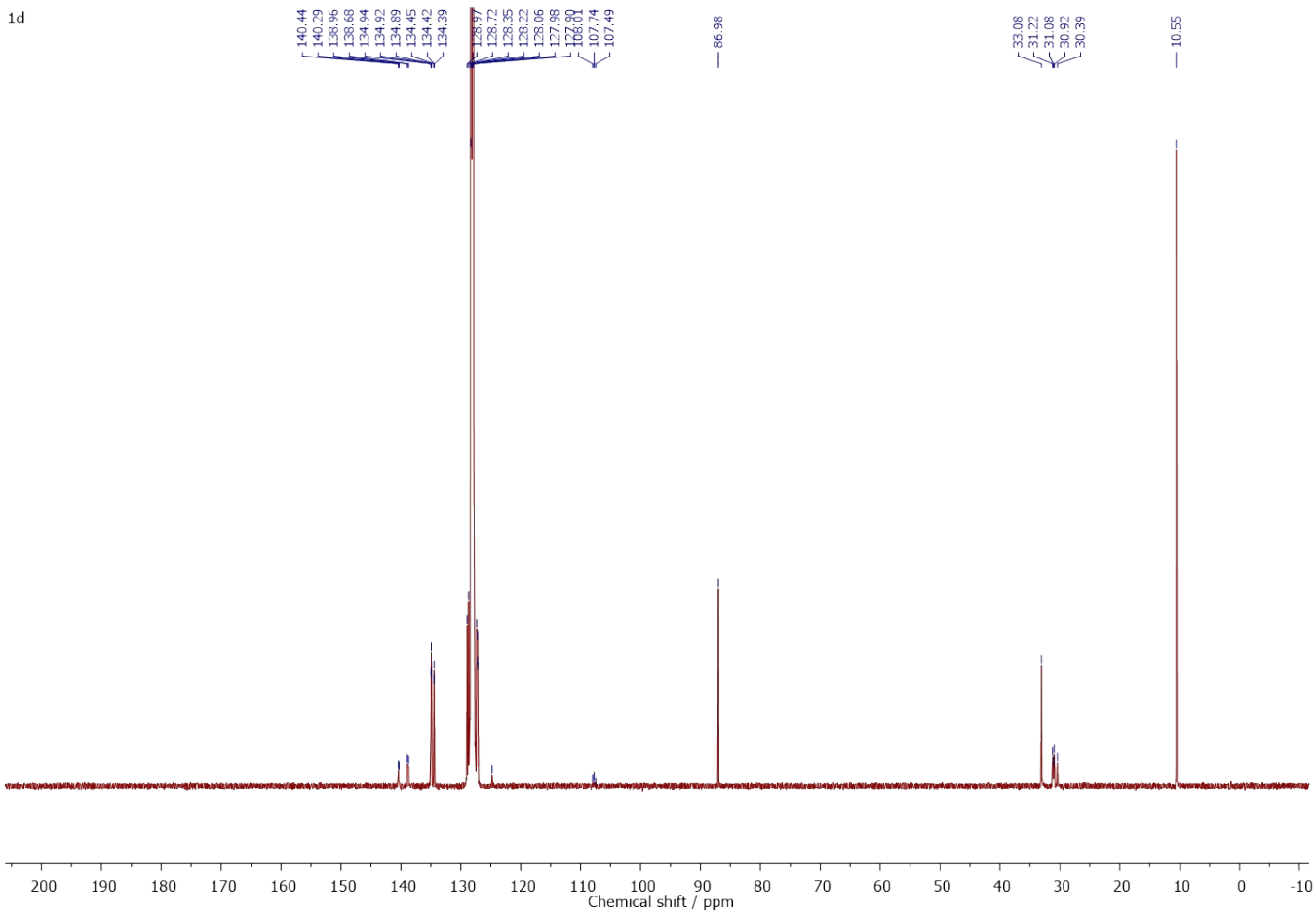

Figure S17. The $^{13}C\{H\}$ NMR spectrum of [**1d**].

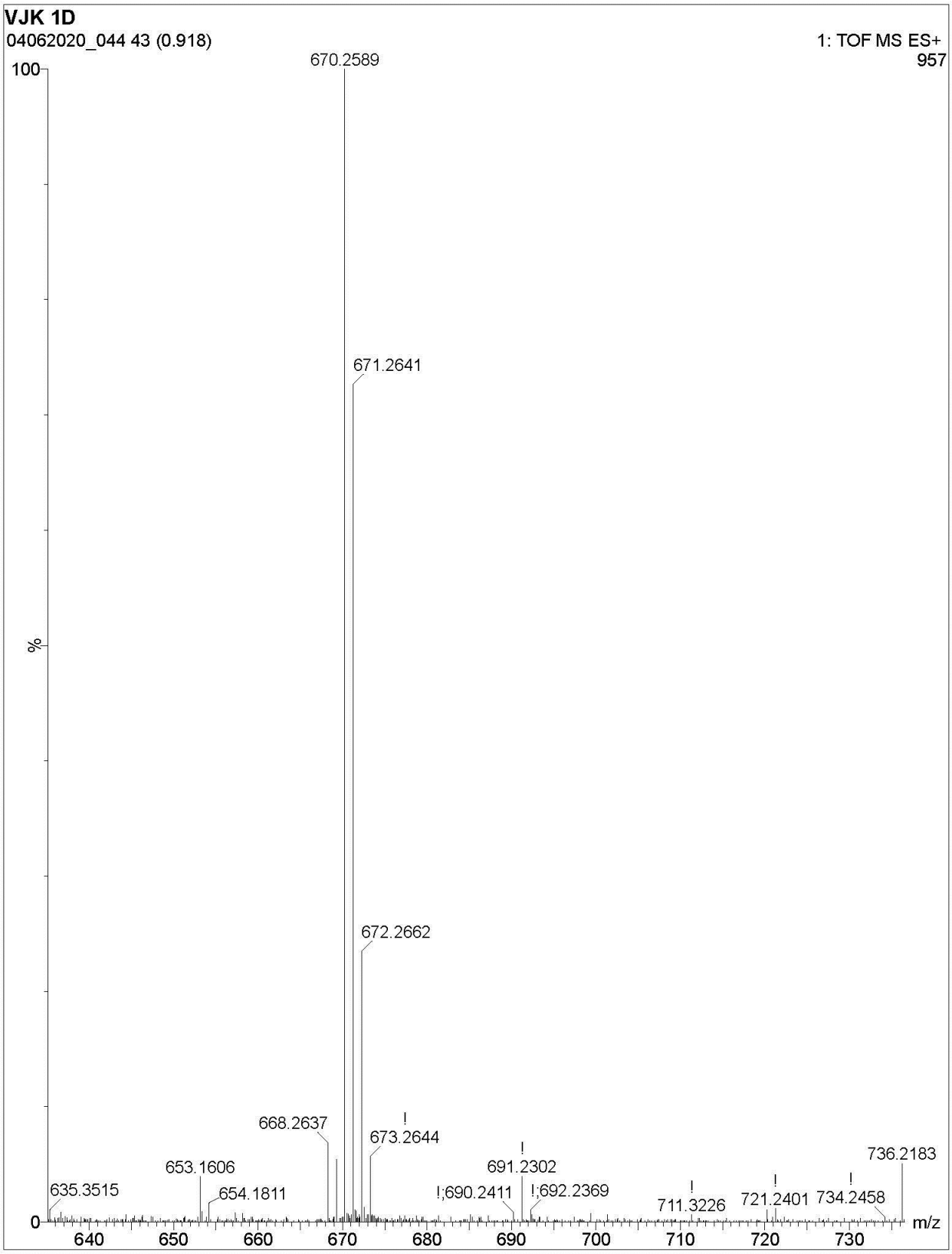

Figure S18. The ESI(+) mass spectrum of [**1d**].

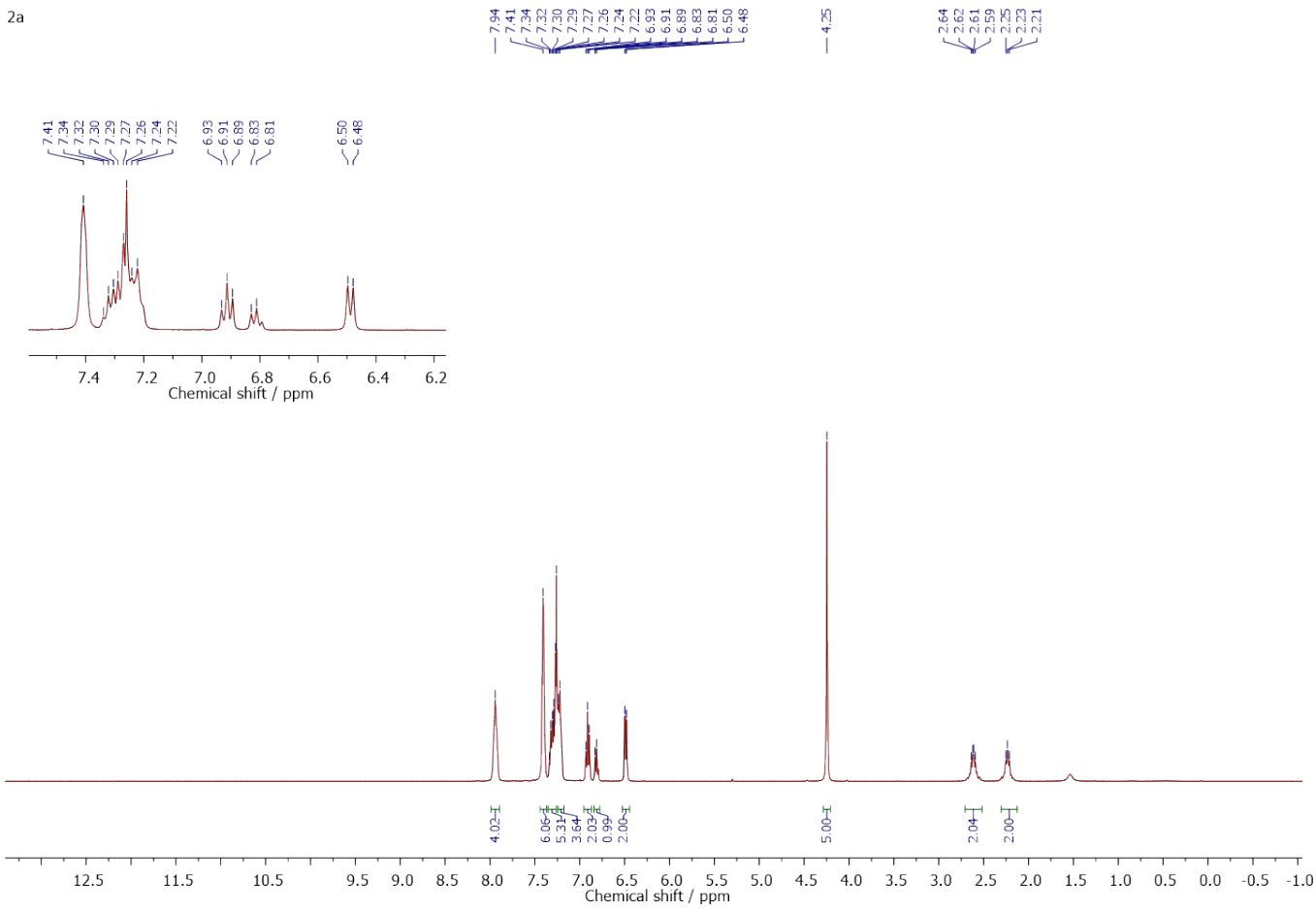

Figure S19. The ^{1}H NMR spectrum of [**2a**].

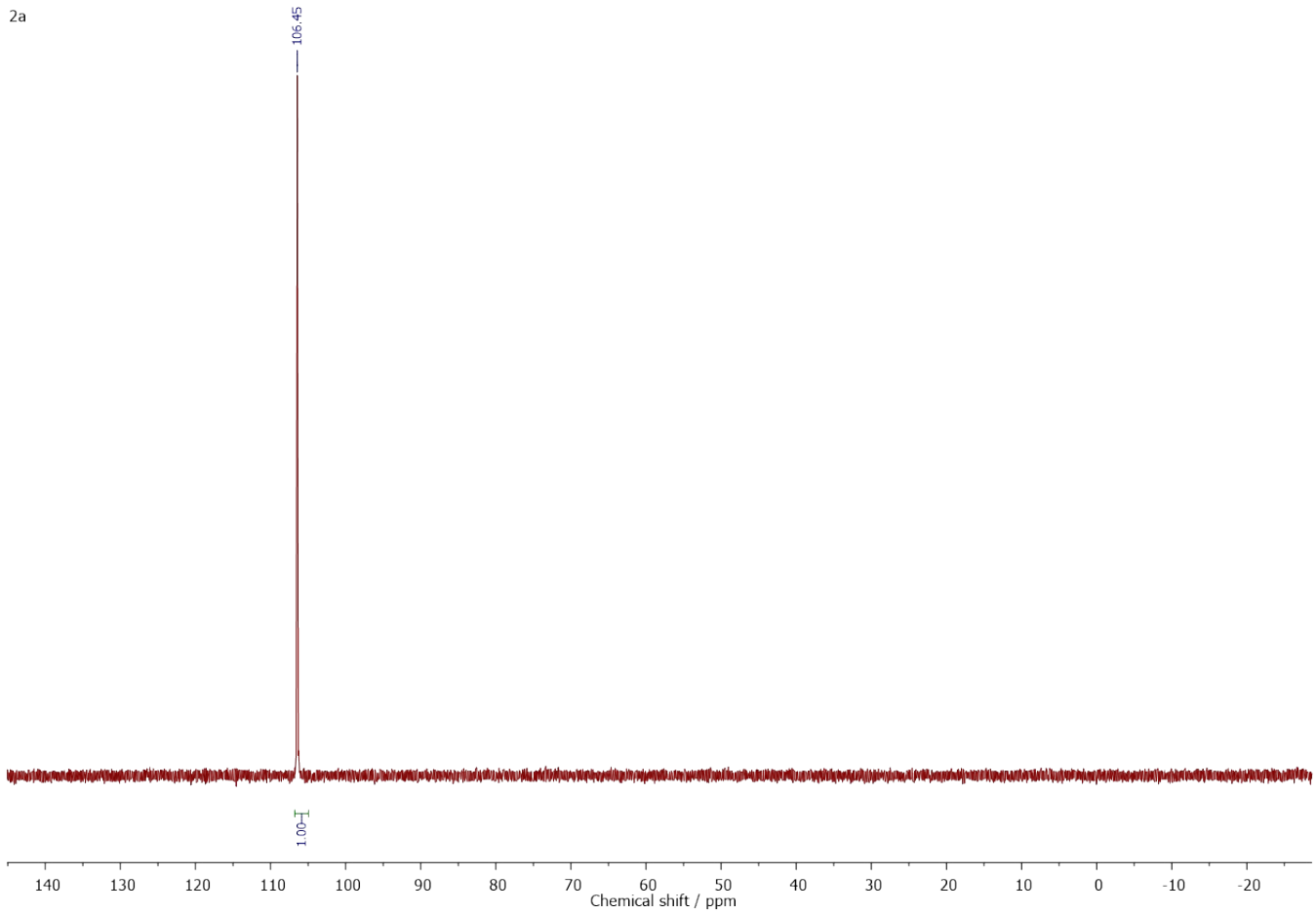

Figure S20. The ^{31}P NMR spectrum of [**2a**].

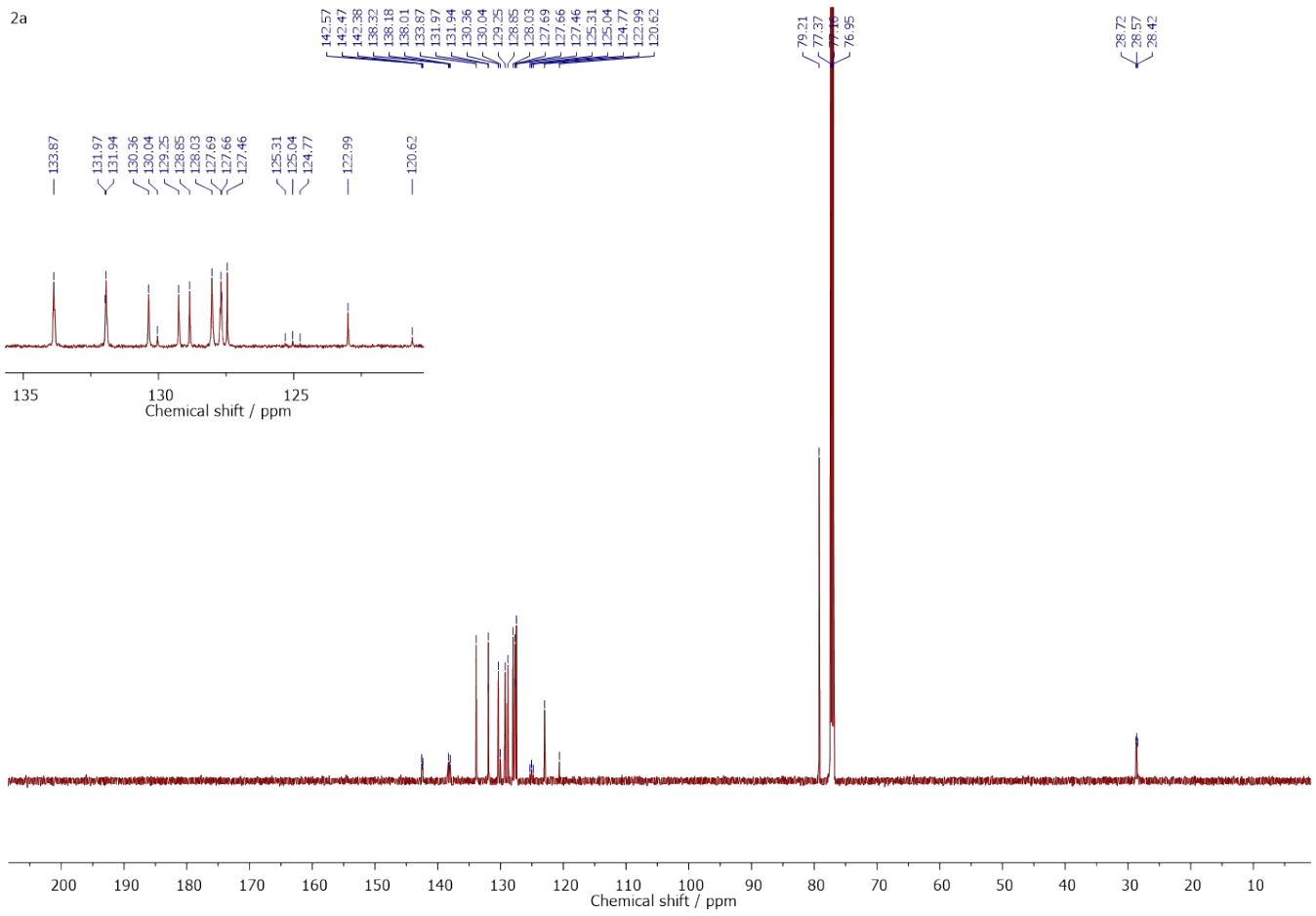

Figure S21. The $^{13}C\{^{1}H\}$ NMR spectrum of [**2a**]. The inset shows an expansion of the aromatic region for clarity.

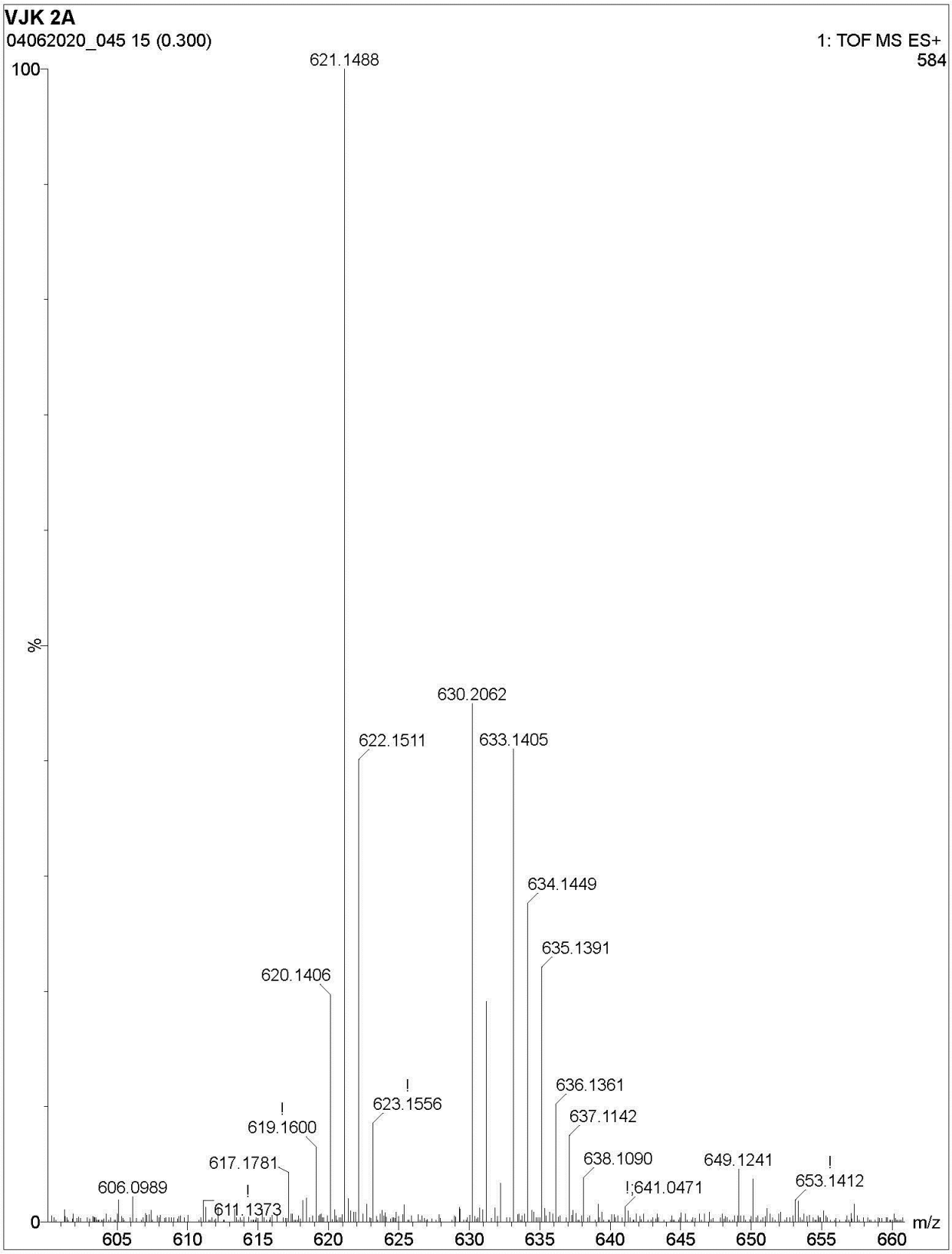

Figure S22. The ESI(+) mass spectrum of [**2a**].

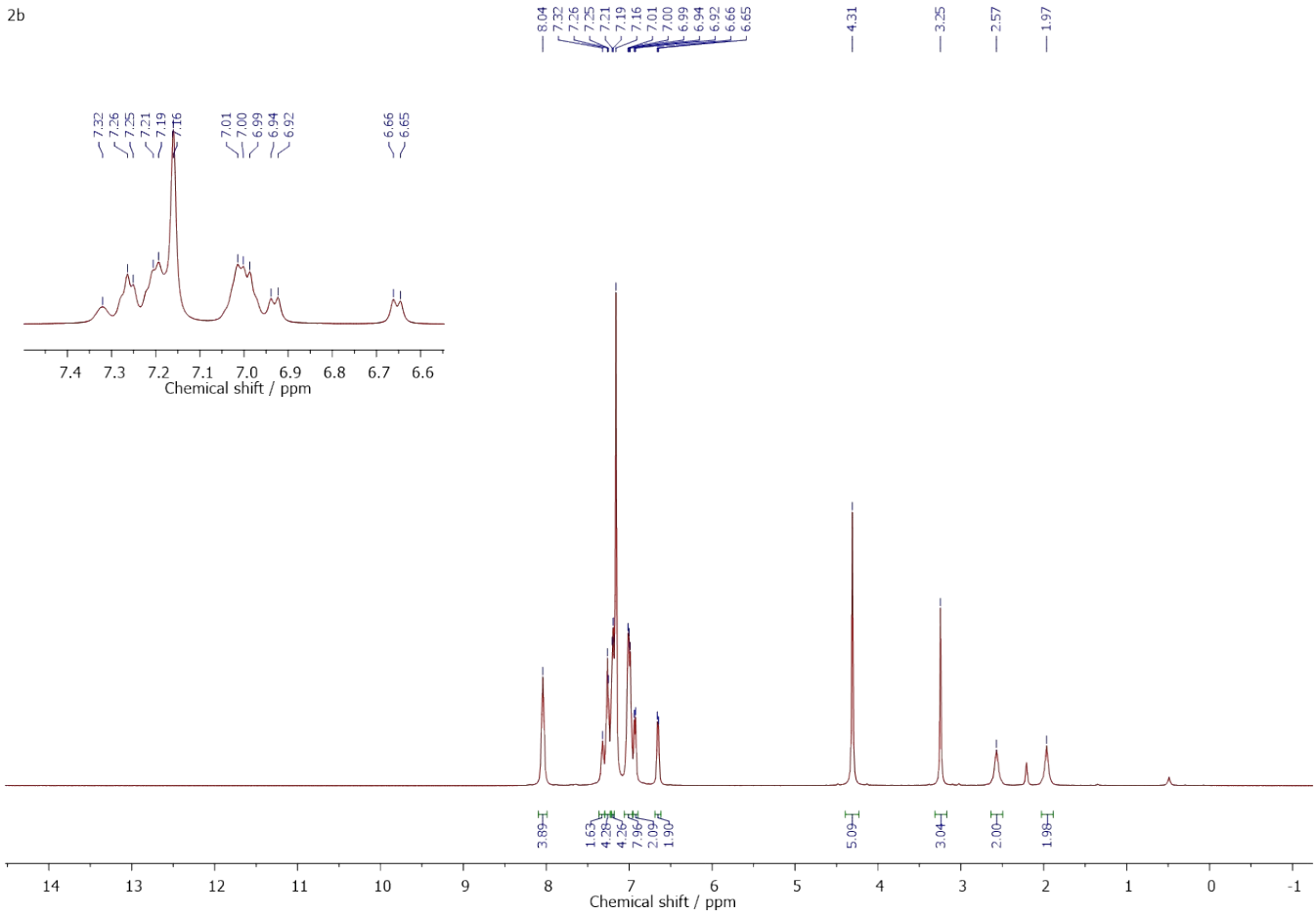

Figure S23. The ^{1}H NMR spectrum of [**2b**]. The inset shows an expansion of the aromatic region for clarity.

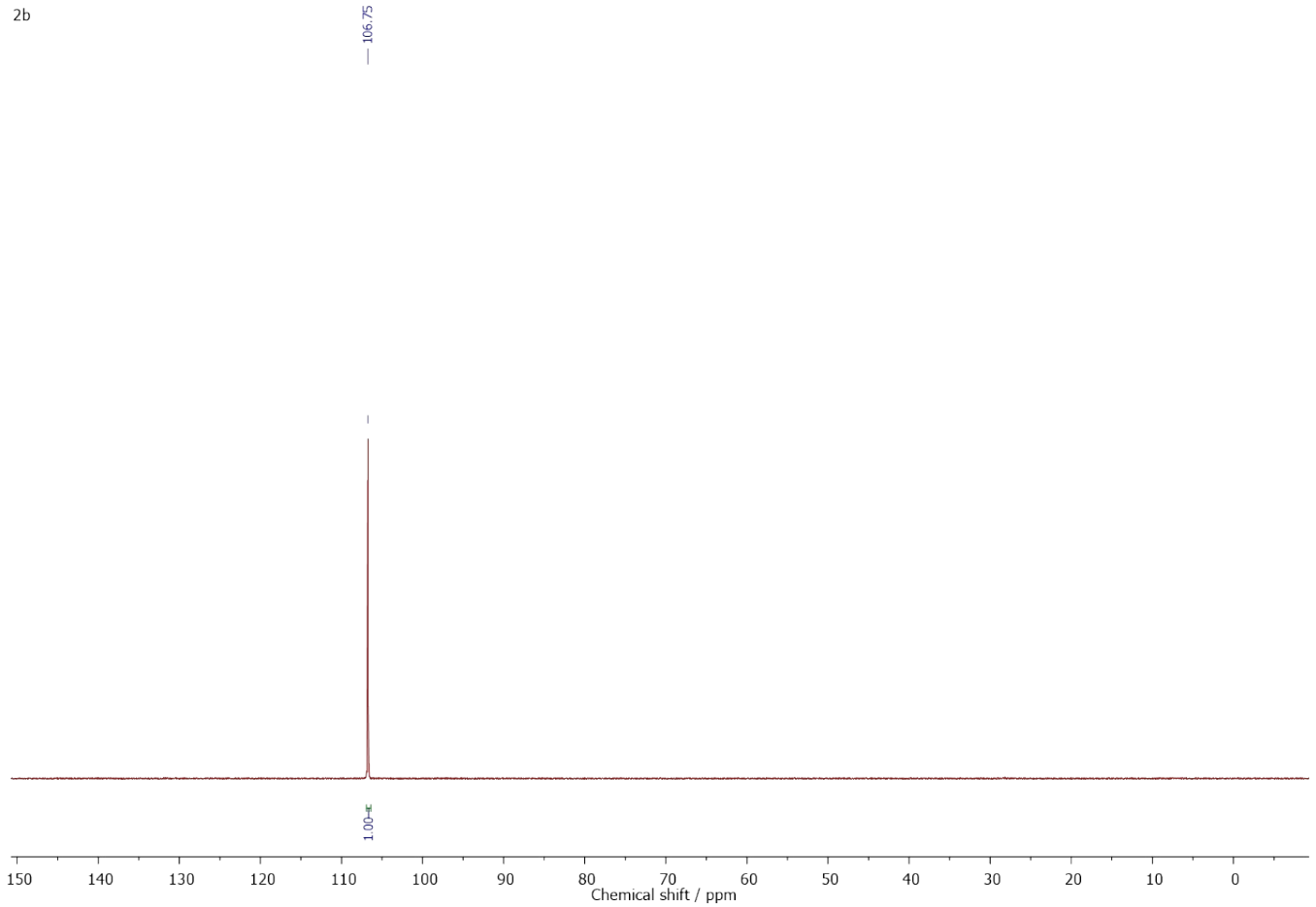

Figure S24. The ^{31}P NMR spectrum of [**2b**].

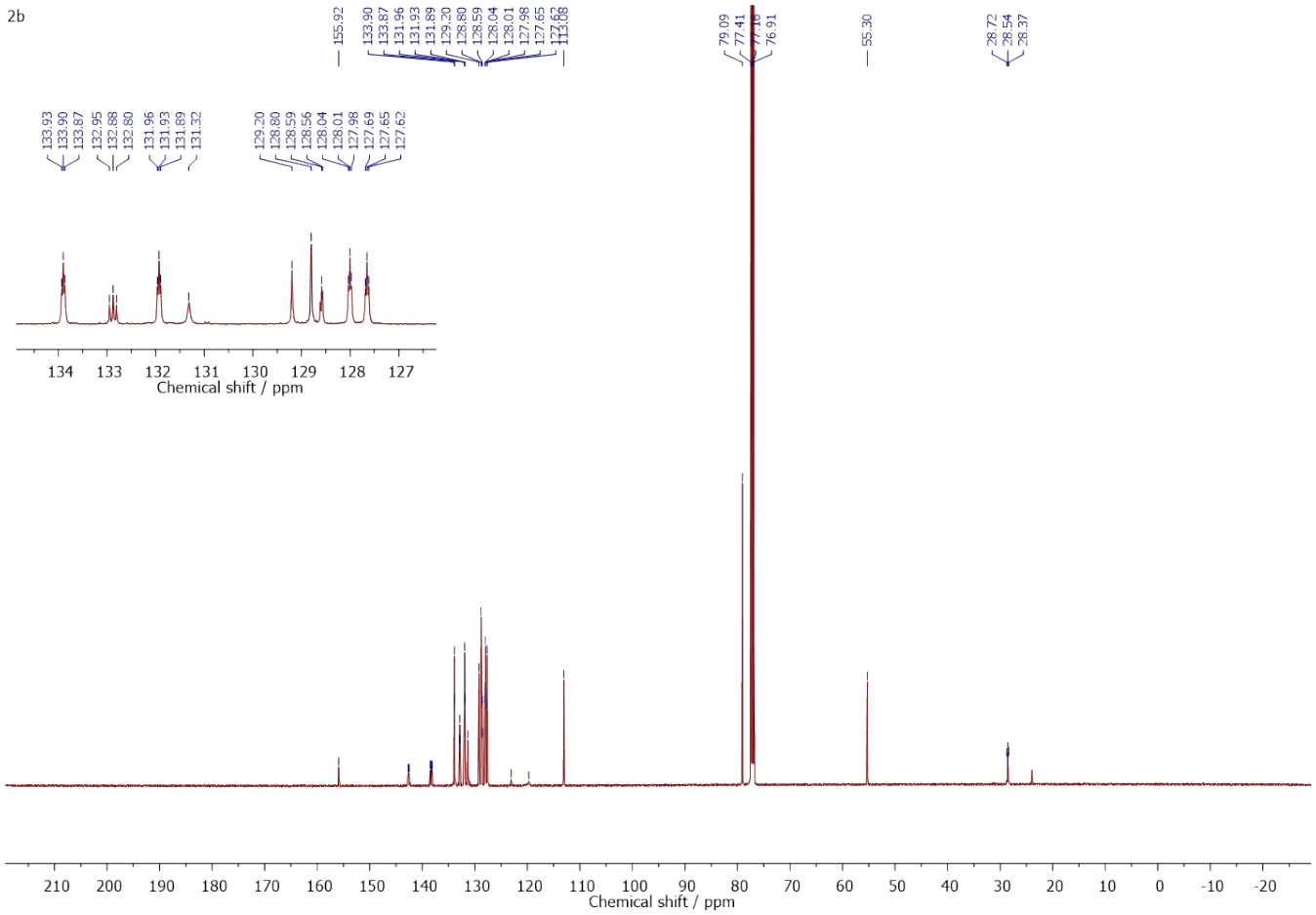

Figure S25. The $^{13}C\{^{1}H\}$ NMR spectrum of [**2b**]. The inset shows an expansion of the aromatic region for clarity.

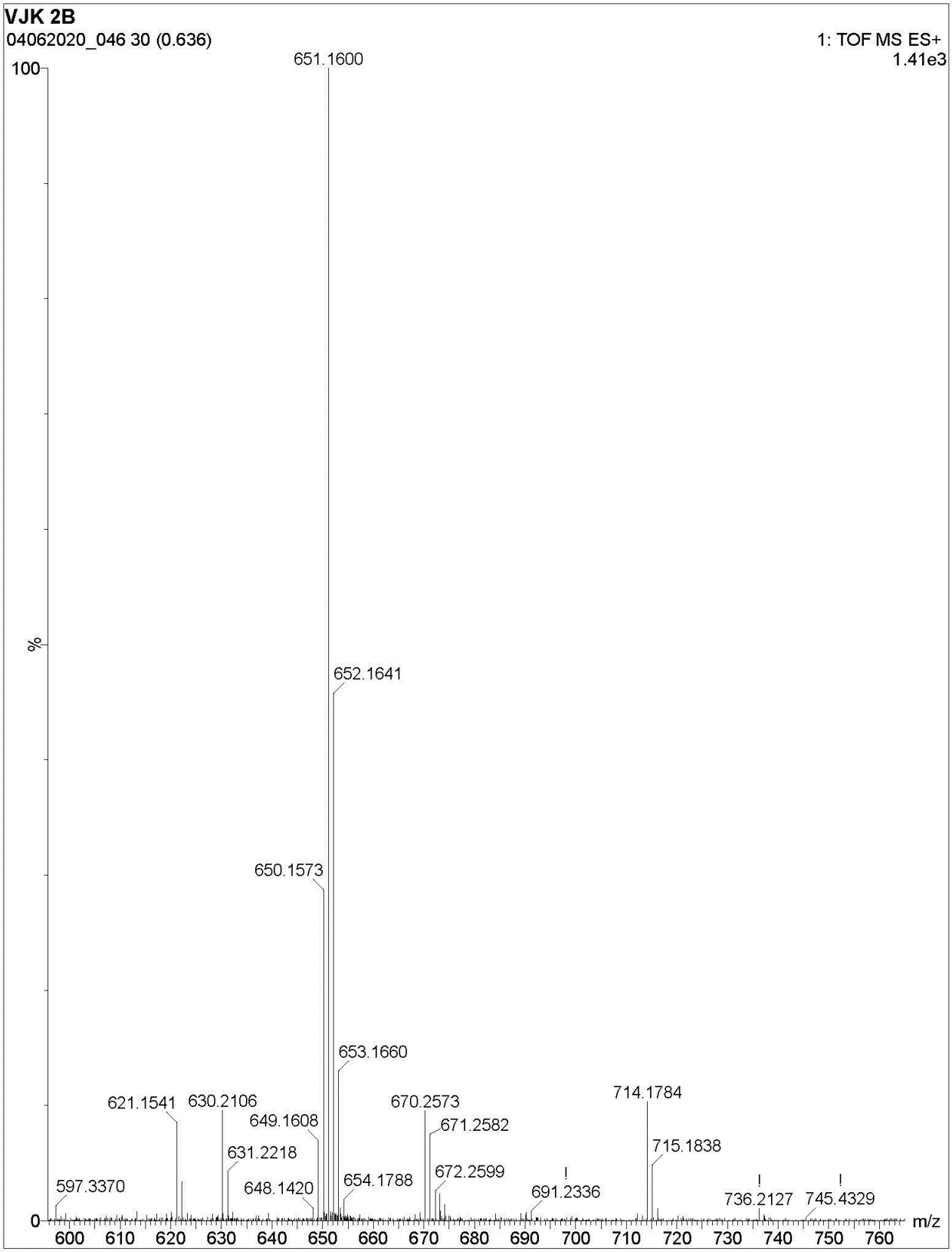

Figure S26. The ESI(+) mass spectrum of [**2b**].

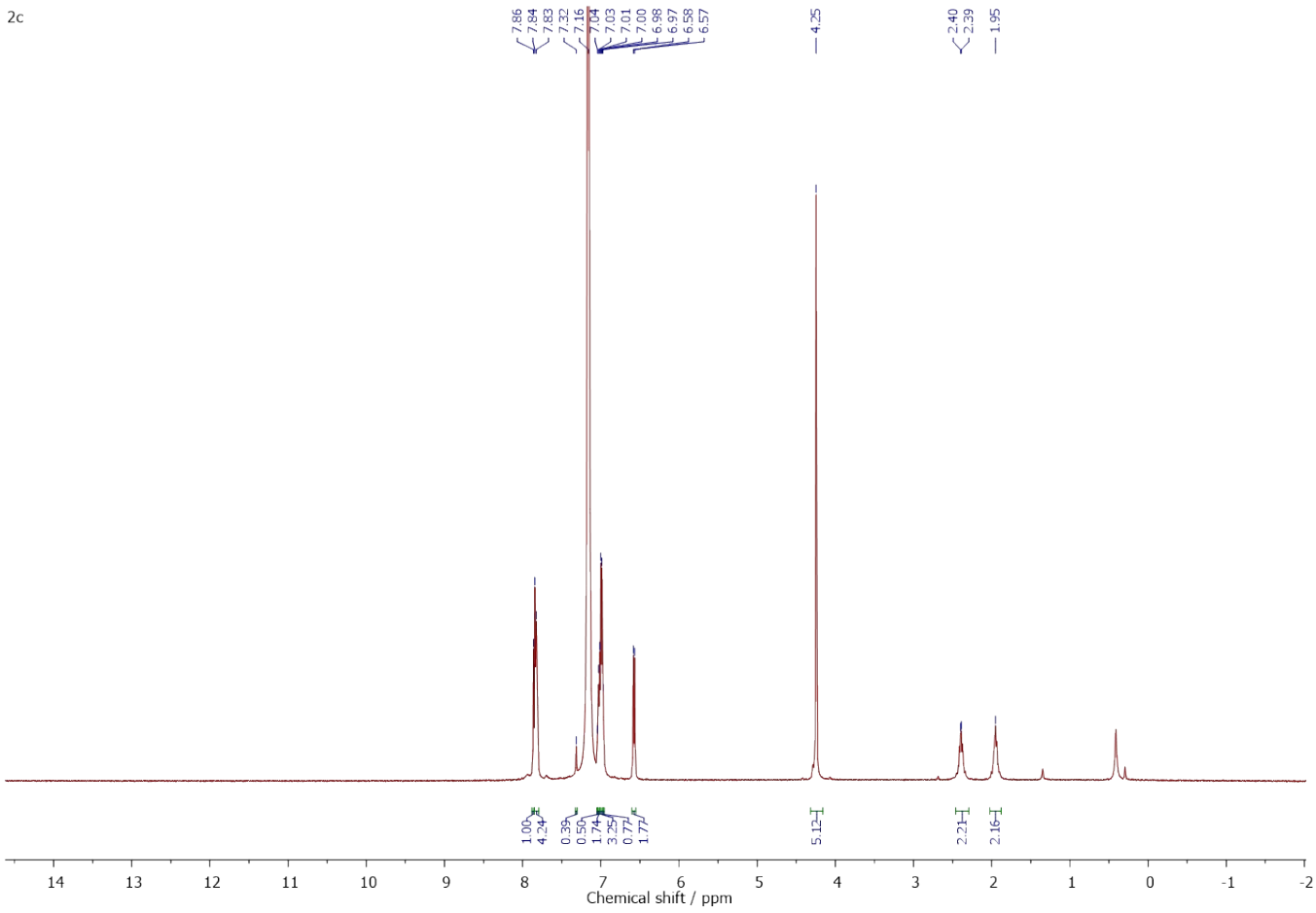

Figure S27. The ^{1}H NMR spectrum of [**2c**].

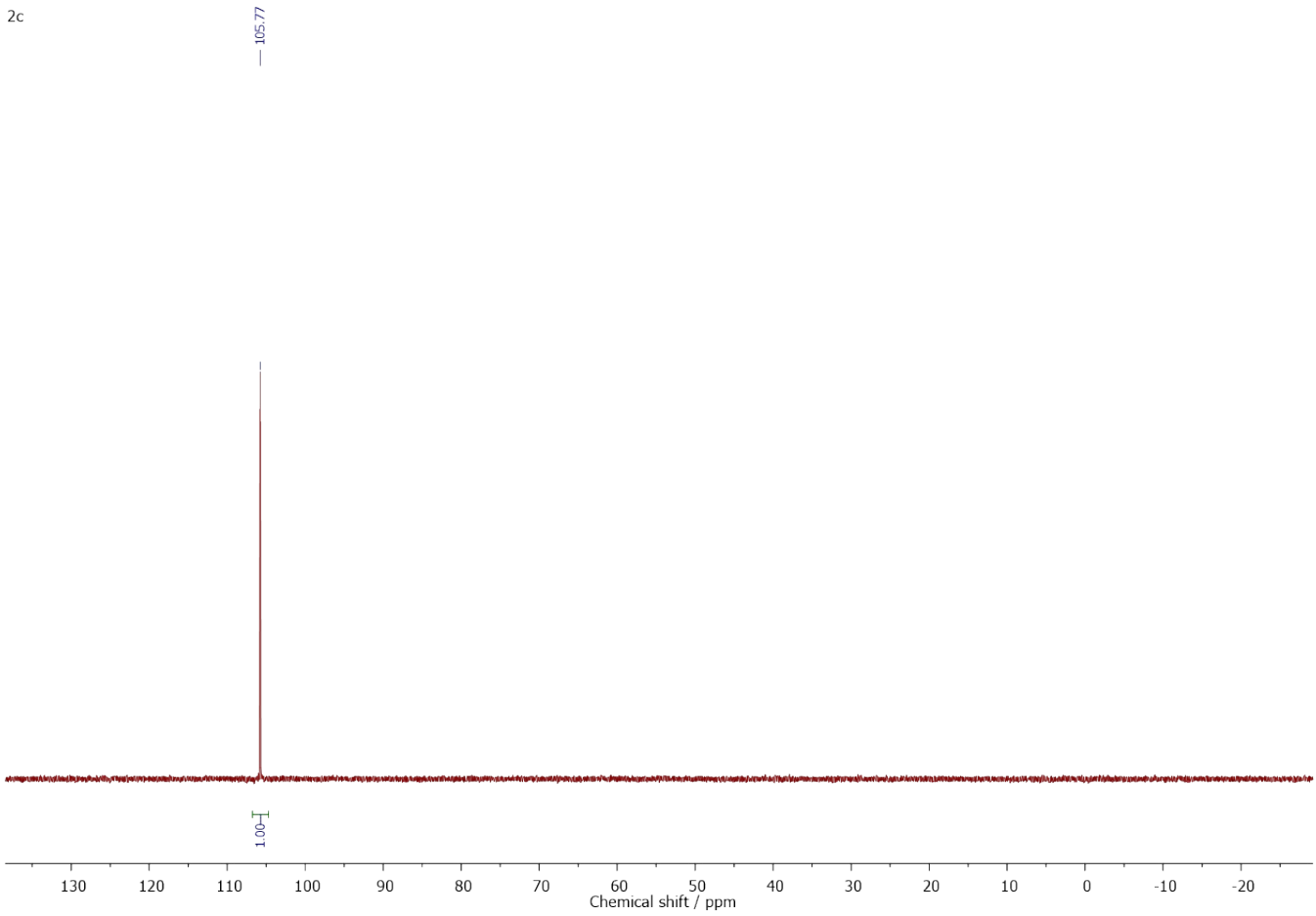

Figure S28. The ^{31}P NMR spectrum of [**2c**].

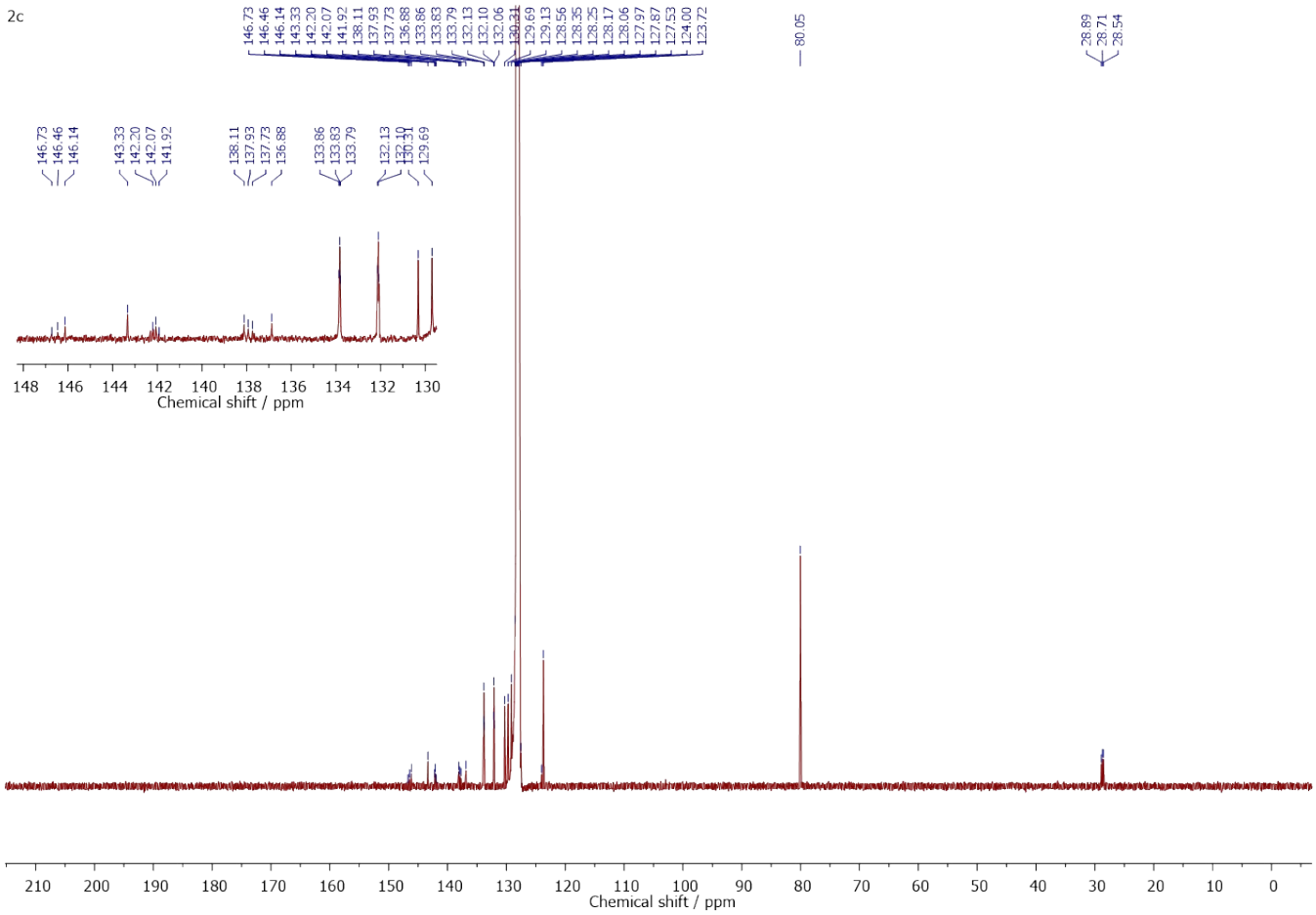

Figure S29. The $^{13}C\{^{1}H\}$ NMR spectrum of [**2c**]. The inset shows an expansion of the aromatic region for clarity.

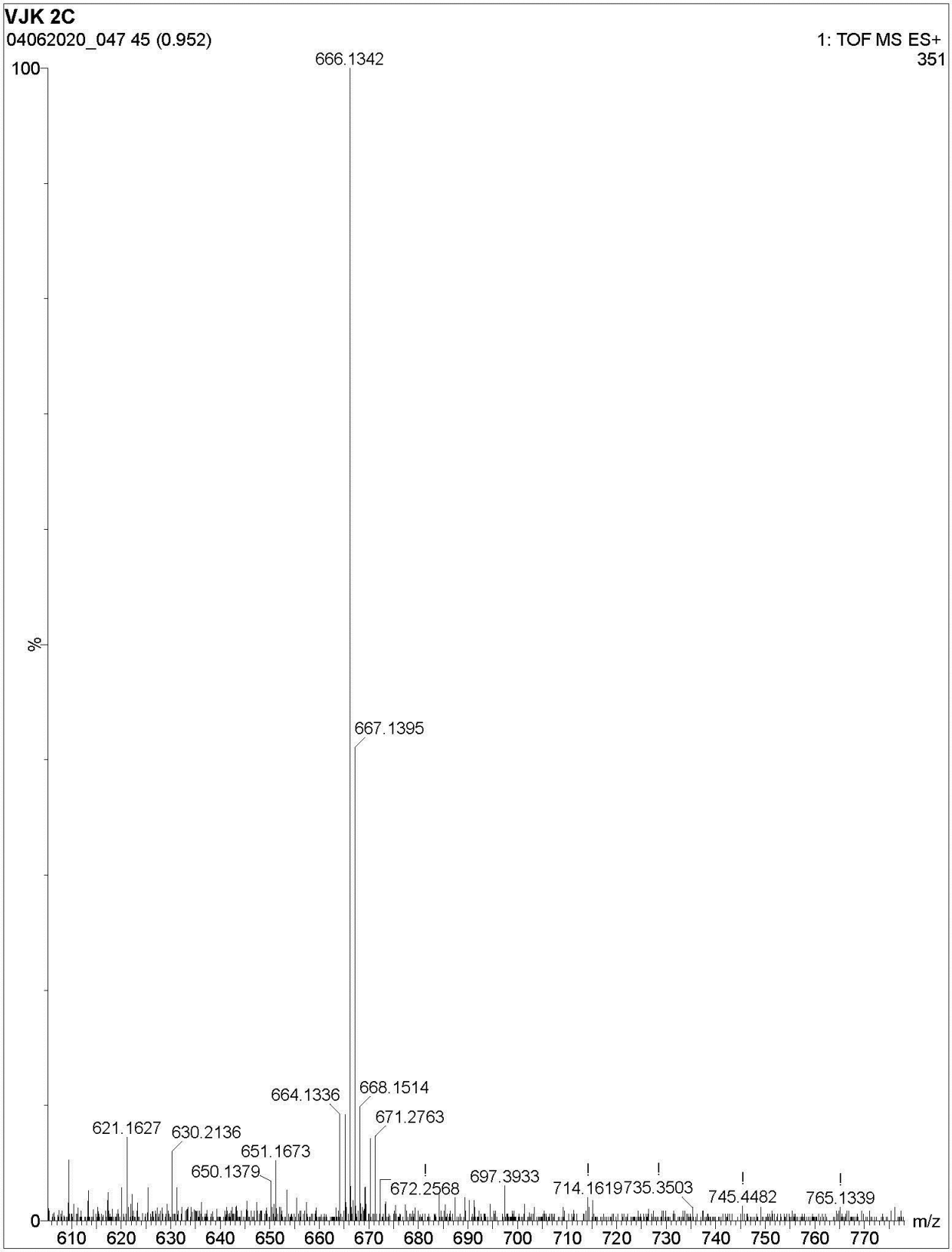

Figure S30. The ESI(+) mass spectrum of [**2c**].

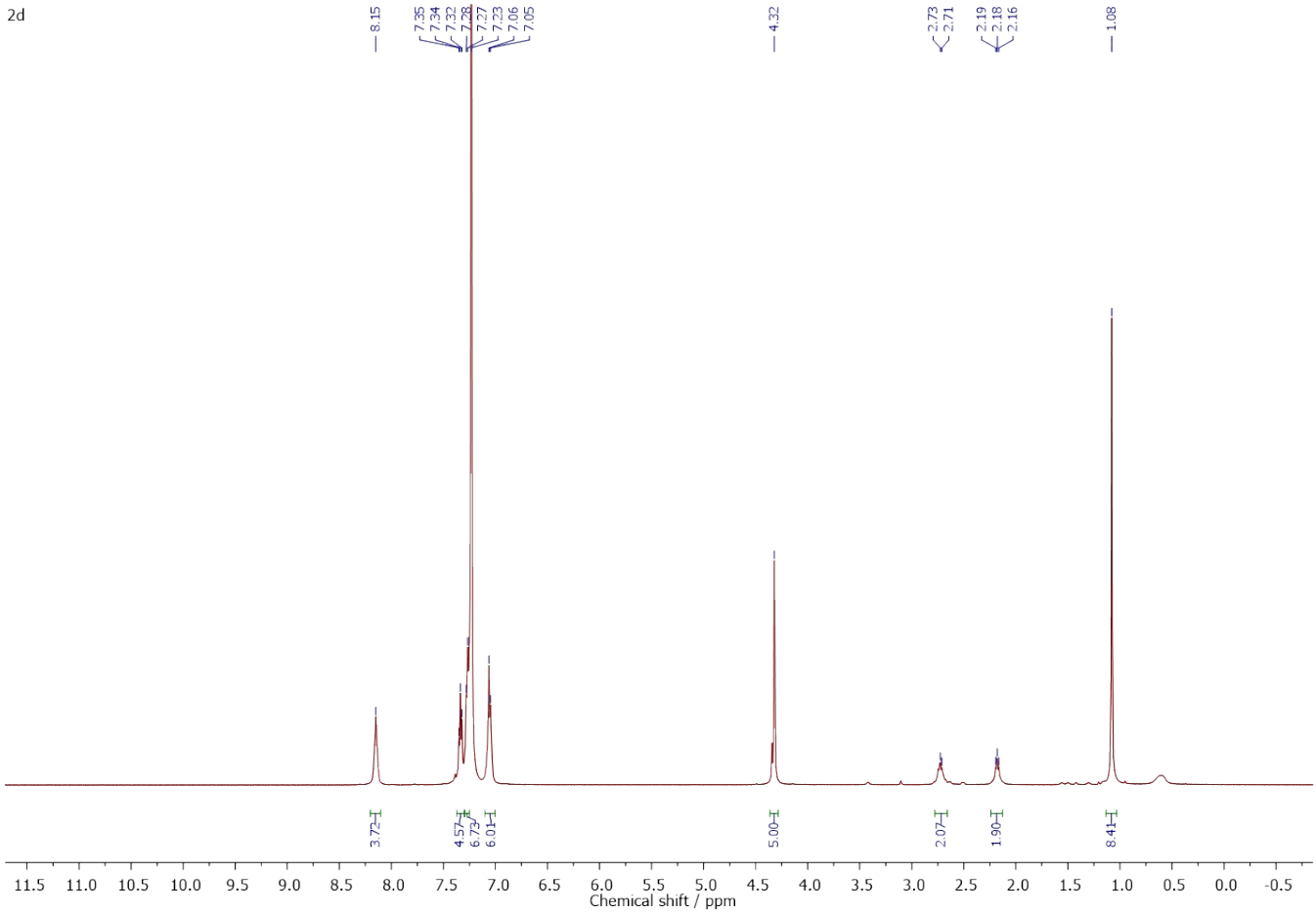

Figure S31. The ^{1}H NMR spectrum of [**2d**].

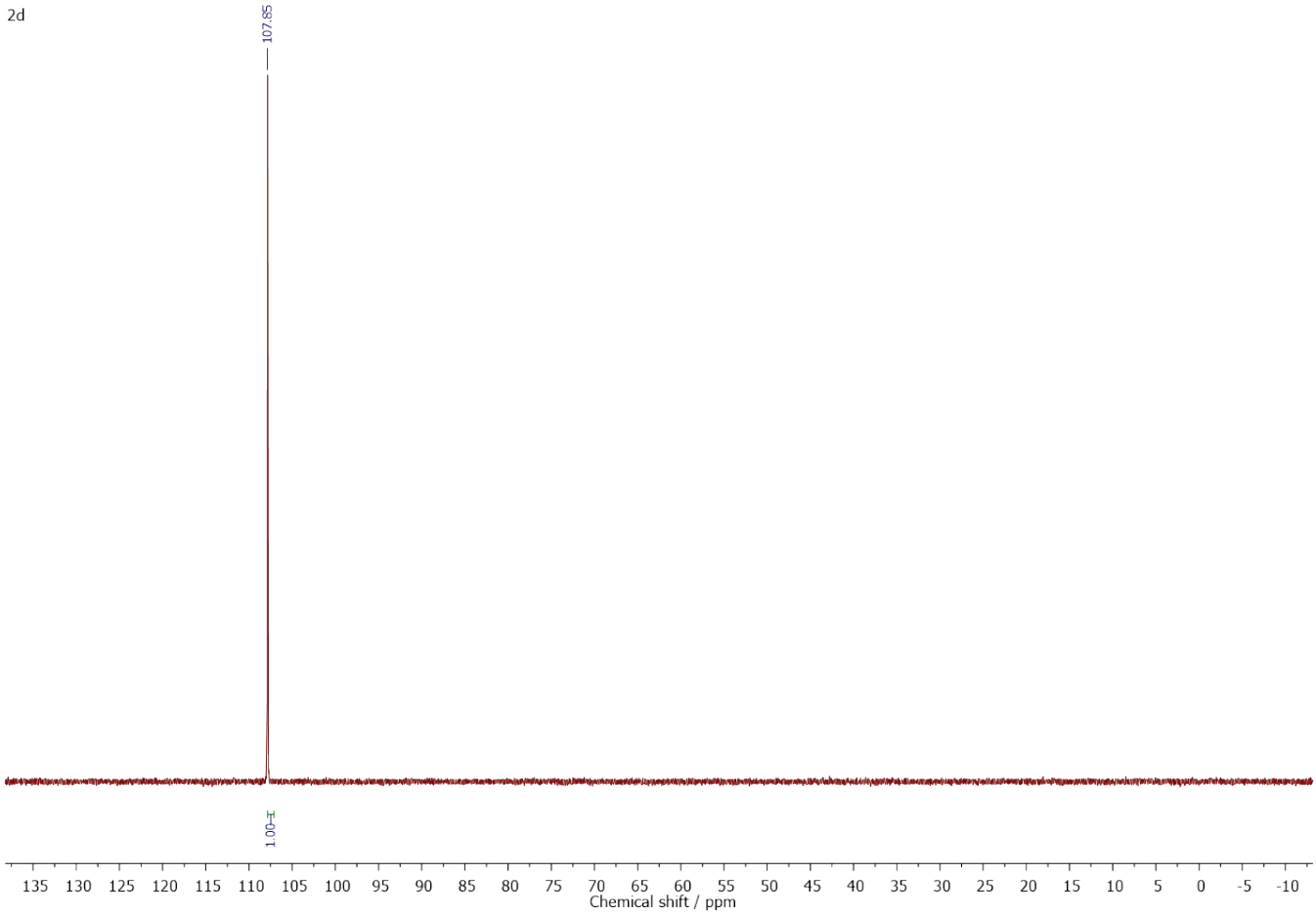

Figure S32. The ^{31}P NMR spectrum of [**2d**].

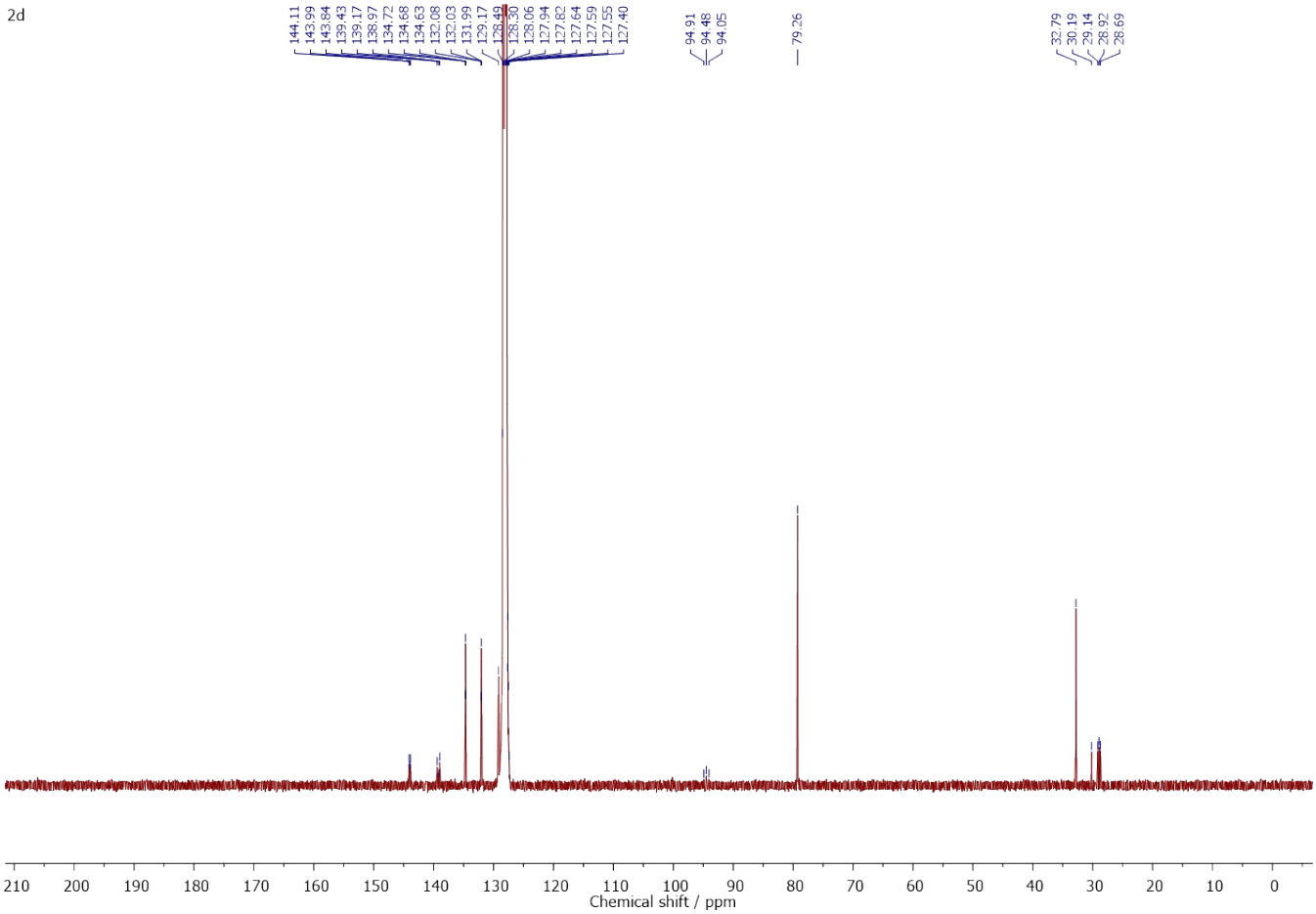

Figure S33. The $^{13}C\{^{1}H\}$ NMR spectrum of [**2d**].

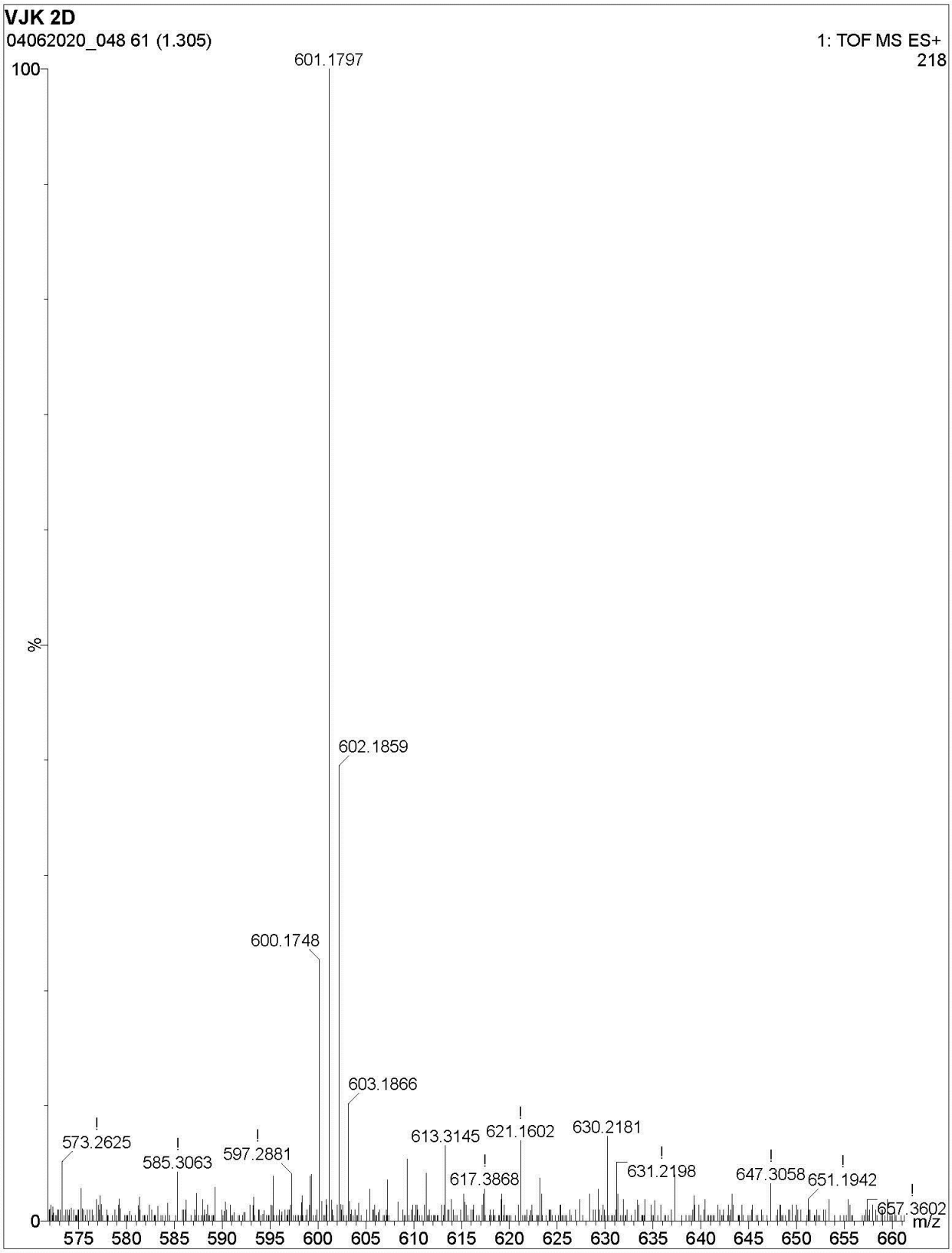

Figure S34. The ESI(+) mass spectrum of [**2d**].

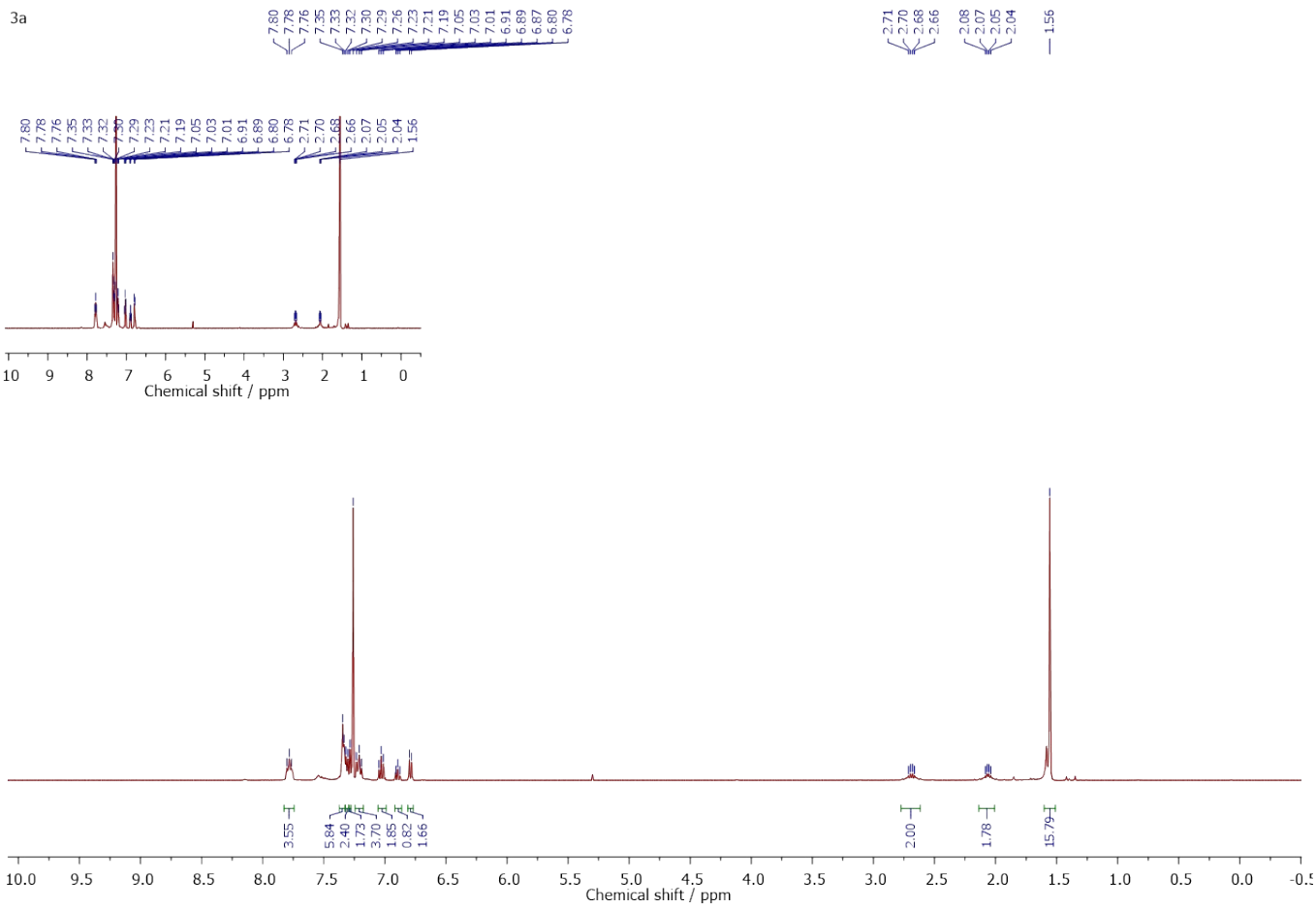

Figure S35. The ^{1}H NMR spectrum of [**3a**]. The inset shows an expansion of the aromatic region for clarity.

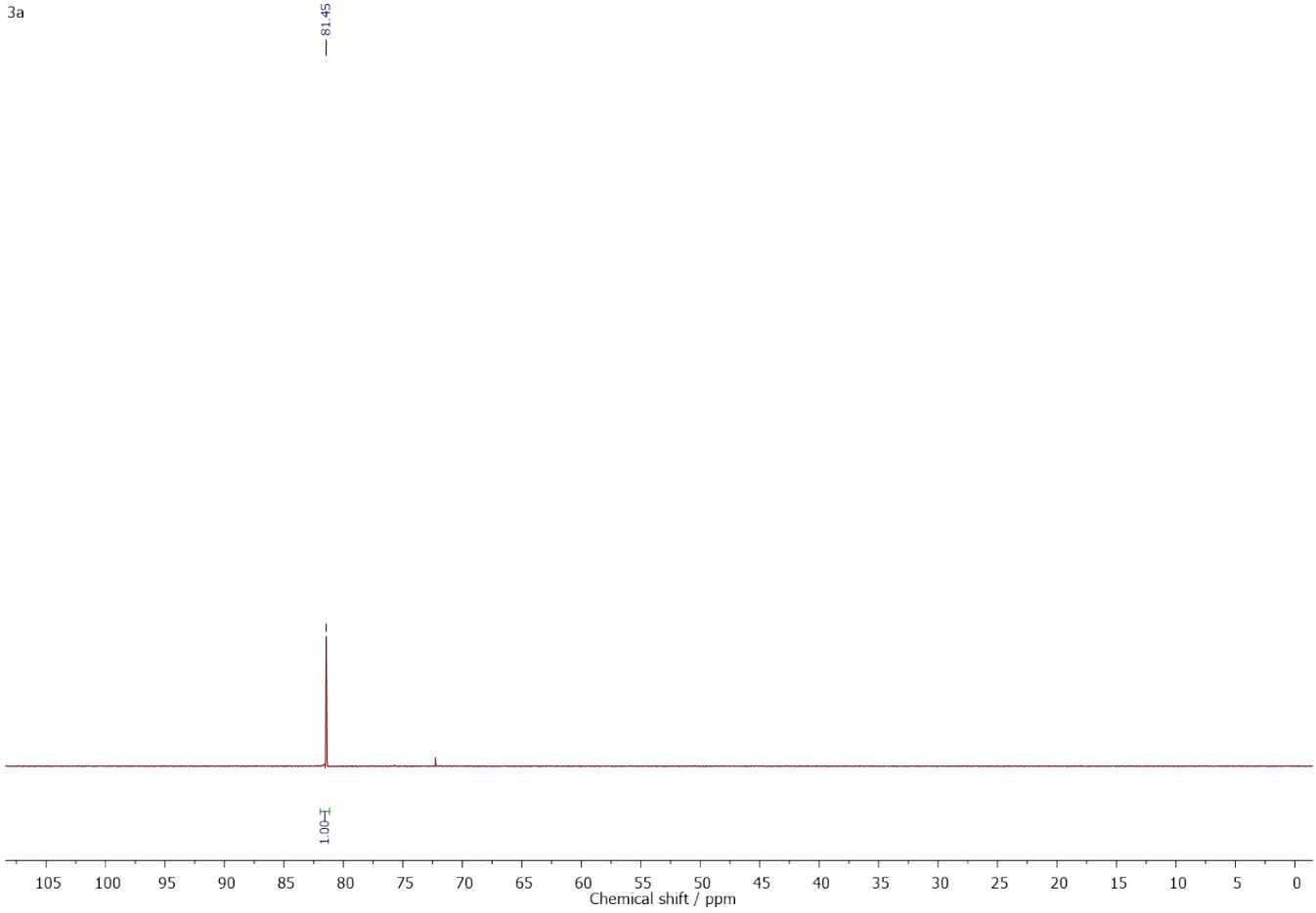

Figure S36. The ^{31}P NMR spectrum of [**3a**].

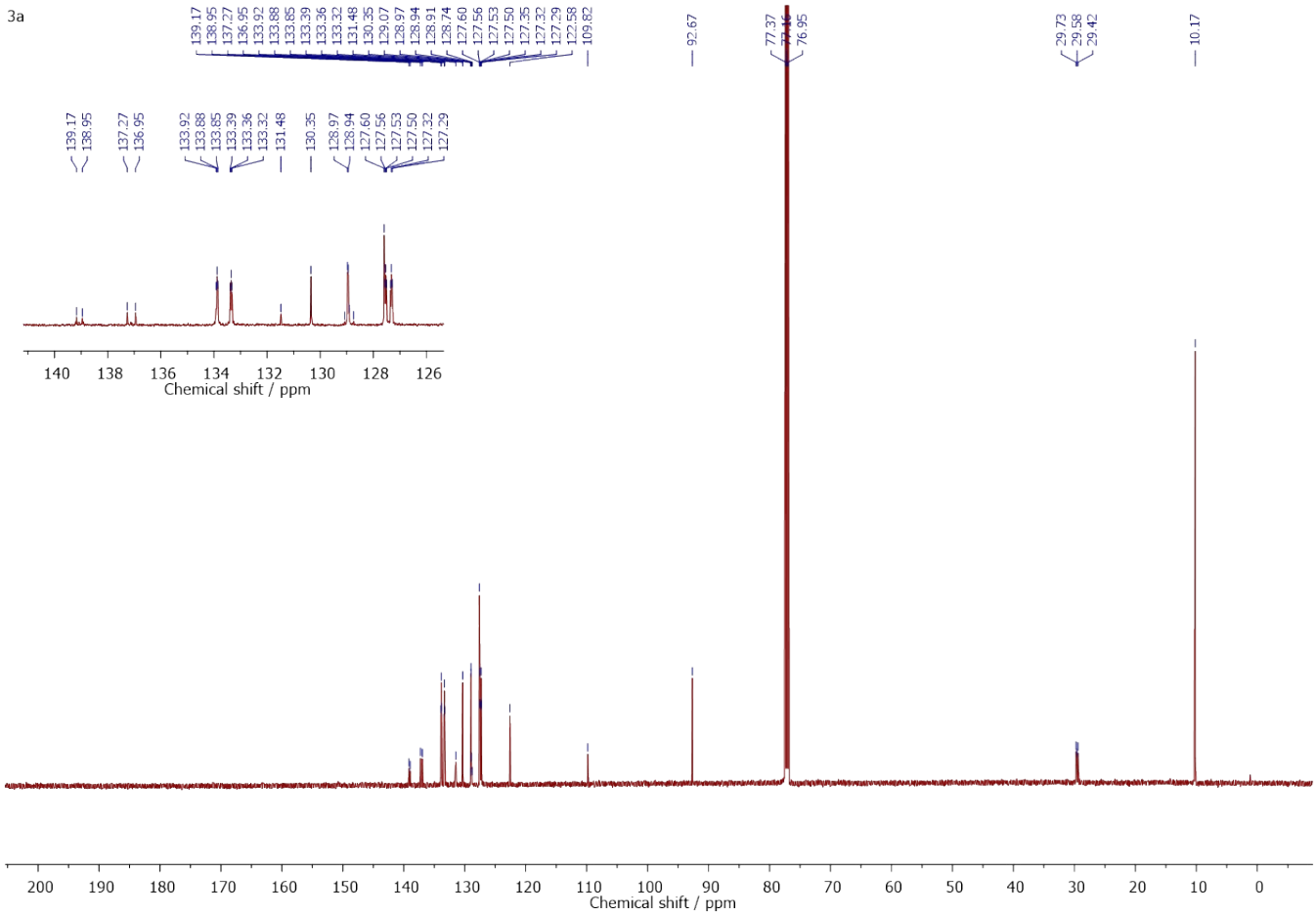

Figure S37. The $^{13}C\{^{1}H\}$ NMR spectrum of [**3a**]. The inset shows an expansion of the aromatic region for clarity.

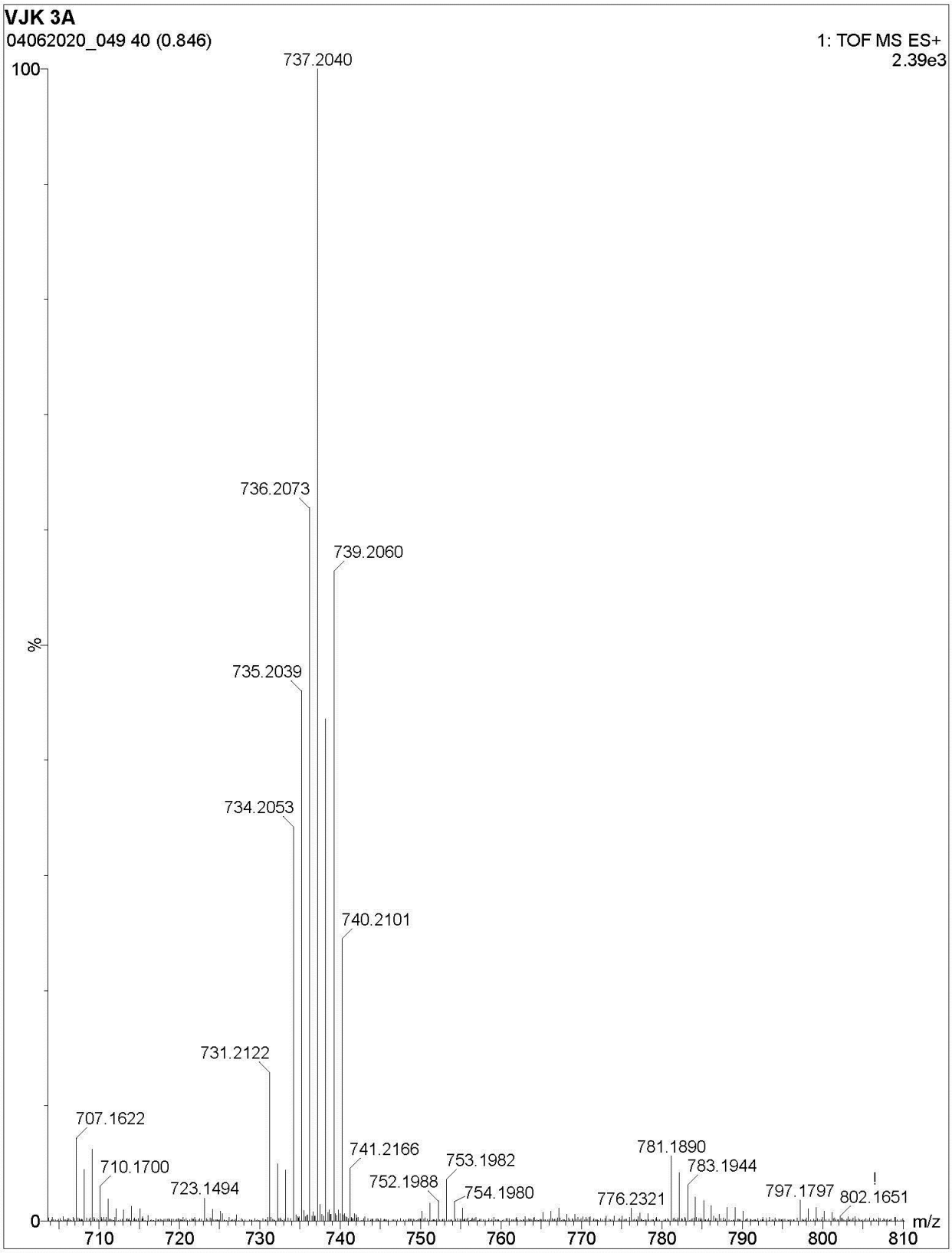

Figure S38. The ESI(+) mass spectrum of [**3a**].

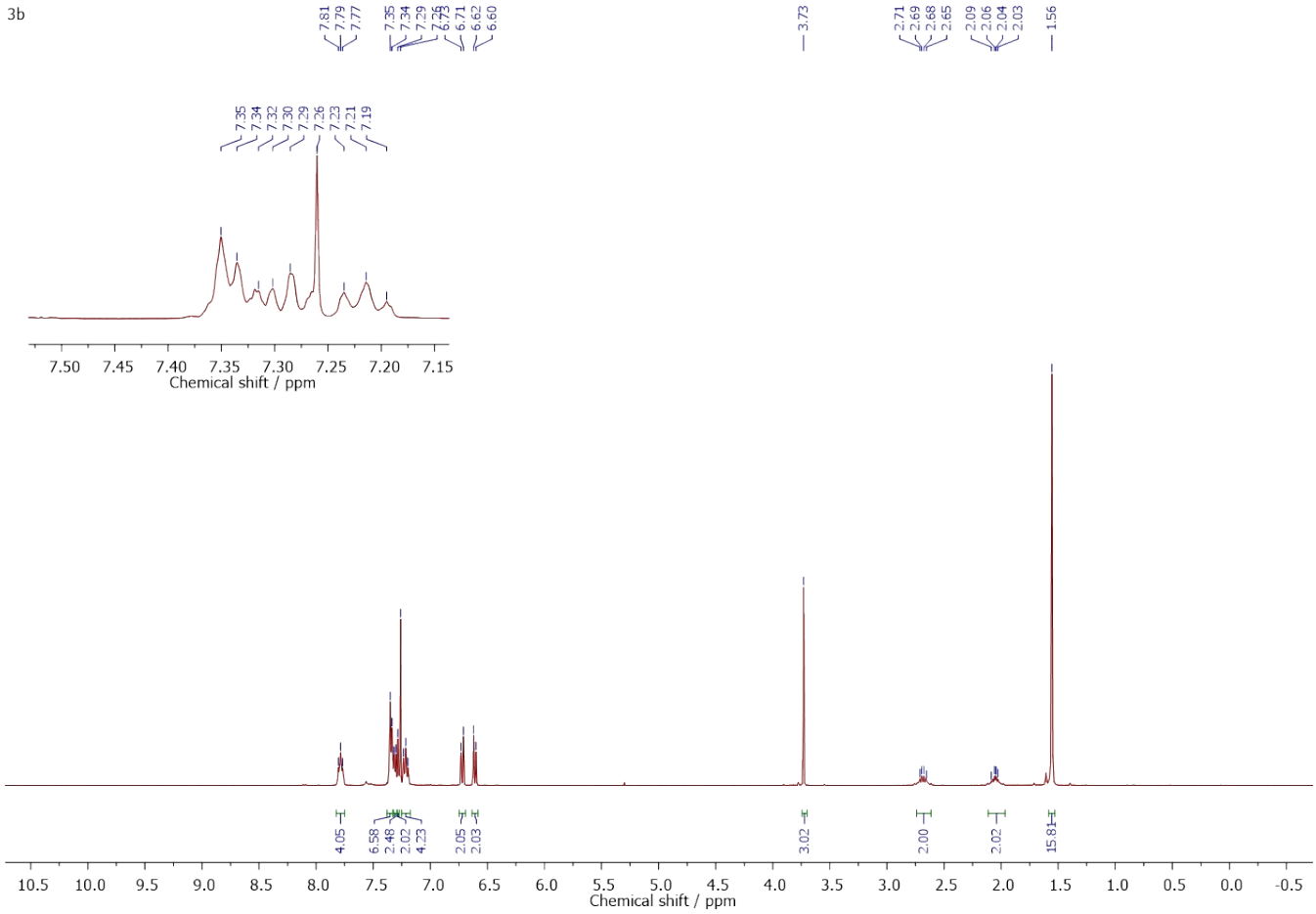

Figure S39. The ^{1}H NMR spectrum of [**3b**]. The inset shows an expansion of the aromatic region for clarity.

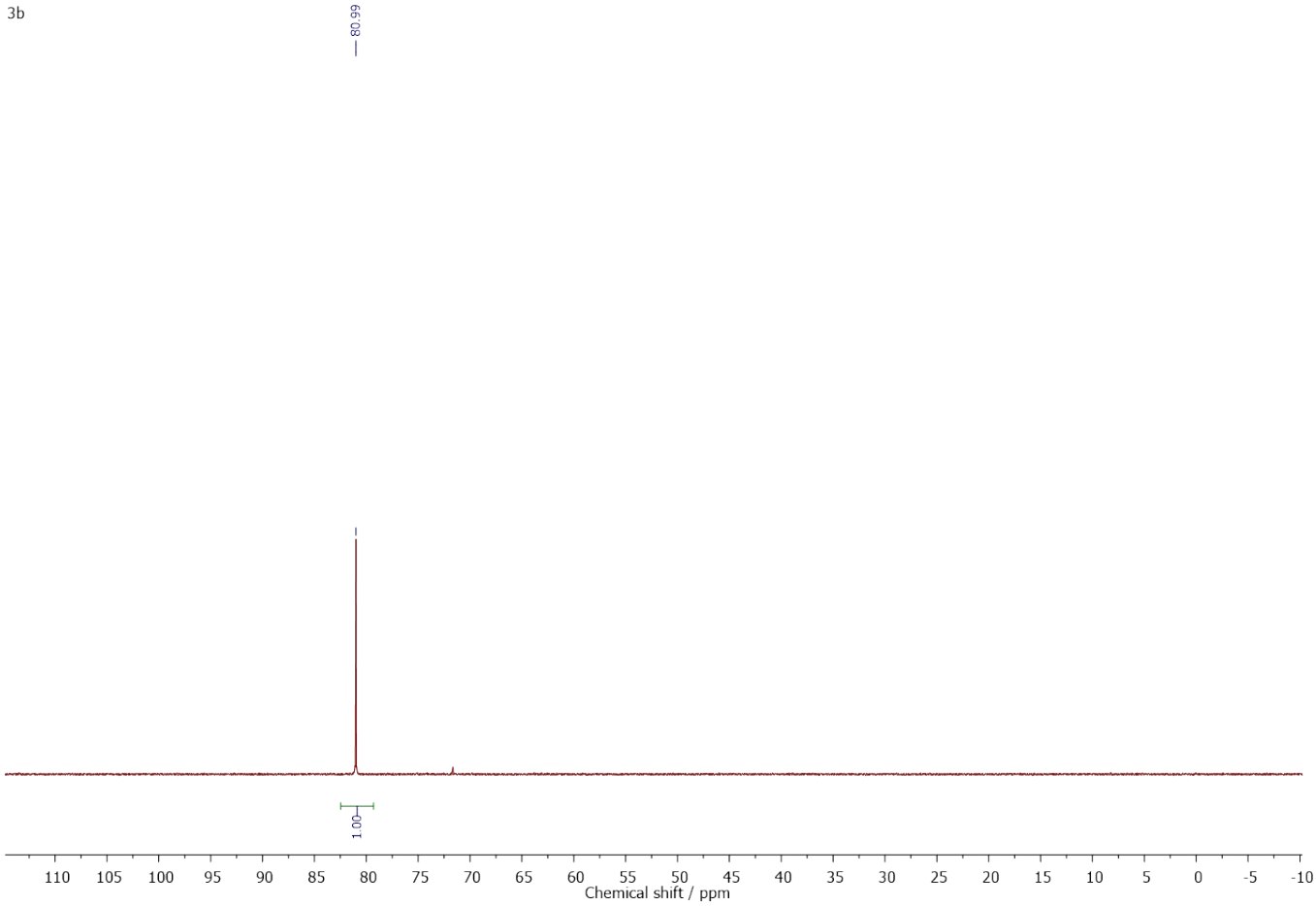

Figure S40. The ^{31}P NMR spectrum of [**3b**].

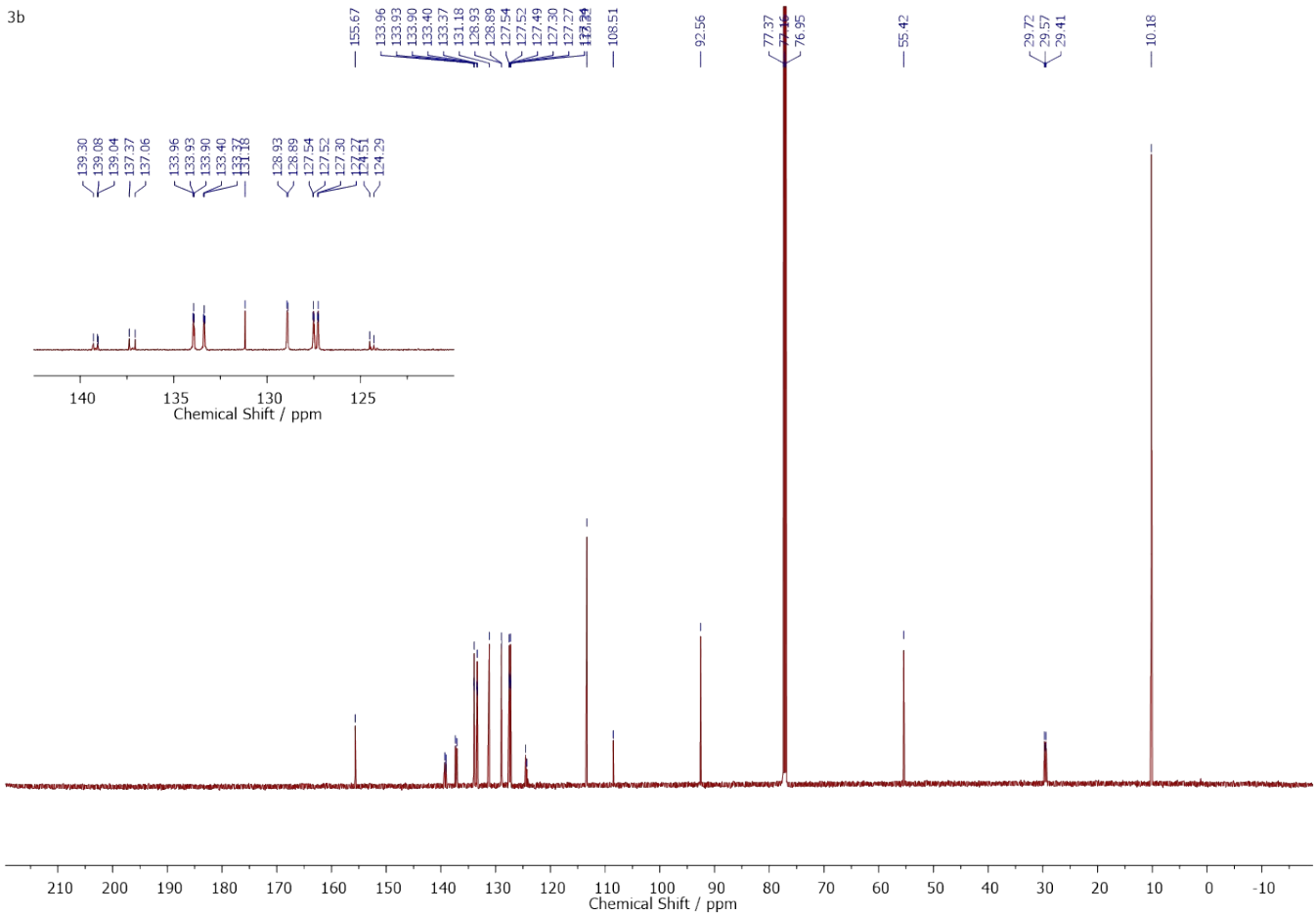

Figure S41. The $^{13}C\{^{1}H\}$ NMR spectrum of [**3b**]. The inset shows an expansion of the aromatic region for clarity.

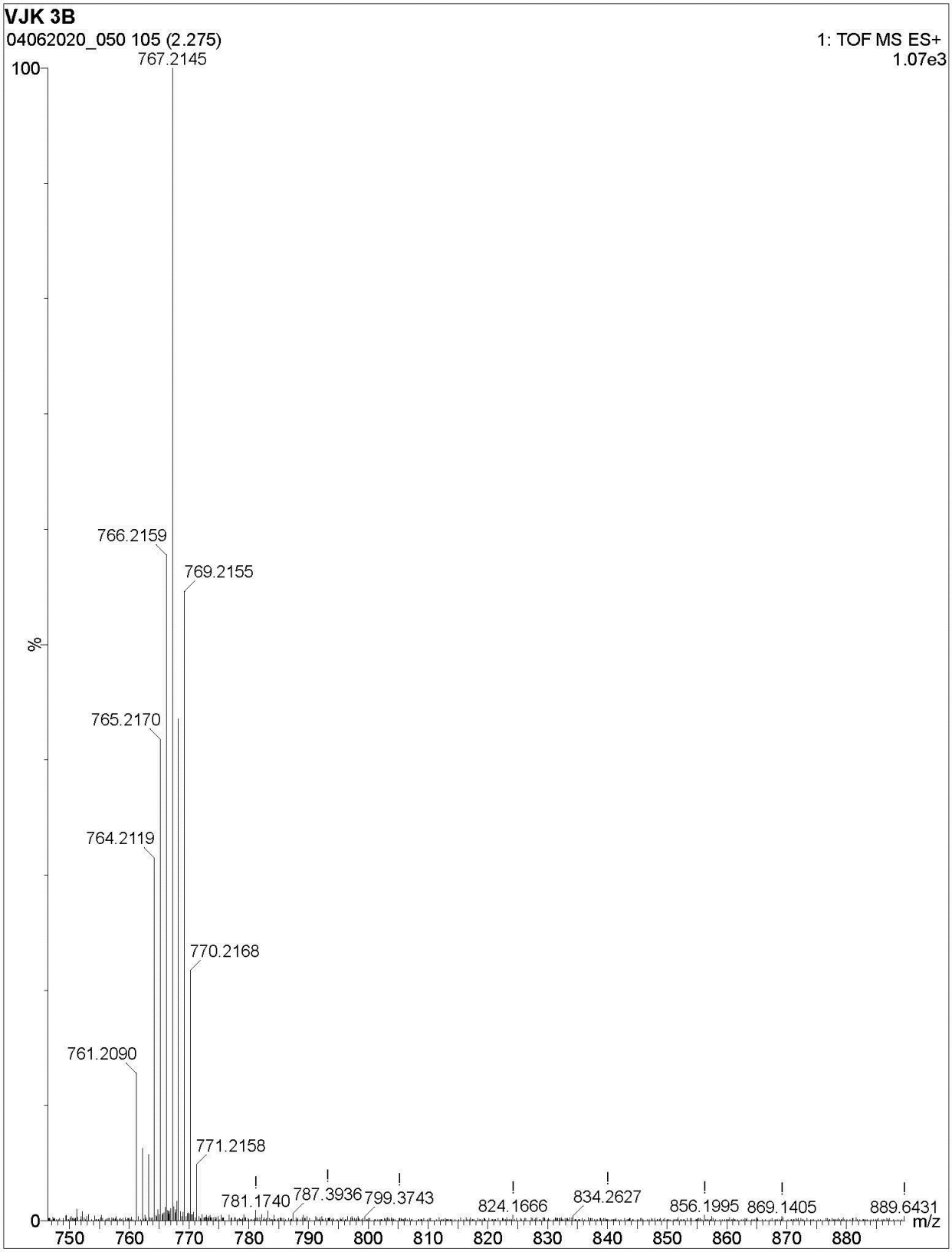

Figure S42. The ESI(+) mass spectrum of [**3b**].

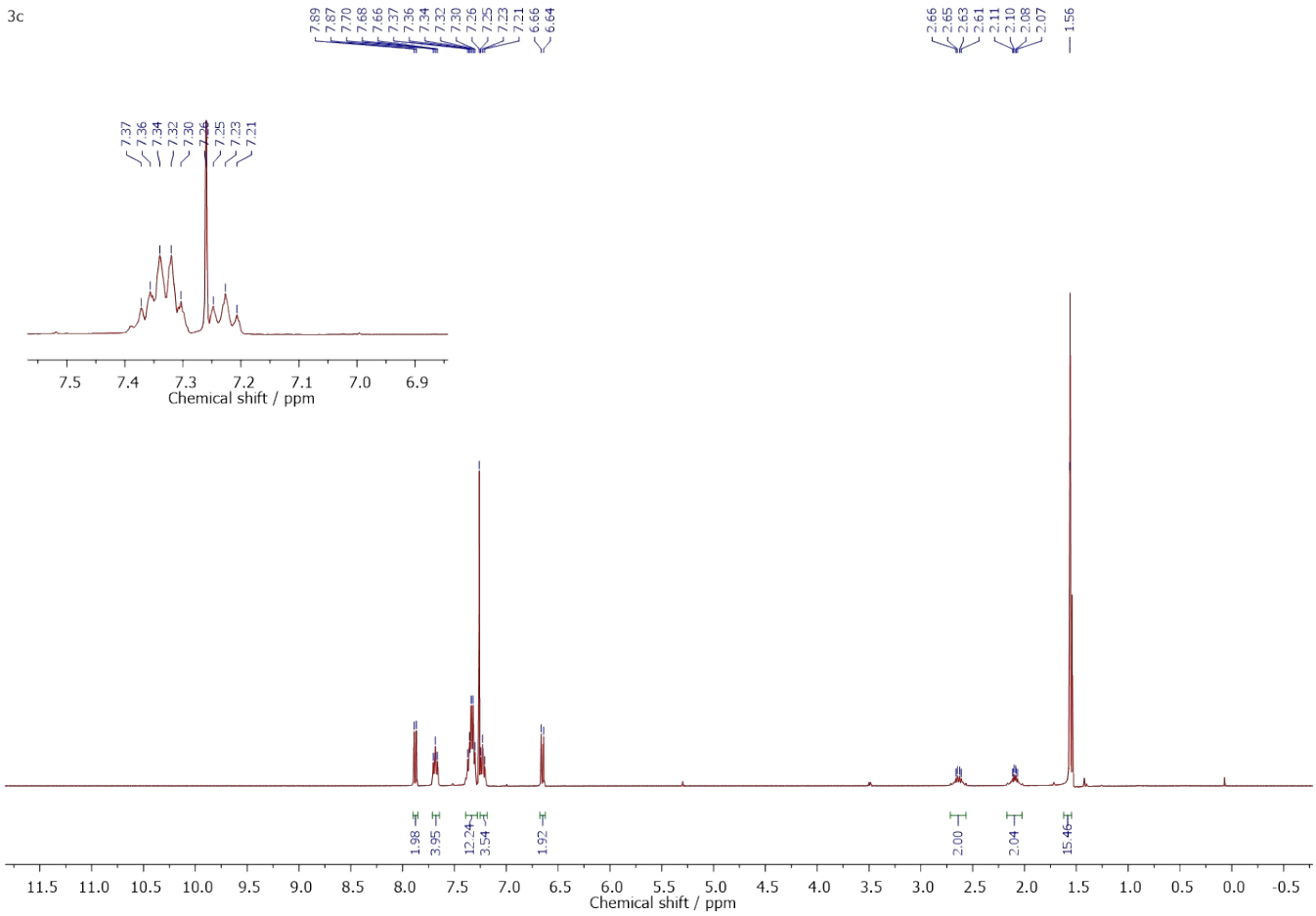

Figure S43. The ^{1}H NMR spectrum of [**3c**]. The inset shows an expansion of the aromatic region for clarity.

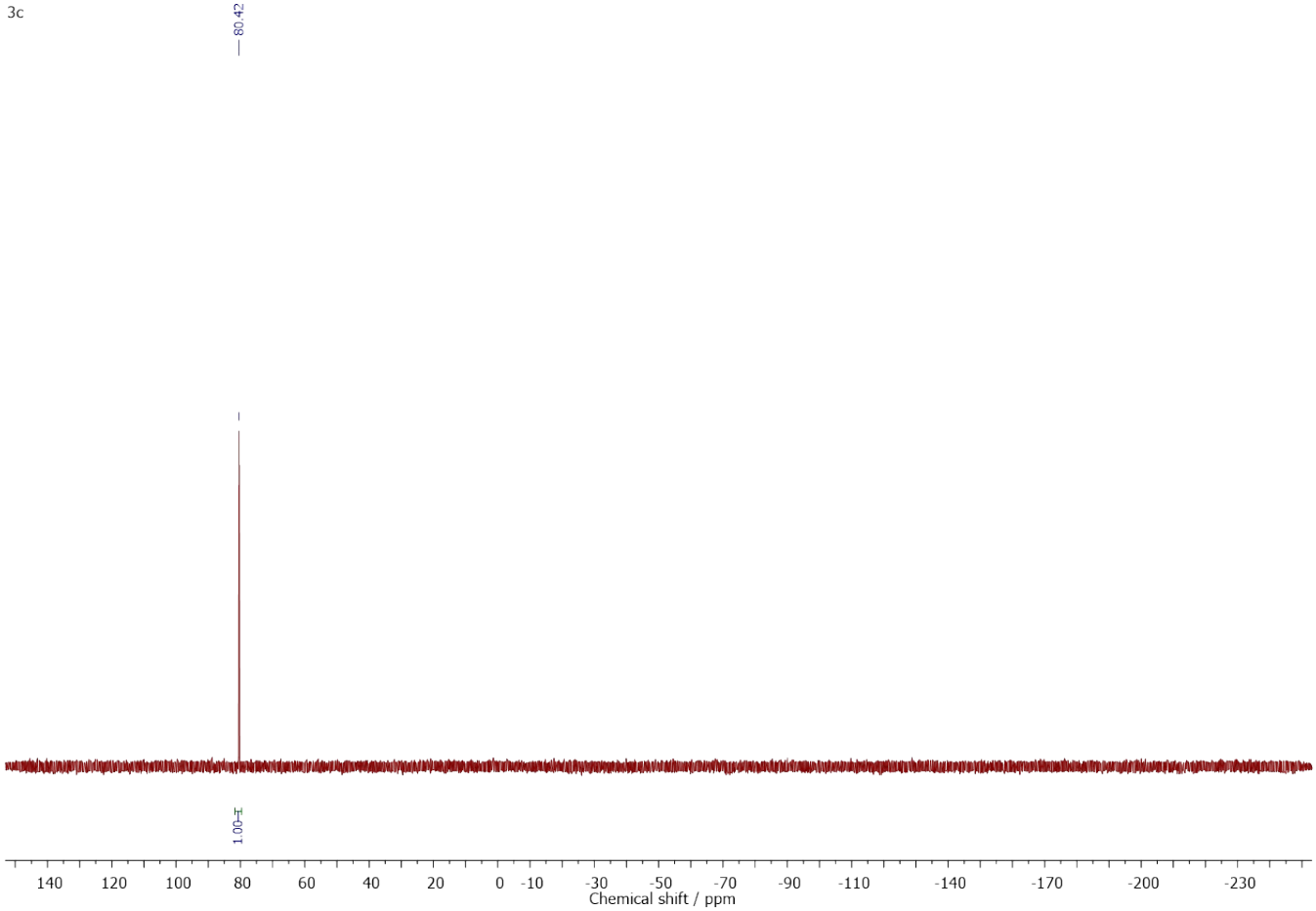

Figure S44. The ^{31}P NMR spectrum of [**3c**].

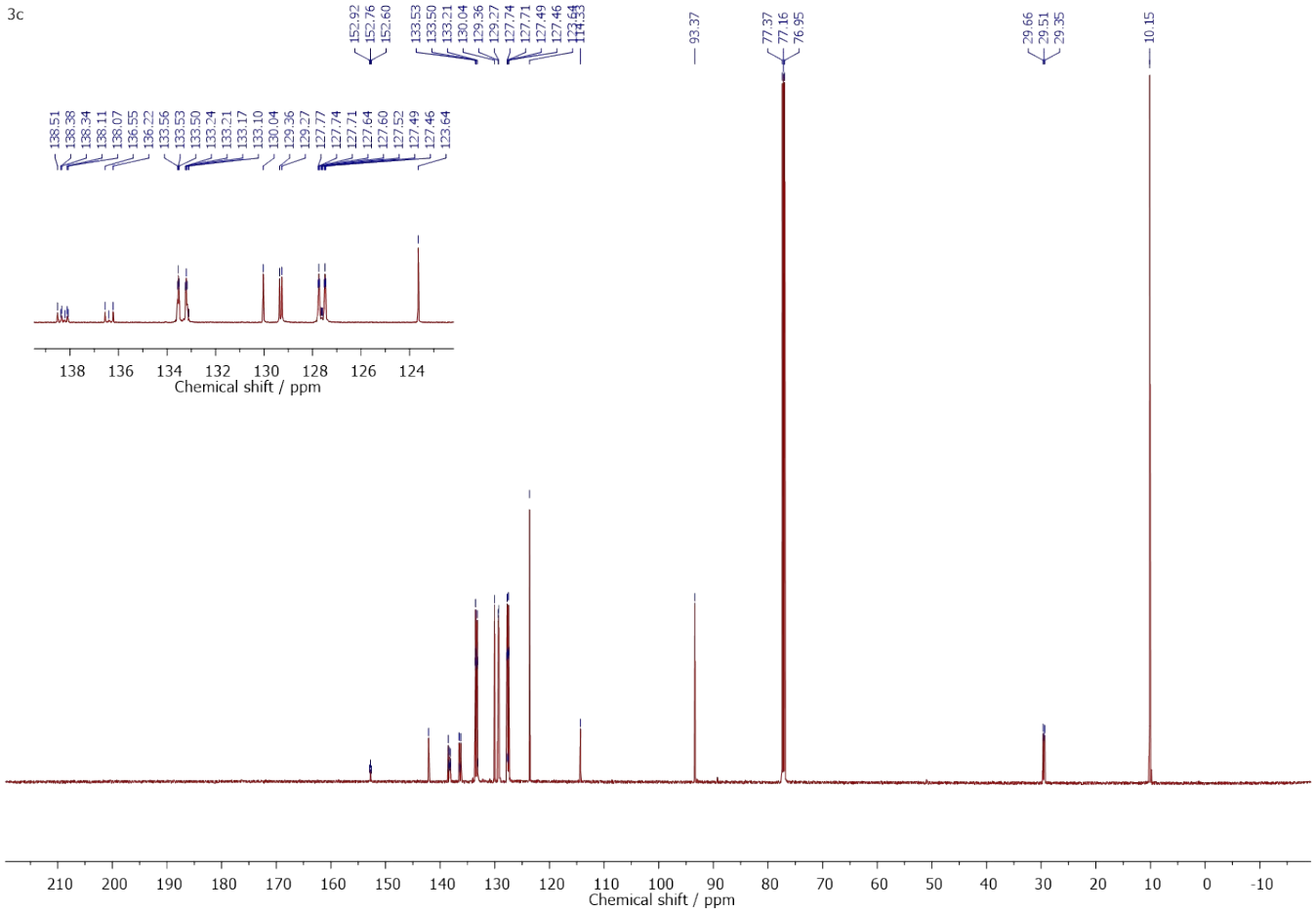

Figure S45. The $^{13}C\{^{1}H\}$ NMR spectrum of [**3c**]. The inset shows an expansion of the aromatic region for clarity.

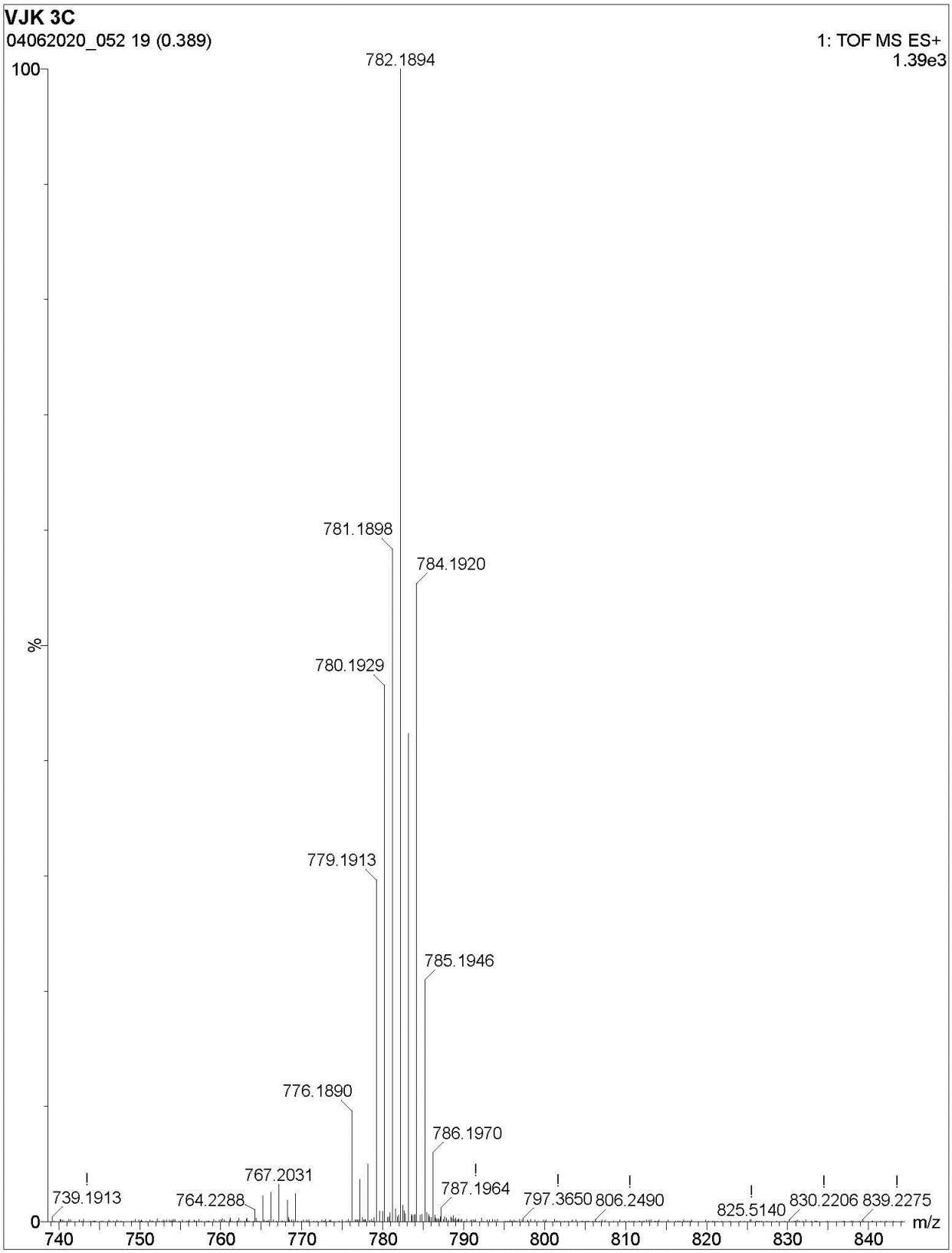

Figure S46. The ESI(+) mass spectrum of [**3c**].

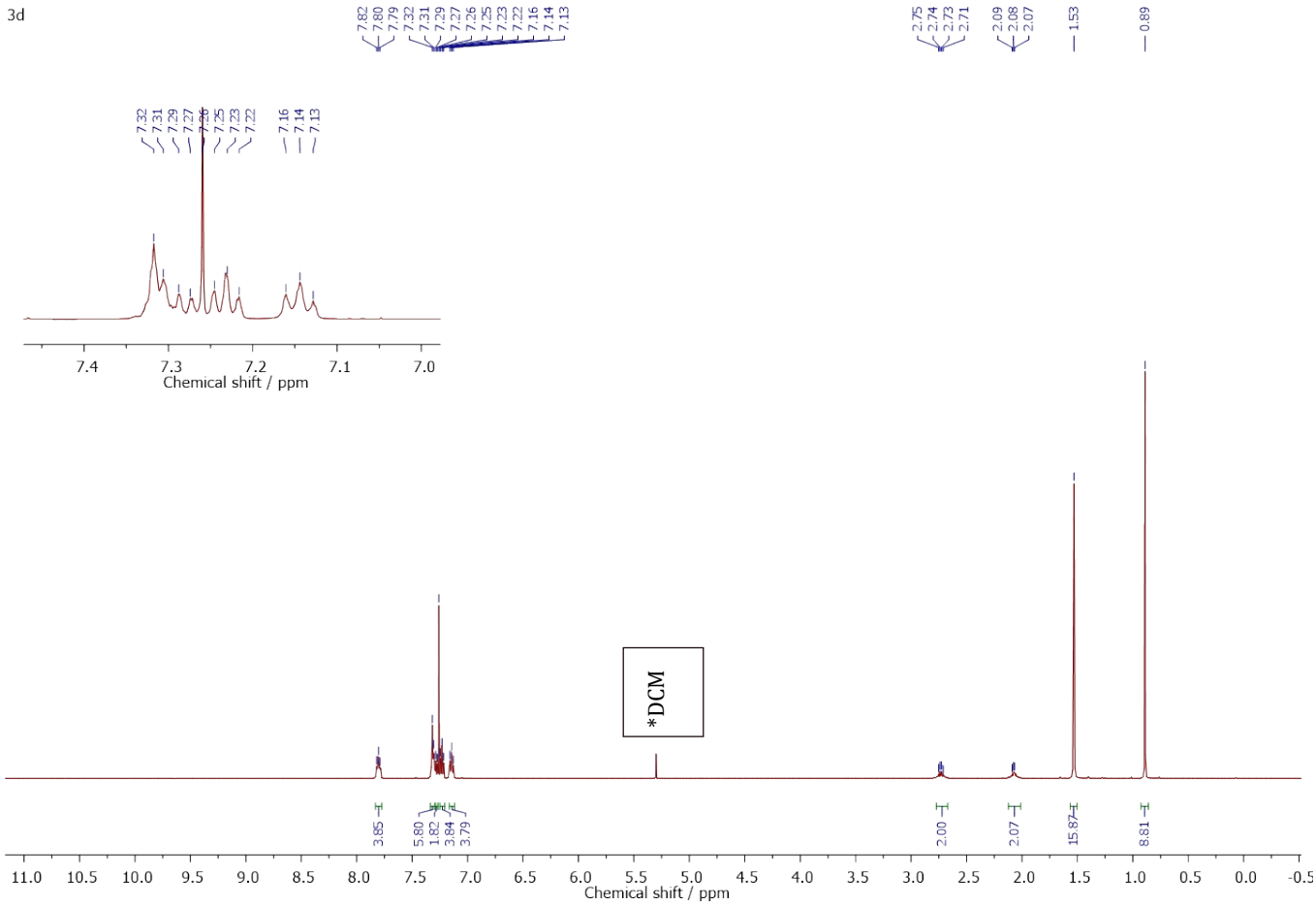

Figure S47. The ^{1}H NMR spectrum of [**3d**]. The inset shows an expansion of the aromatic region for clarity.

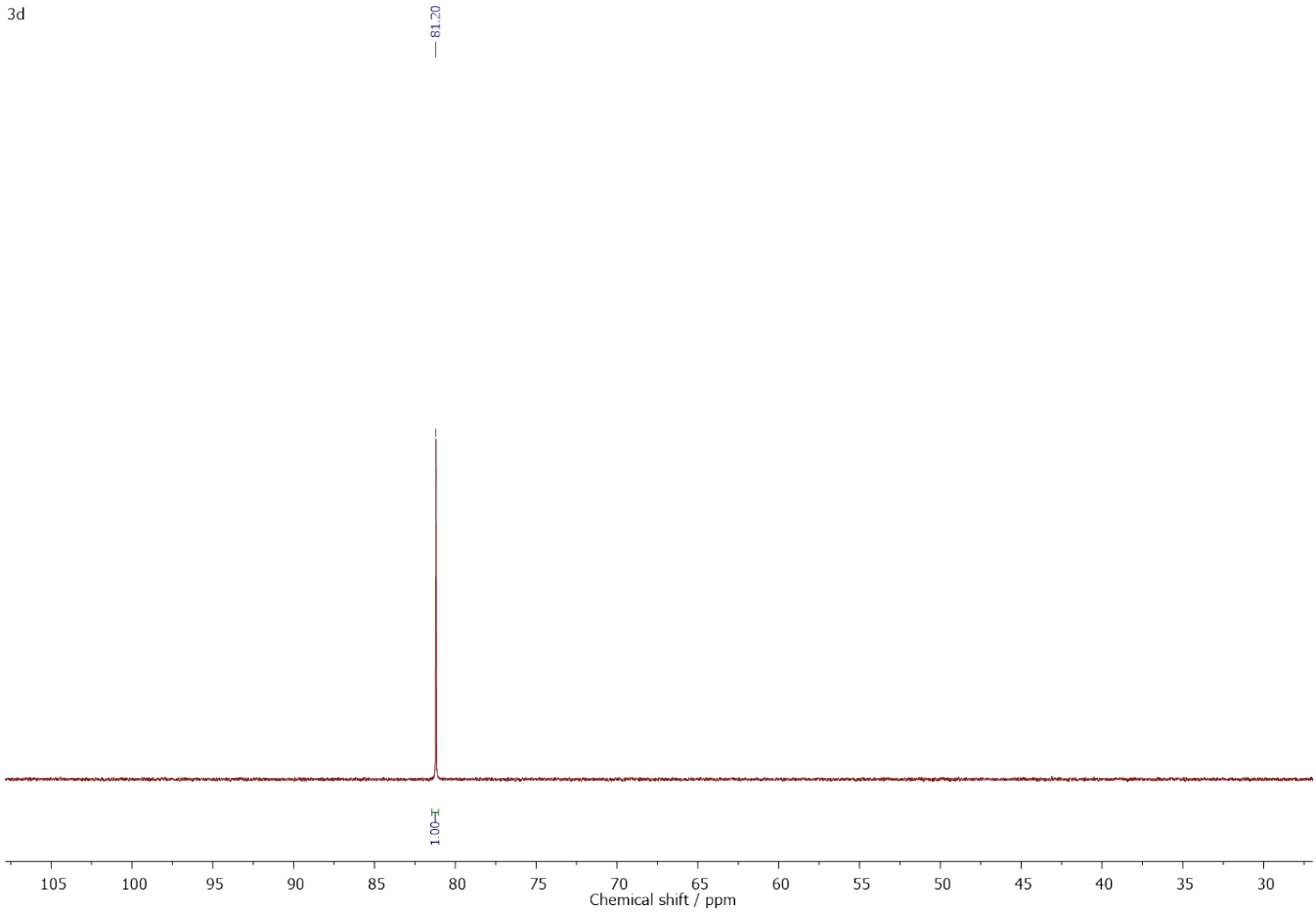

Figure S48. The ^{31}P NMR spectrum of [**3d**].

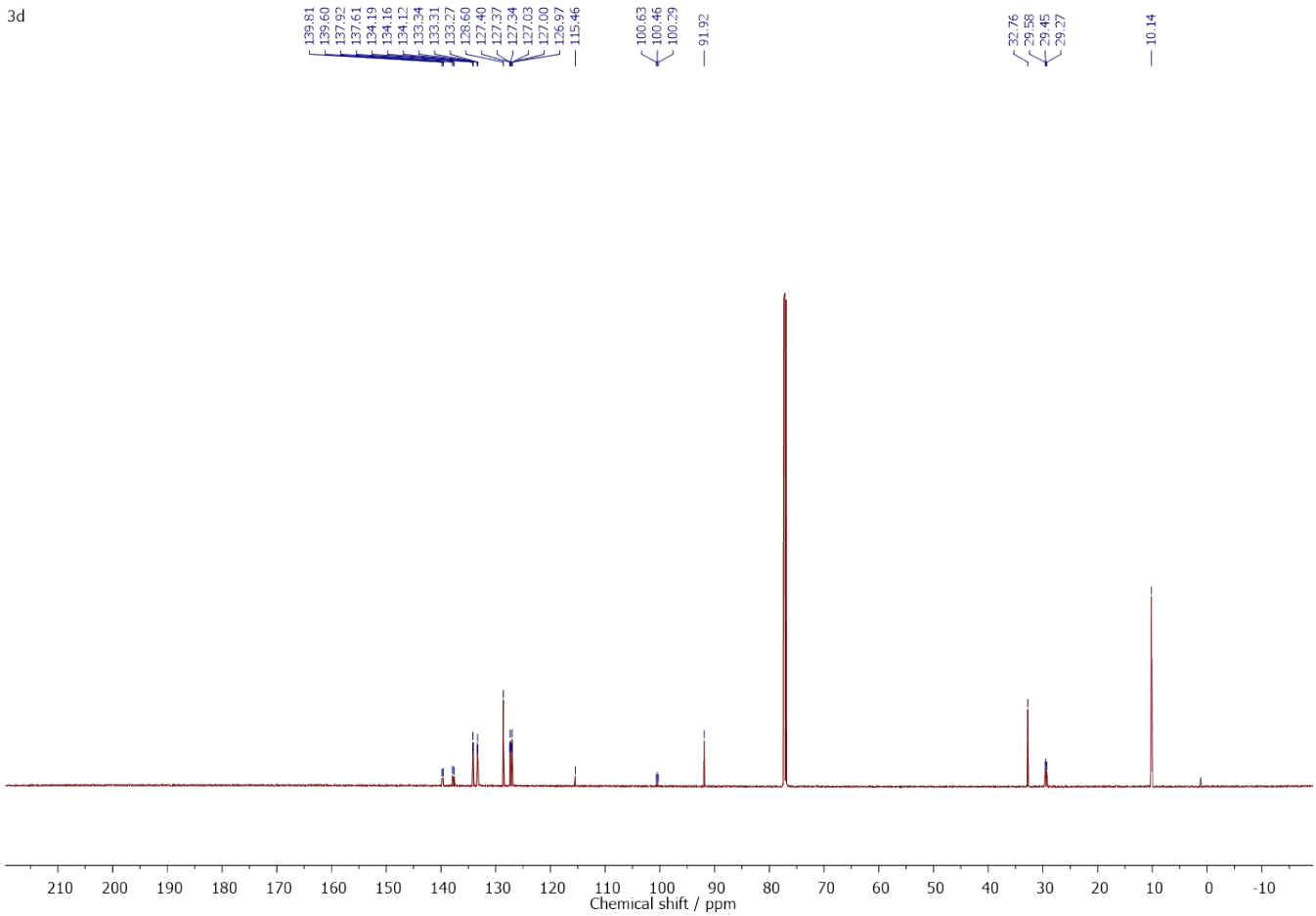

Figure S49. The $^{13}C\{^{1}H\}$ NMR spectrum of [**3d**].

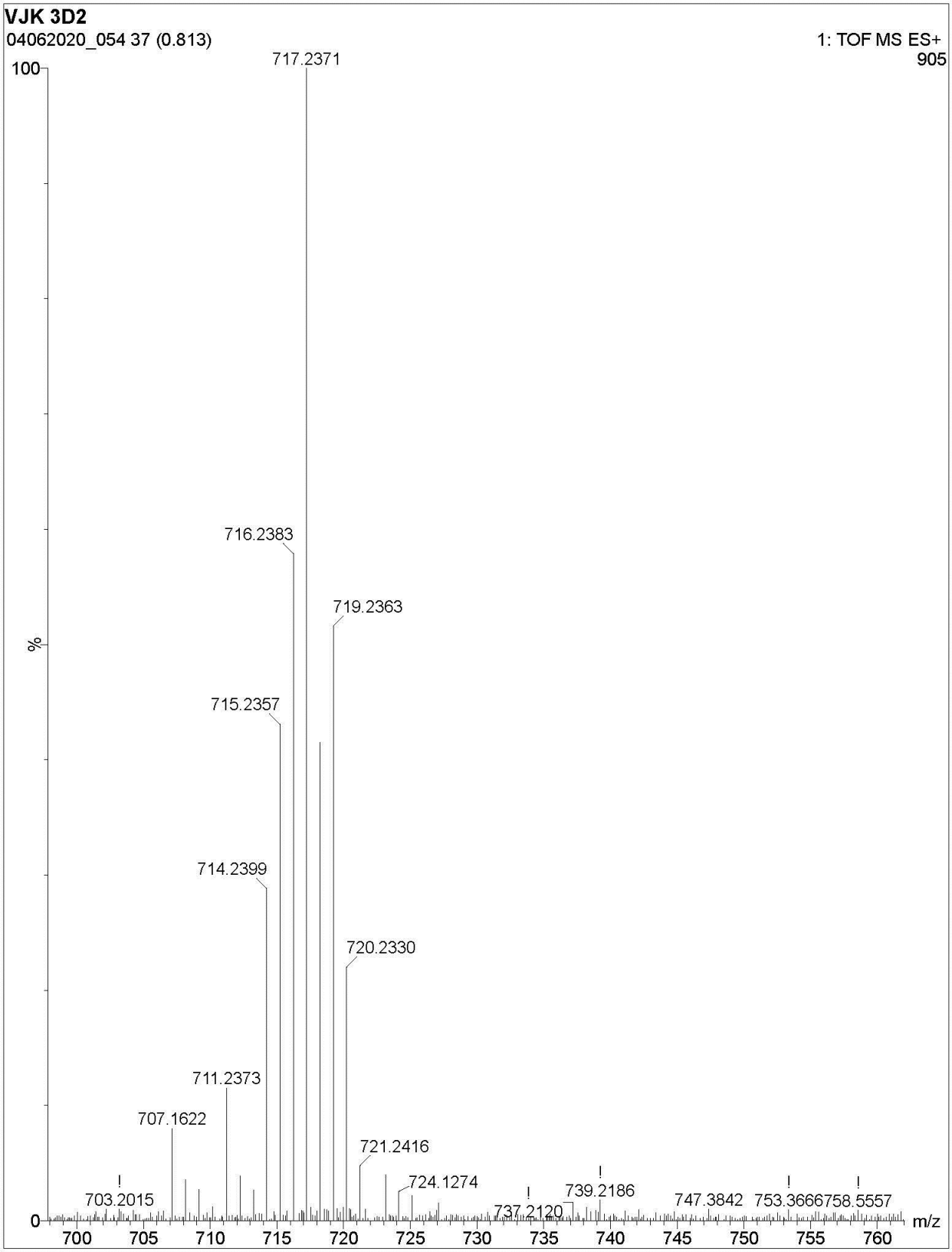

Figure S50. The ESI(+) mass spectrum of [**3d**].

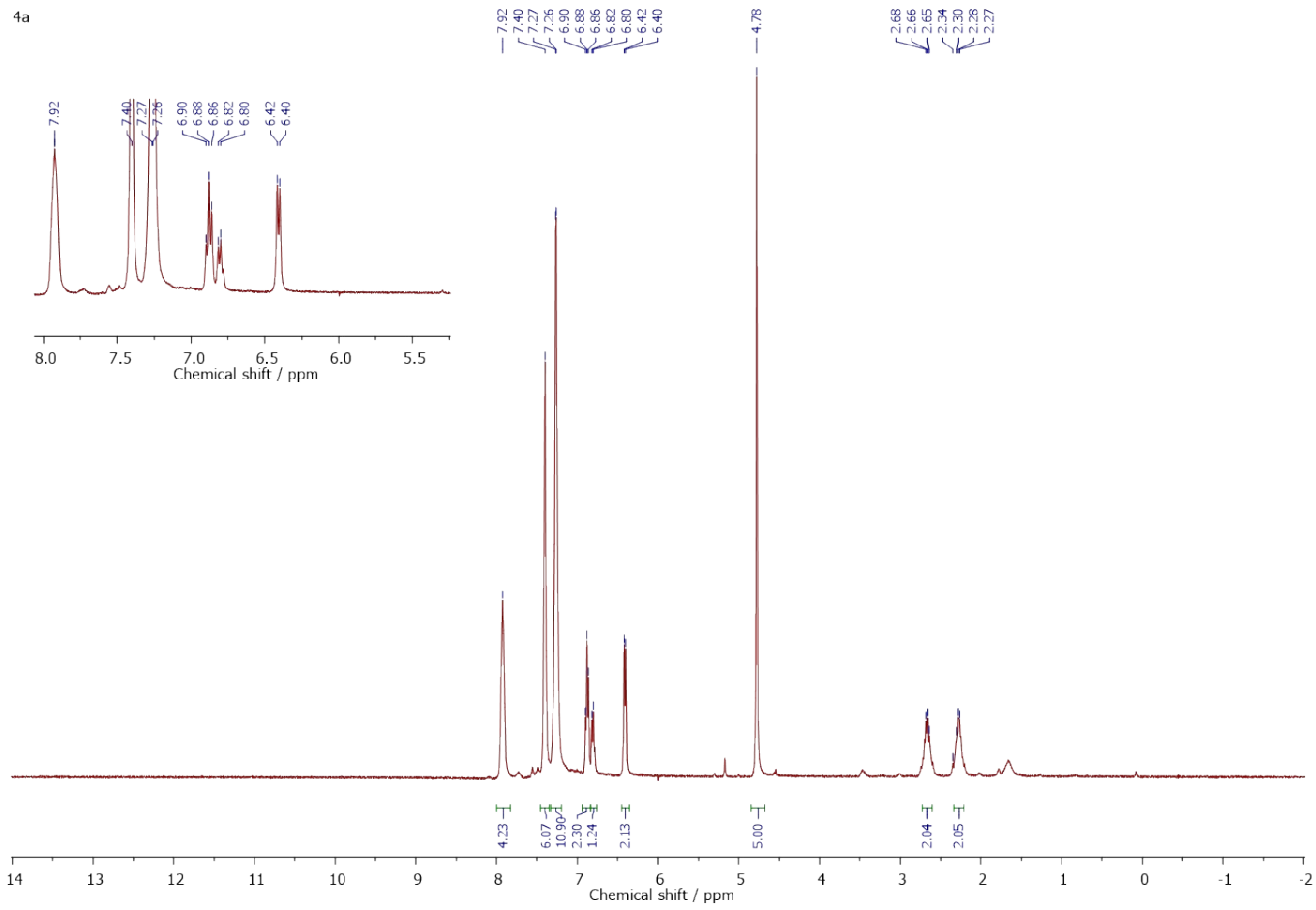

Figure S51. The ^{1}H NMR spectrum of [**4a**]. The inset shows an expansion of the aromatic region for clarity.

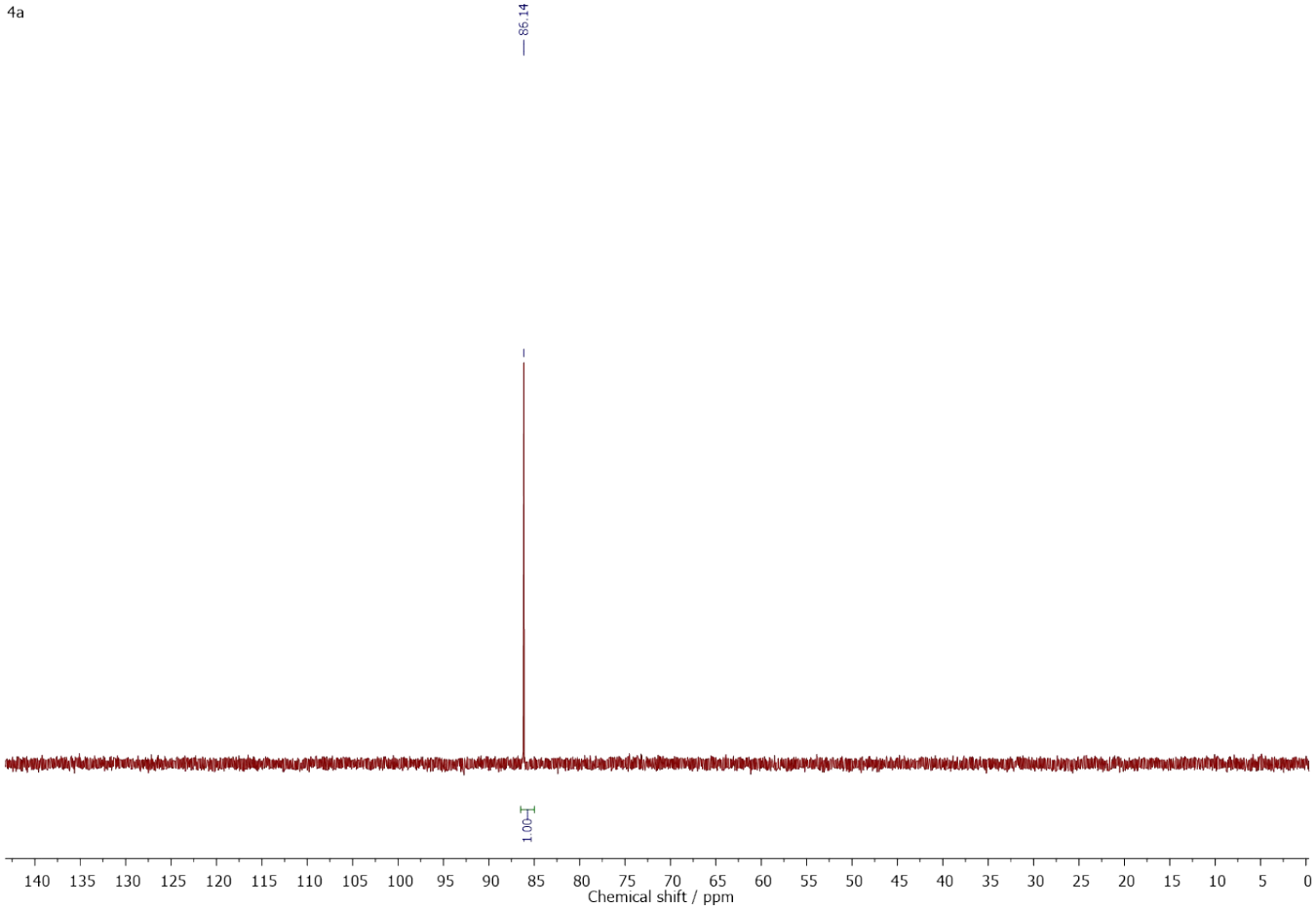

Figure S52. The ^{31}P NMR spectrum of [**4a**].

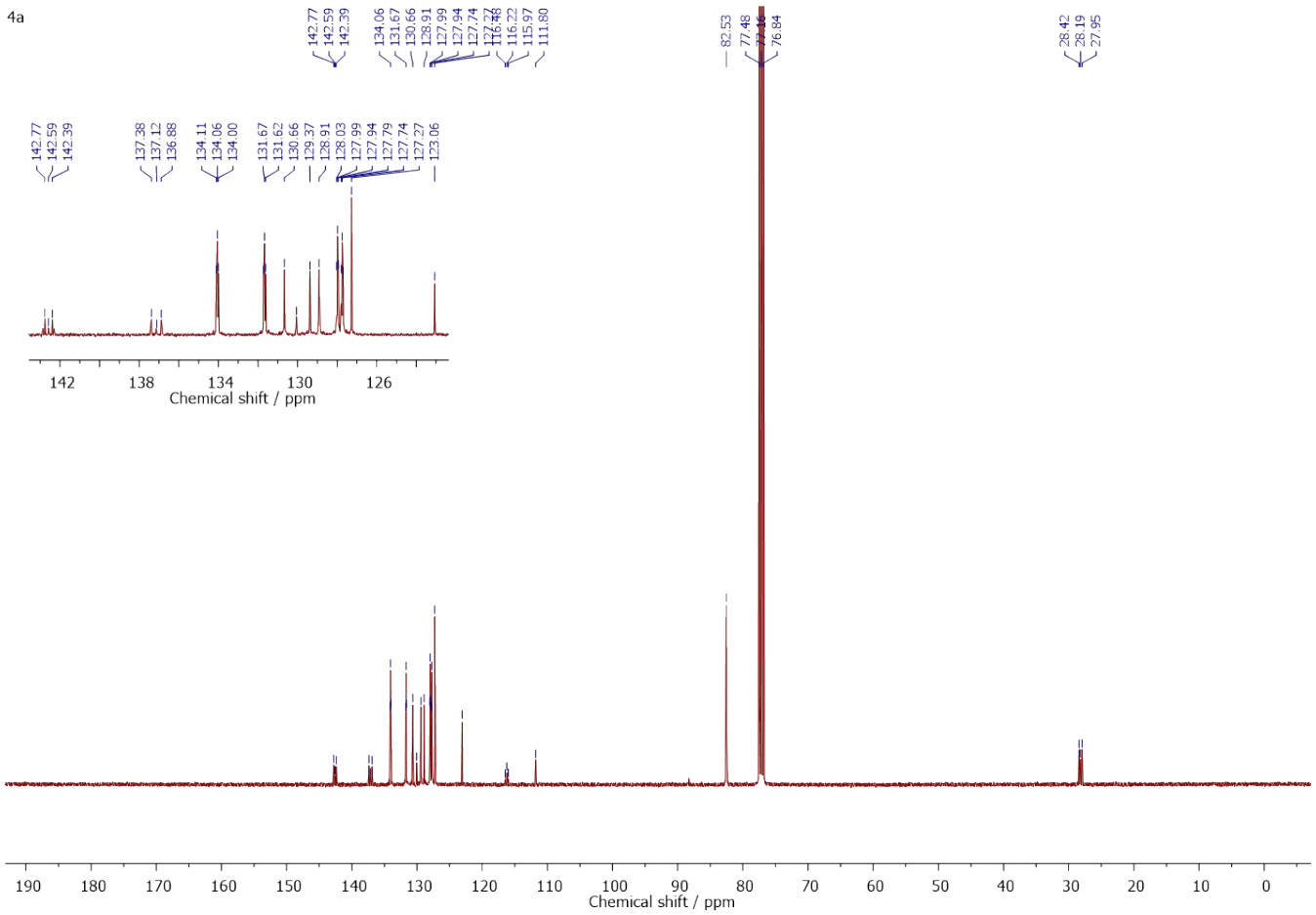

Figure S53. The $^{13}C\{^{1}H\}$ NMR spectrum of [**4a**]. The inset shows an expansion of the aromatic region for clarity.

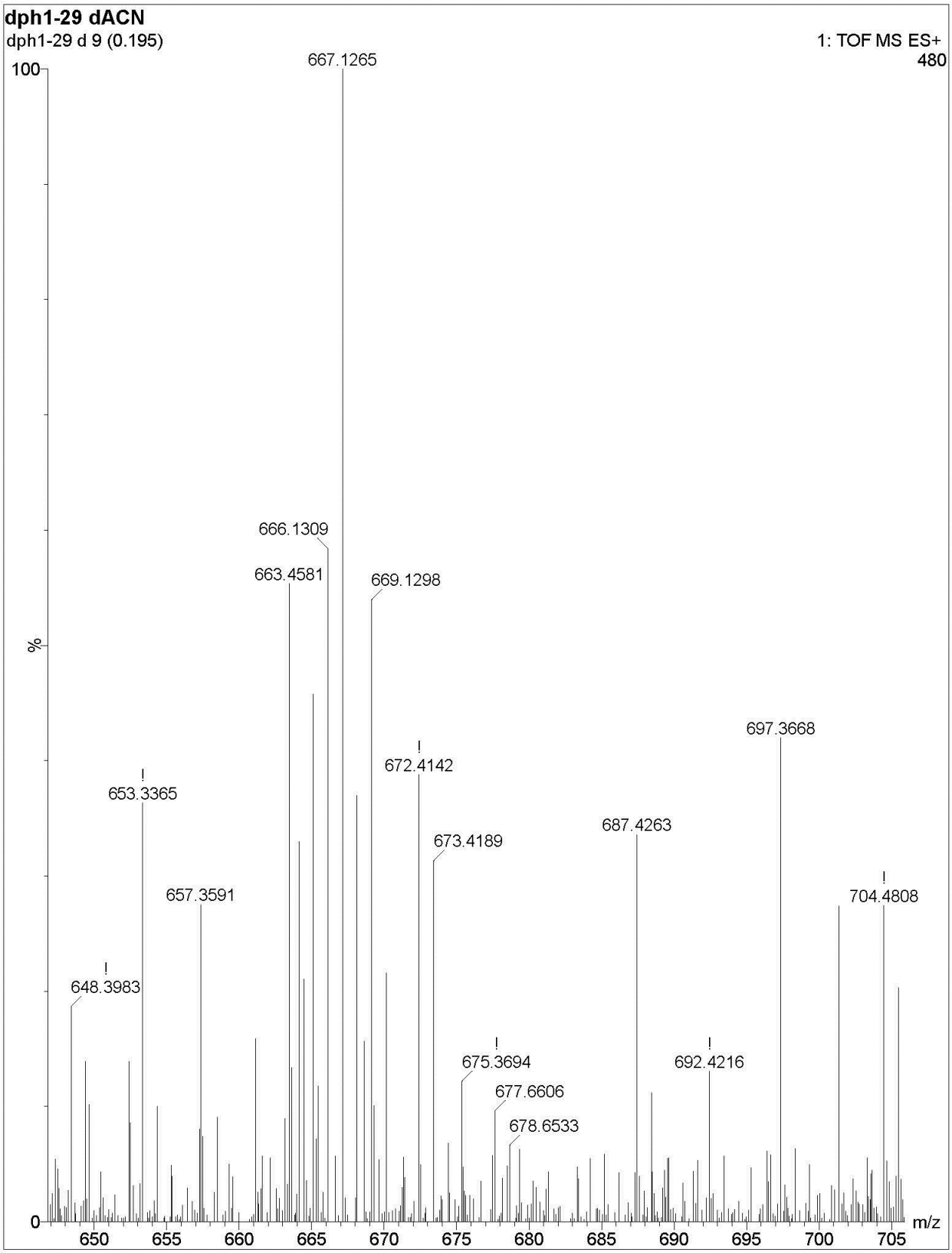

Figure S54. The ESI(+) mass spectrum of [**4a**].

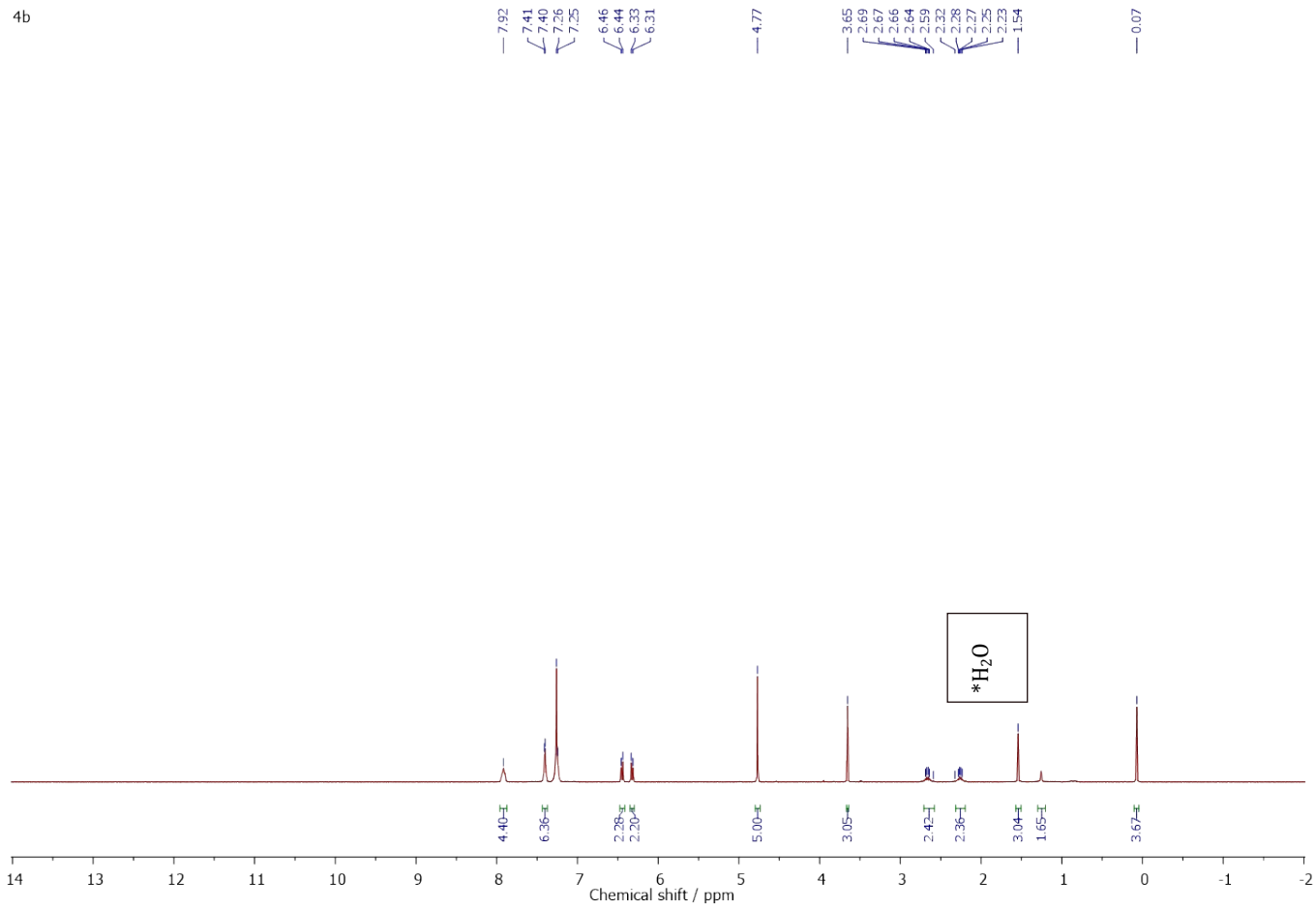

Figure S55. The ^{1}H NMR spectrum of [**4b**].

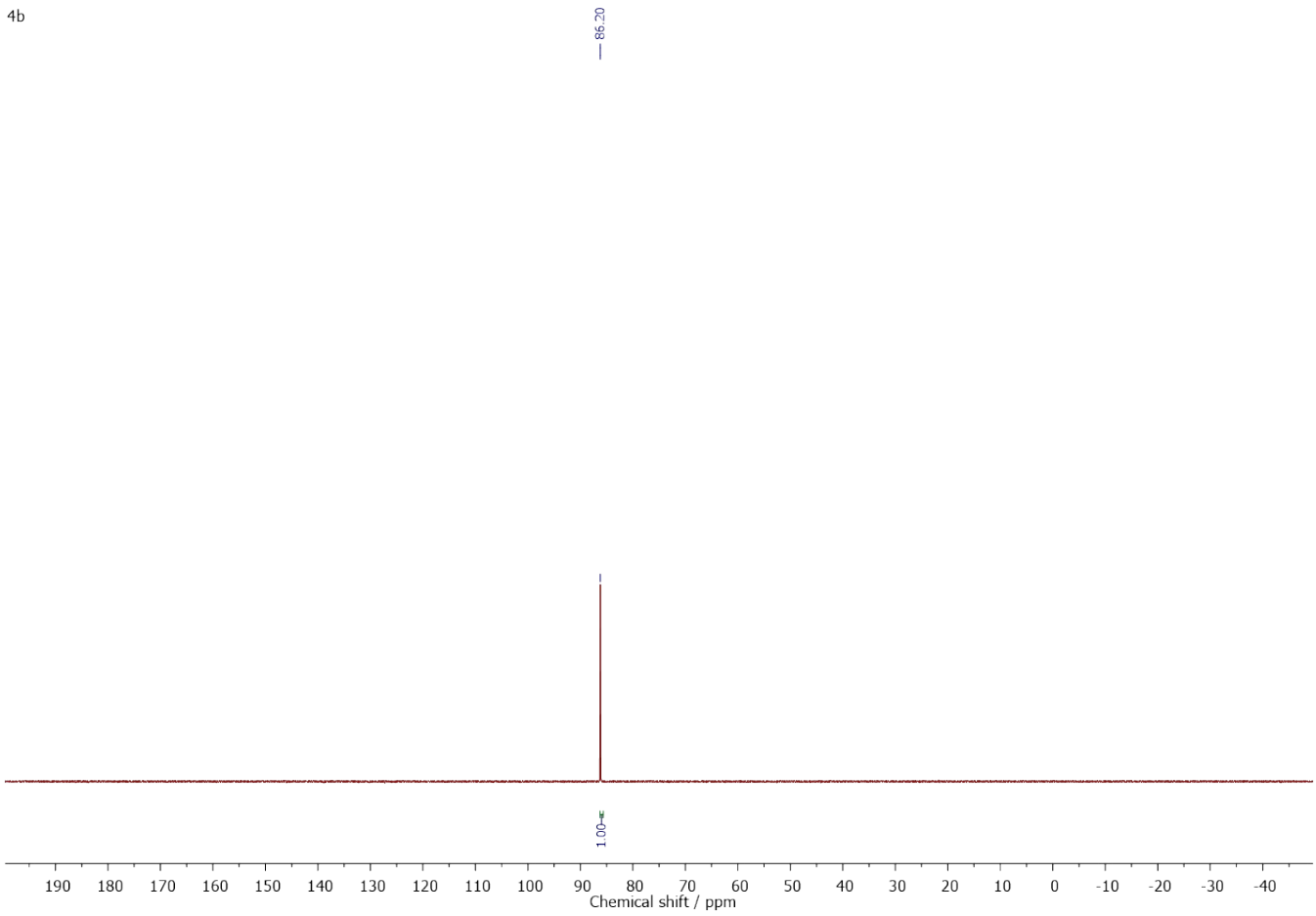

Figure S56. The ^{31}P NMR spectrum of [**4b**].

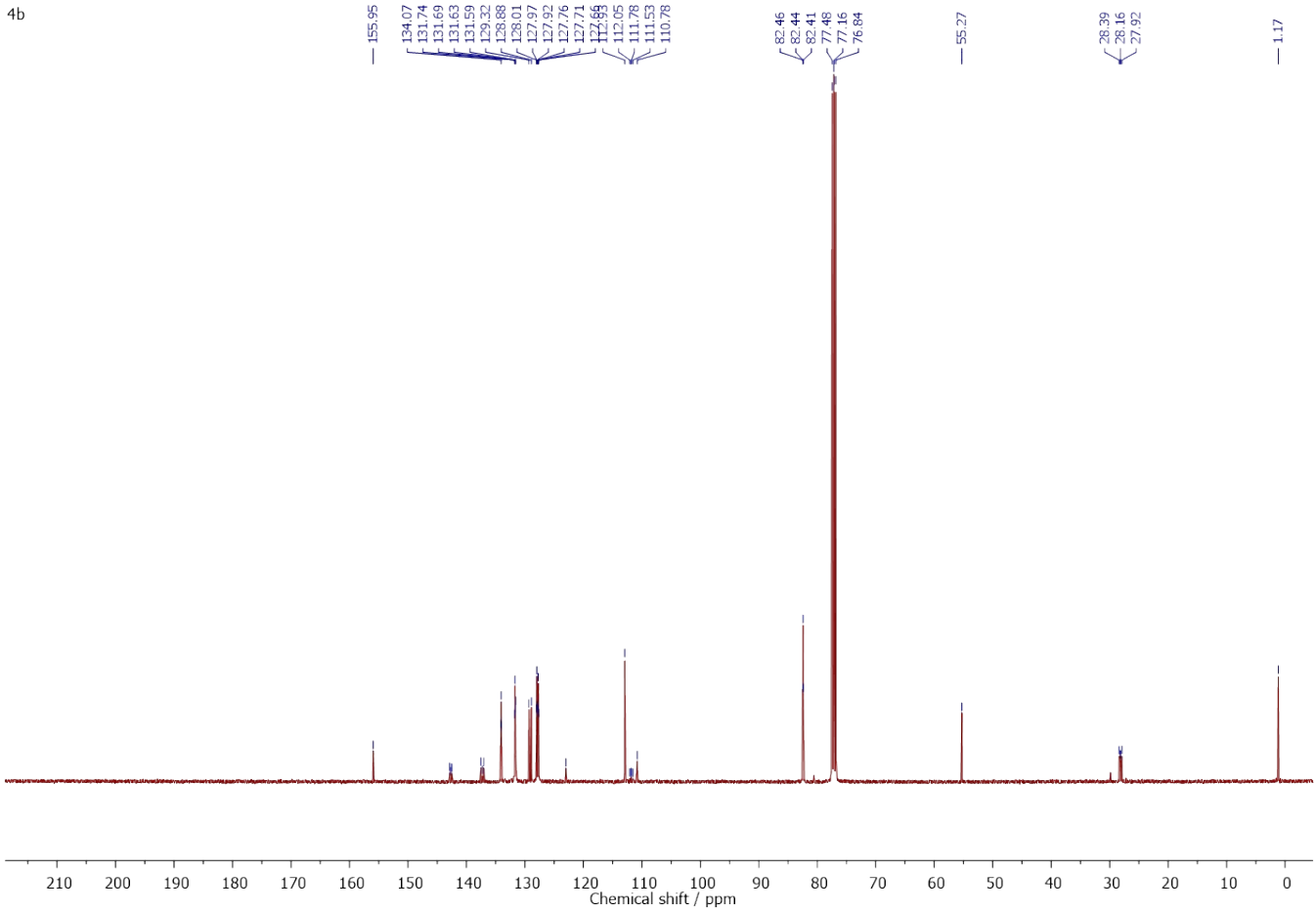

Figure S57. The $^{13}C\{^{1}H\}$ NMR spectrum of [**4b**].

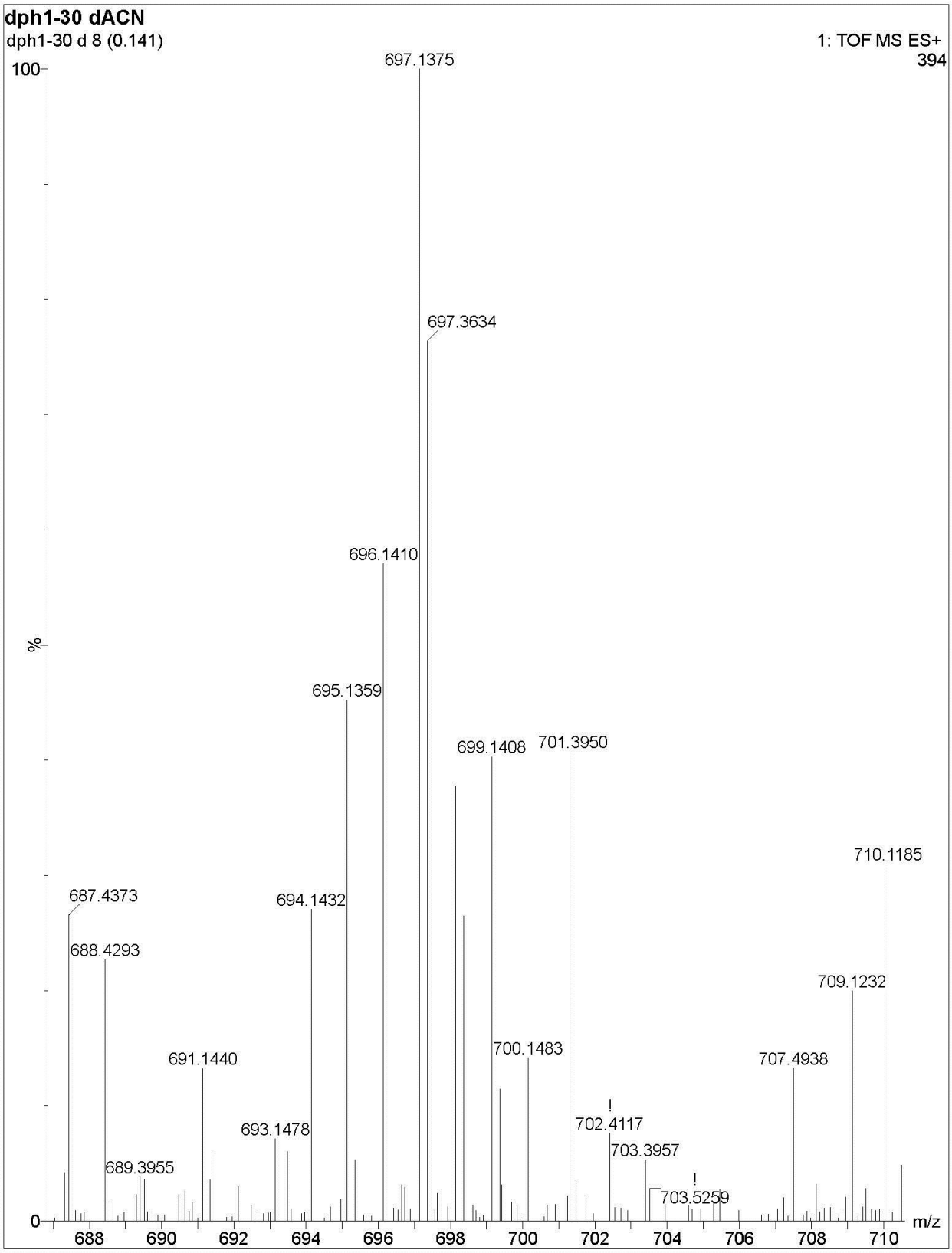

Figure S58. The ESI(+) mass spectrum of [**4b**].

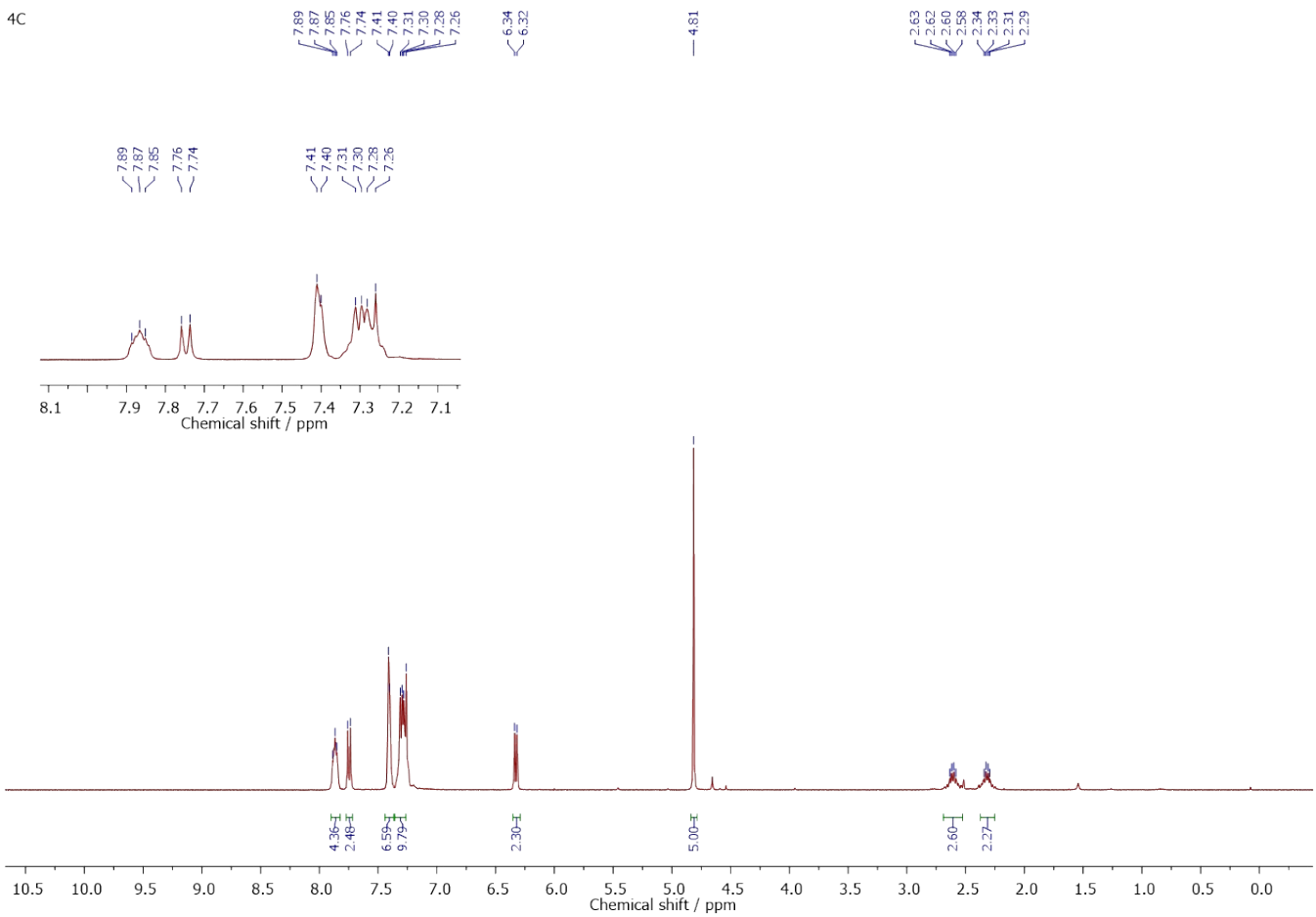

Figure S59. The ^{1}H NMR spectrum of [**4c**]. The inset shows an expansion of the aromatic region for clarity.

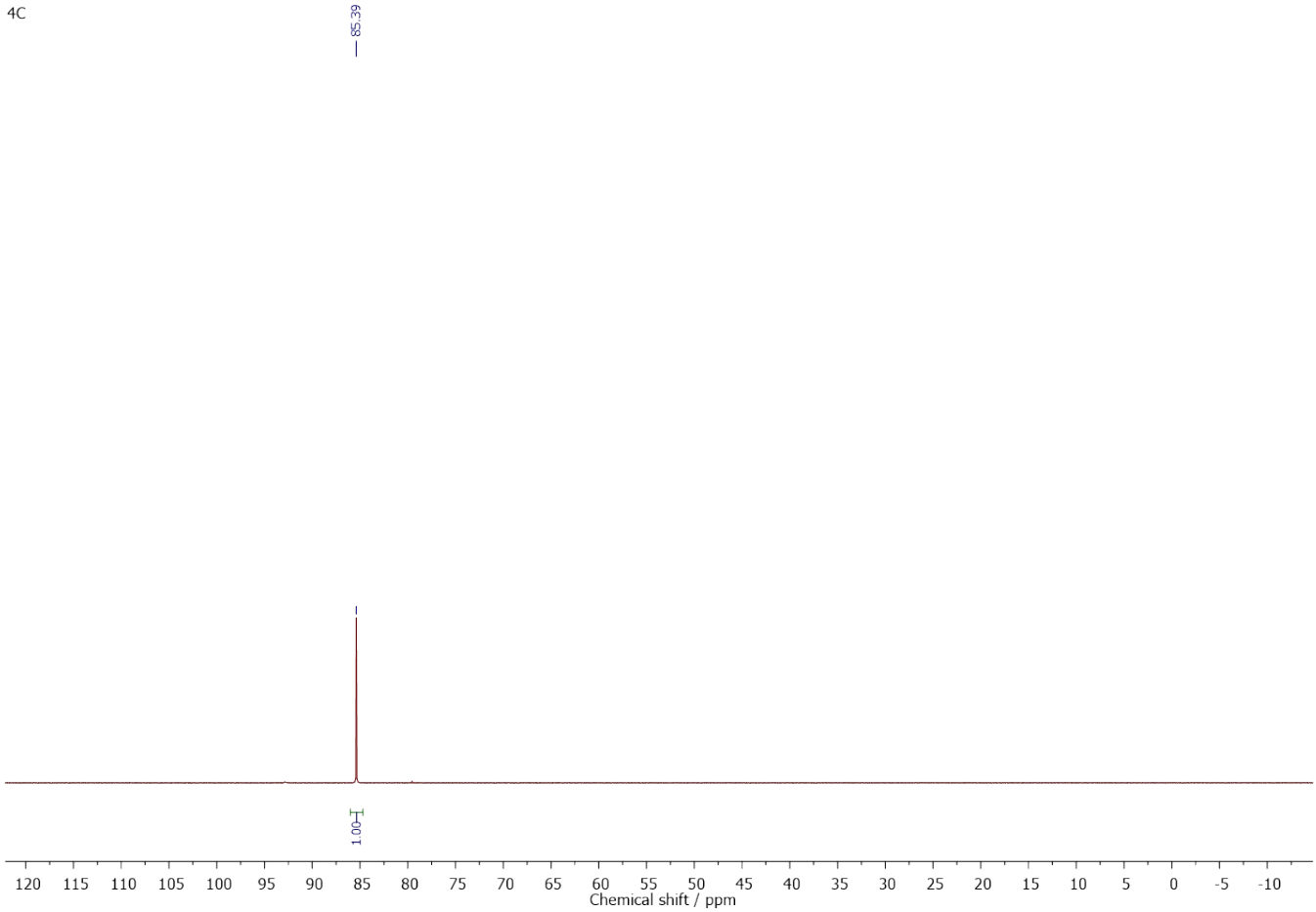

Figure S60. The ^{31}P NMR spectrum of [**4c**].

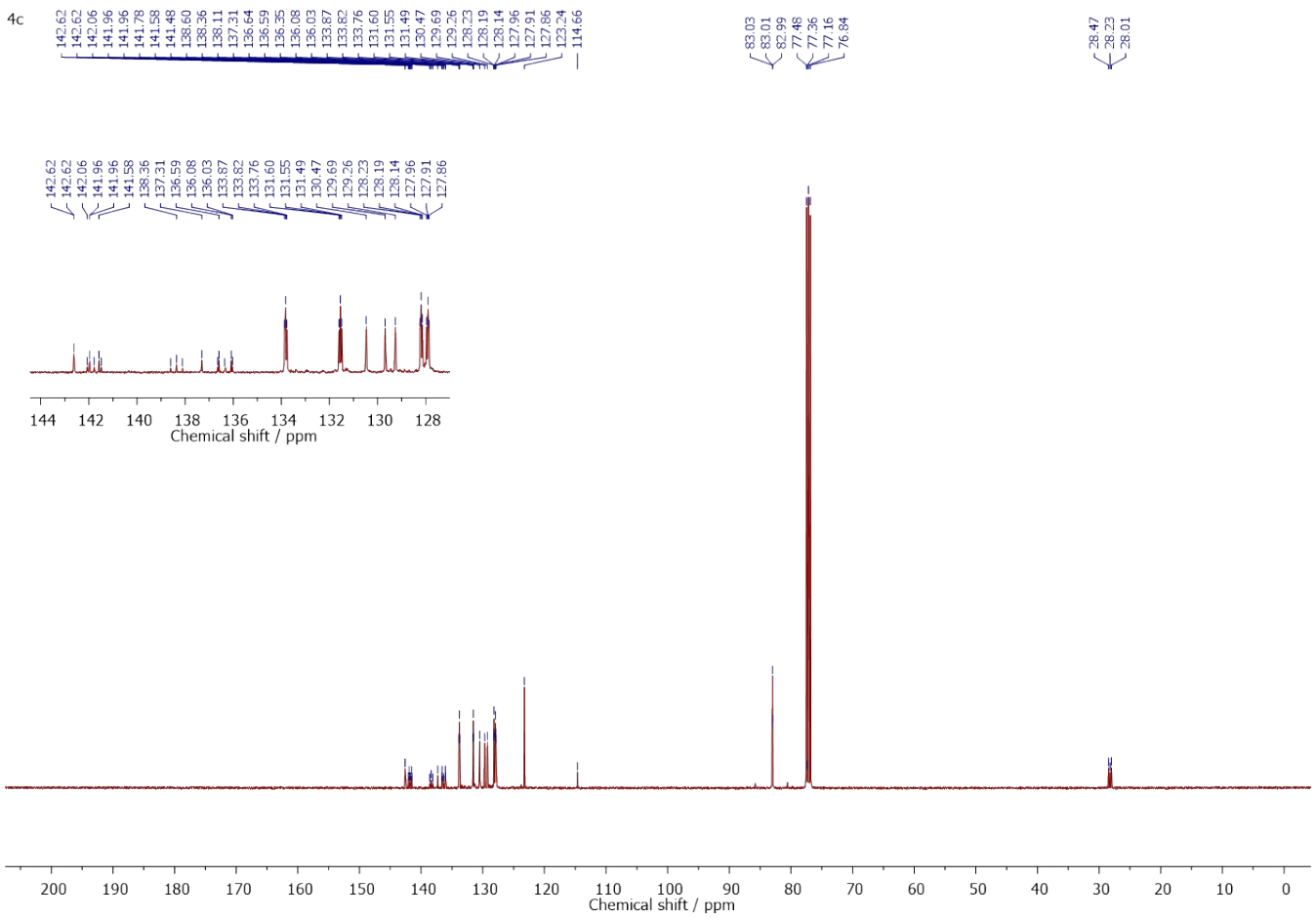

Figure S61. The $^{13}C\{^{1}H\}$ NMR spectrum of [**4c**]. The inset shows an expansion of the aromatic region for clarity.

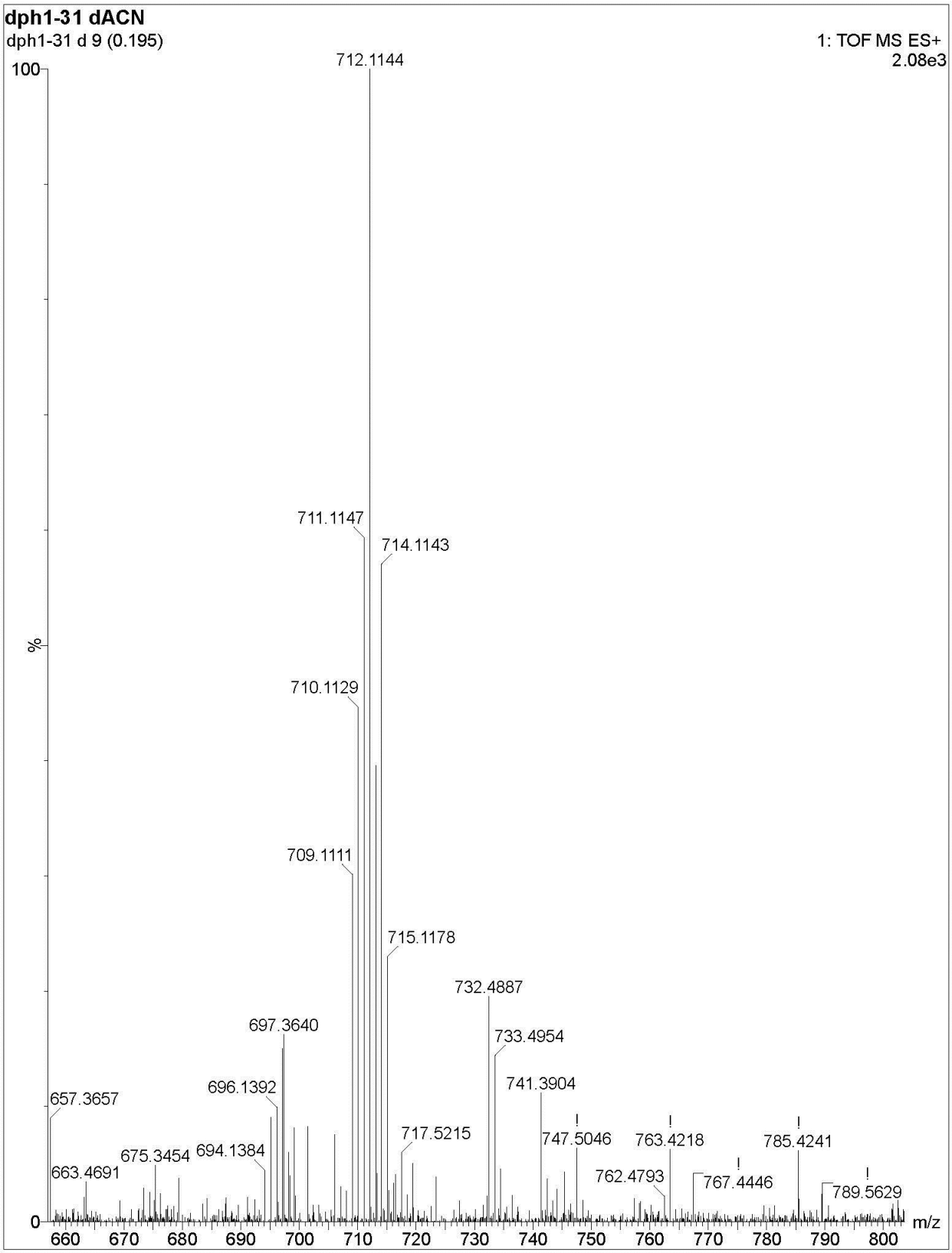

Figure S62. The ESI(+) mass spectrum of [**4c**].

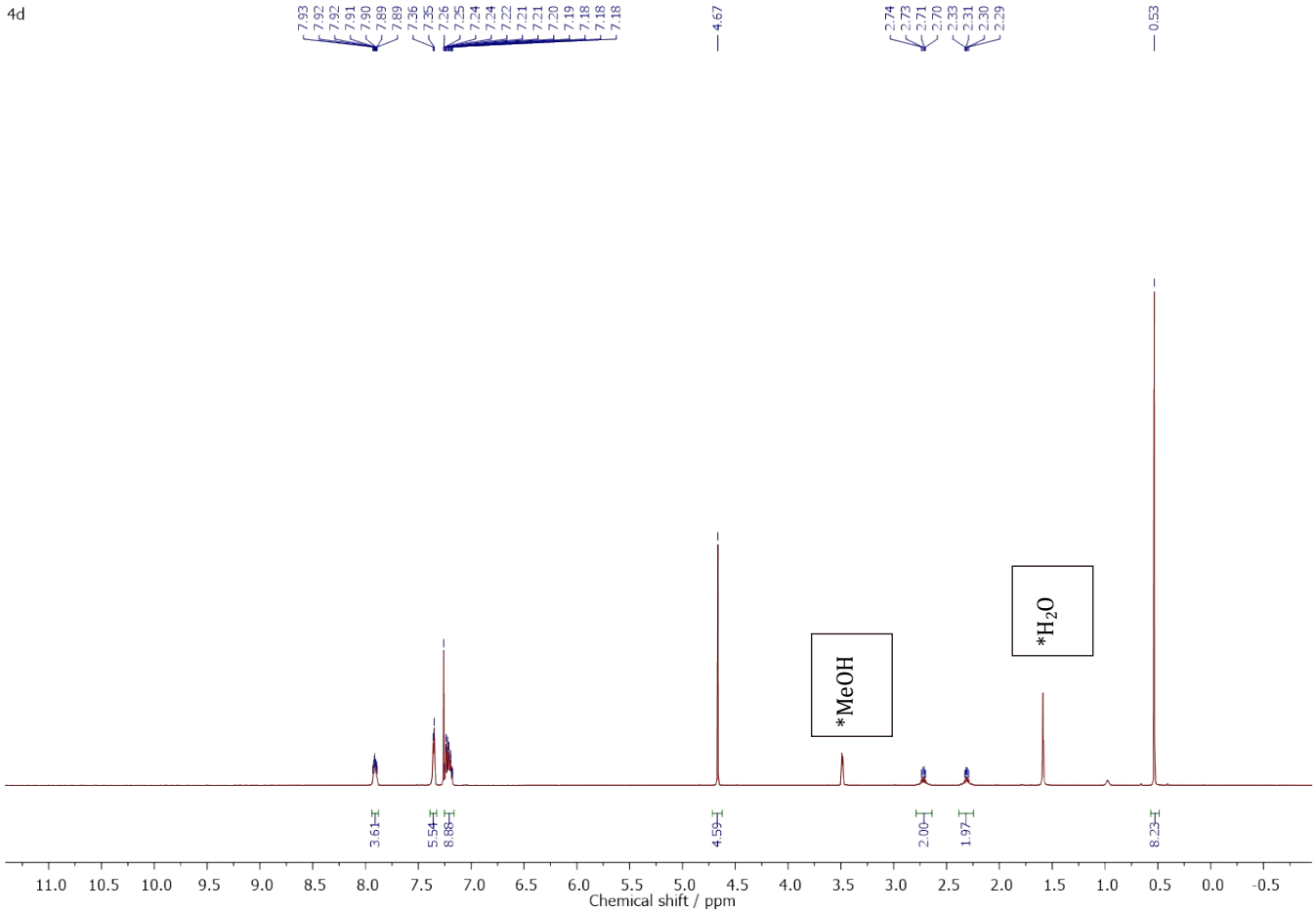

Figure S63. The ^{1}H NMR spectrum of [**4d**].

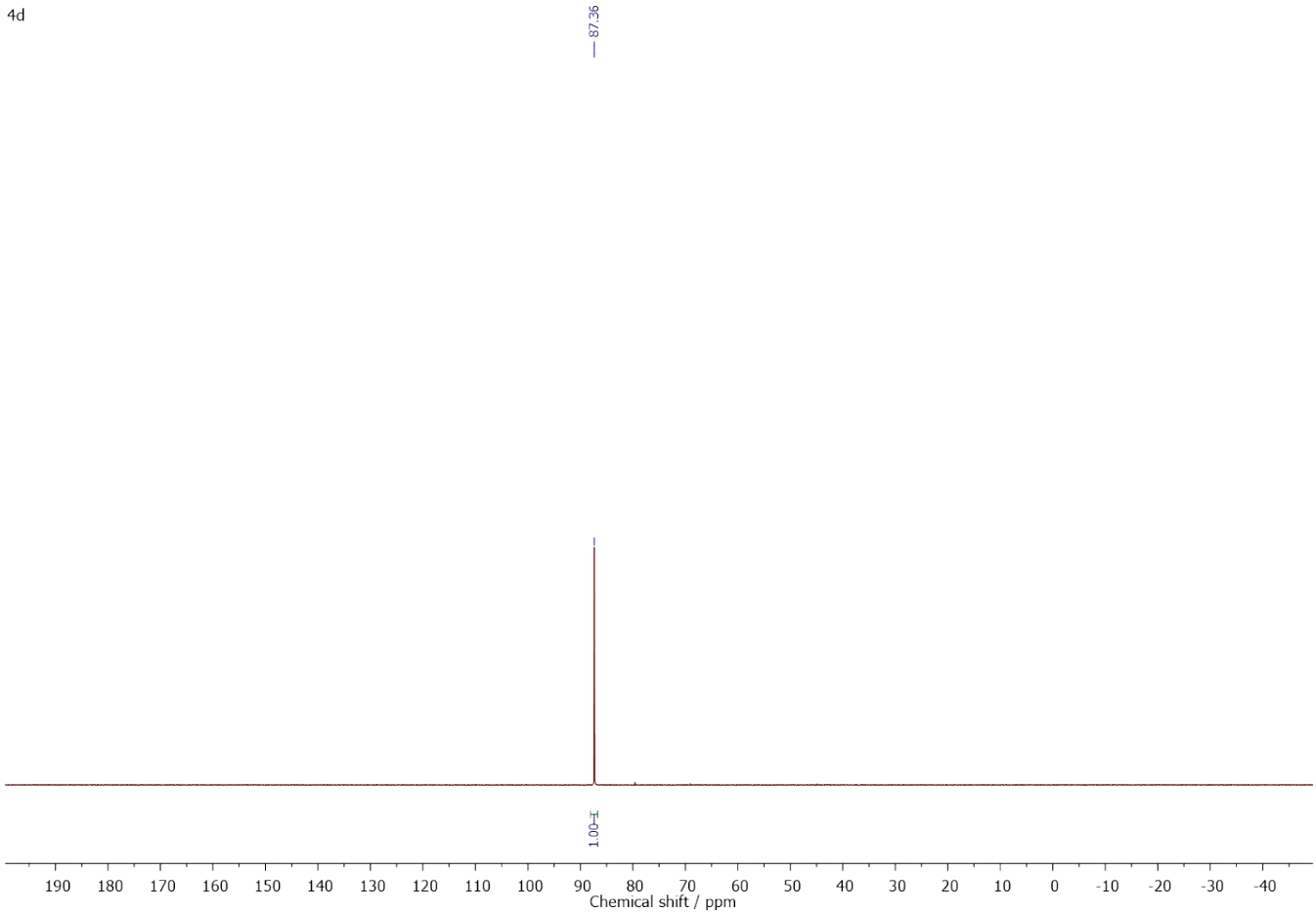

Figure S64. The ^{31}P NMR spectrum of [**4d**].

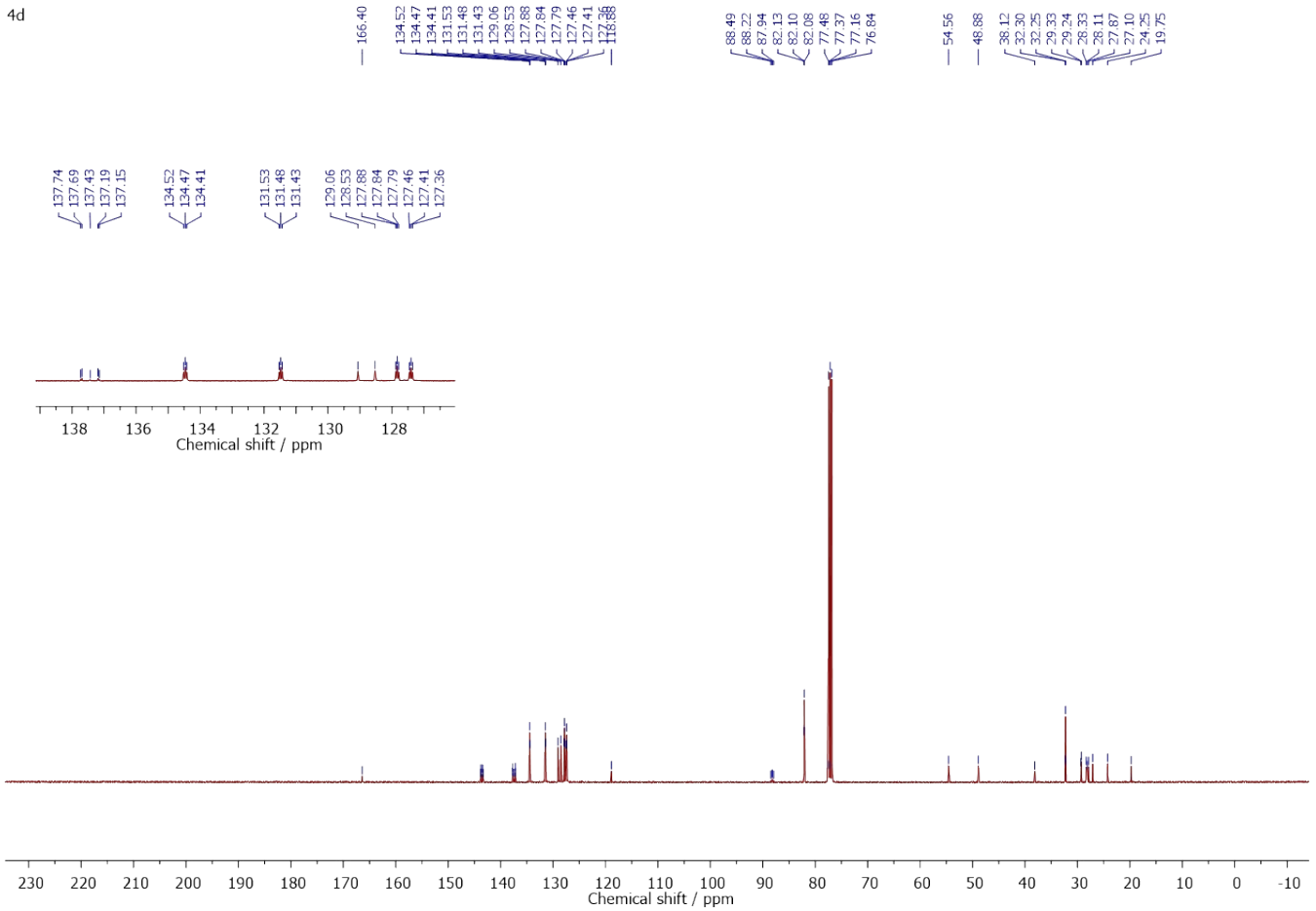

Figure S65. The $^{13}C\{^{1}H\}$ NMR spectrum of [**4d**]. The inset shows an expansion of the aromatic region for clarity.

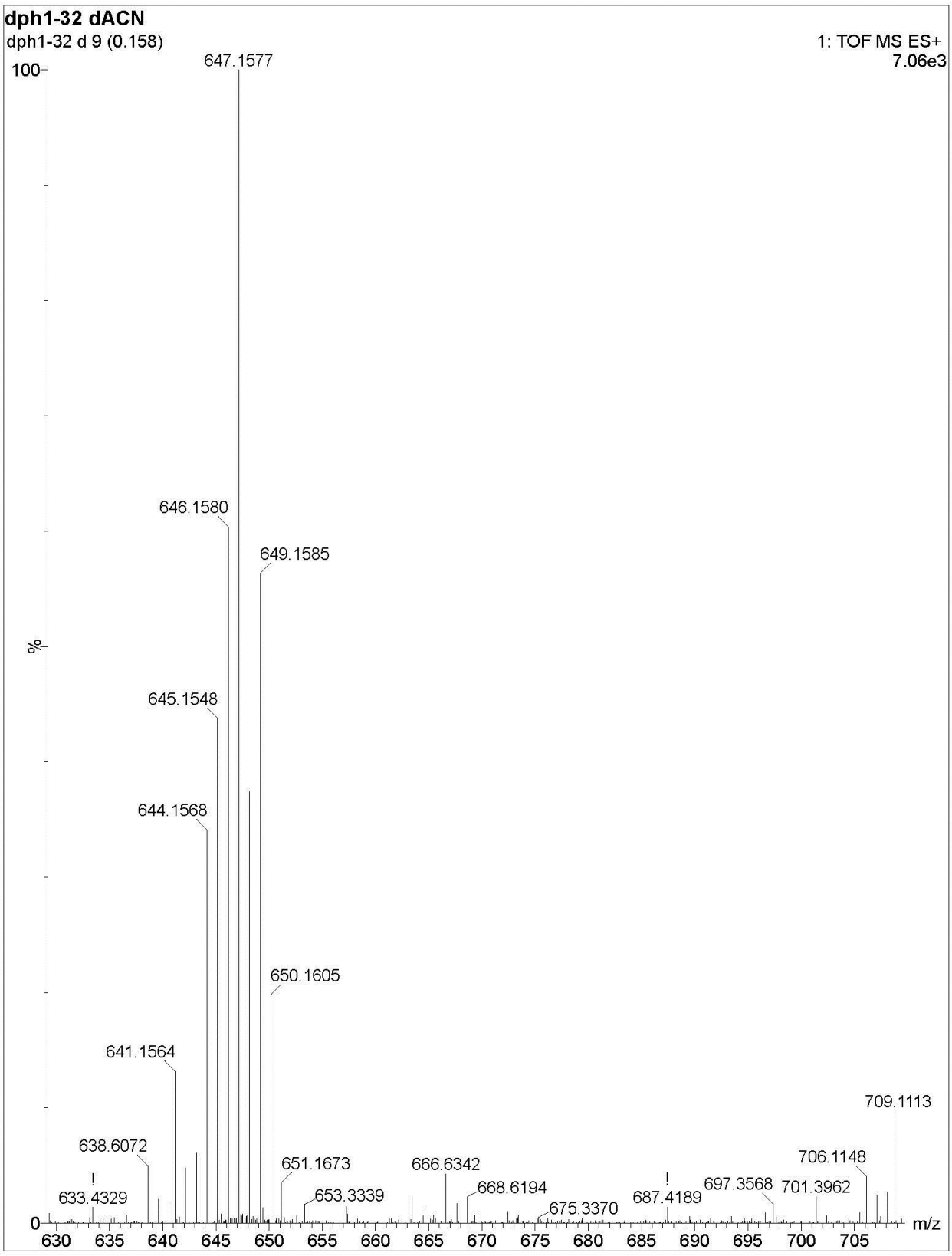

Figure S66. The ESI(+) mass spectrum of [**4d**].

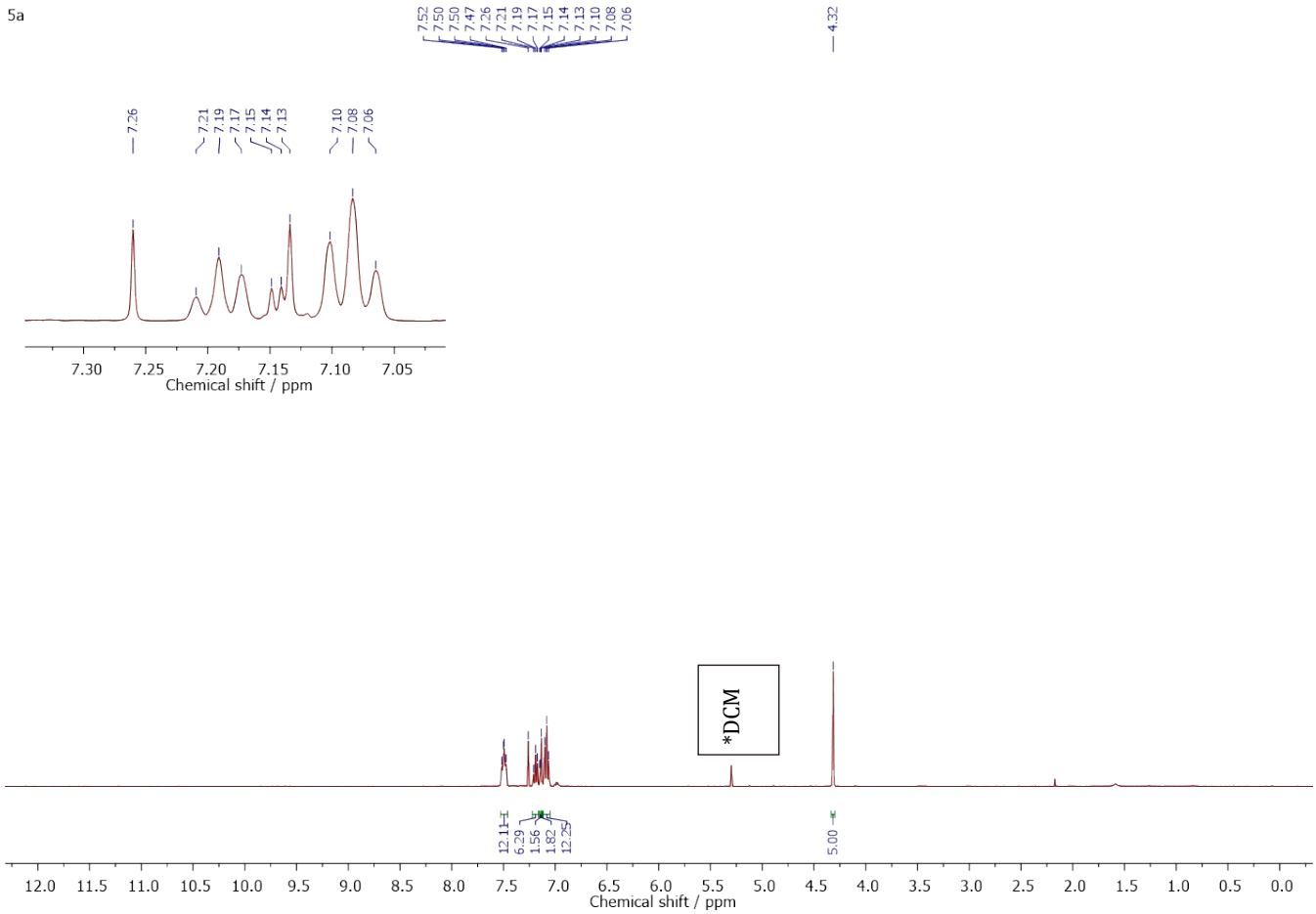

Figure S67. The ^{1}H NMR spectrum of [**5a**]. The inset shows an expansion of the aromatic region for clarity.

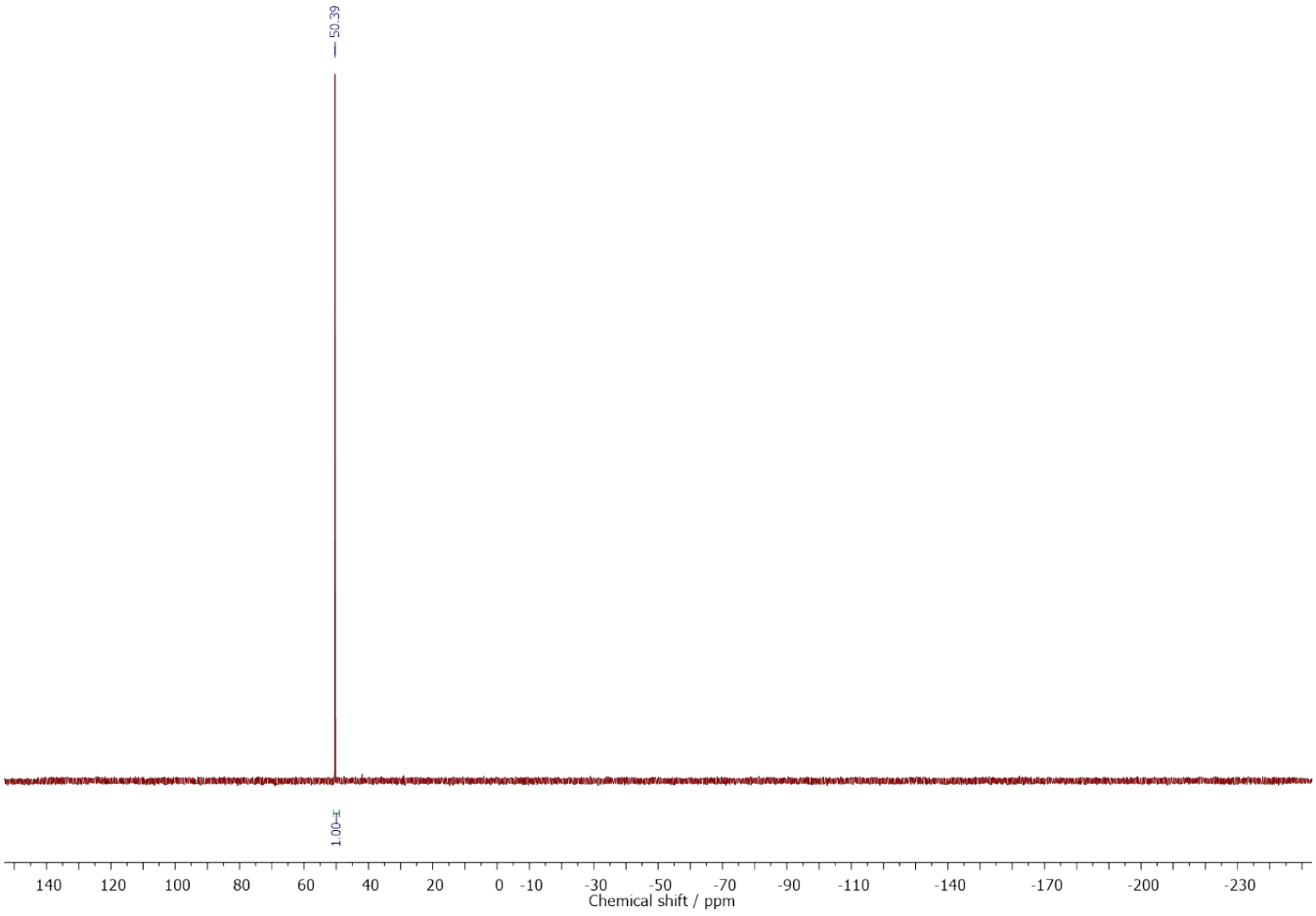

Figure S68. The ^{31}P NMR spectrum of [**5a**].

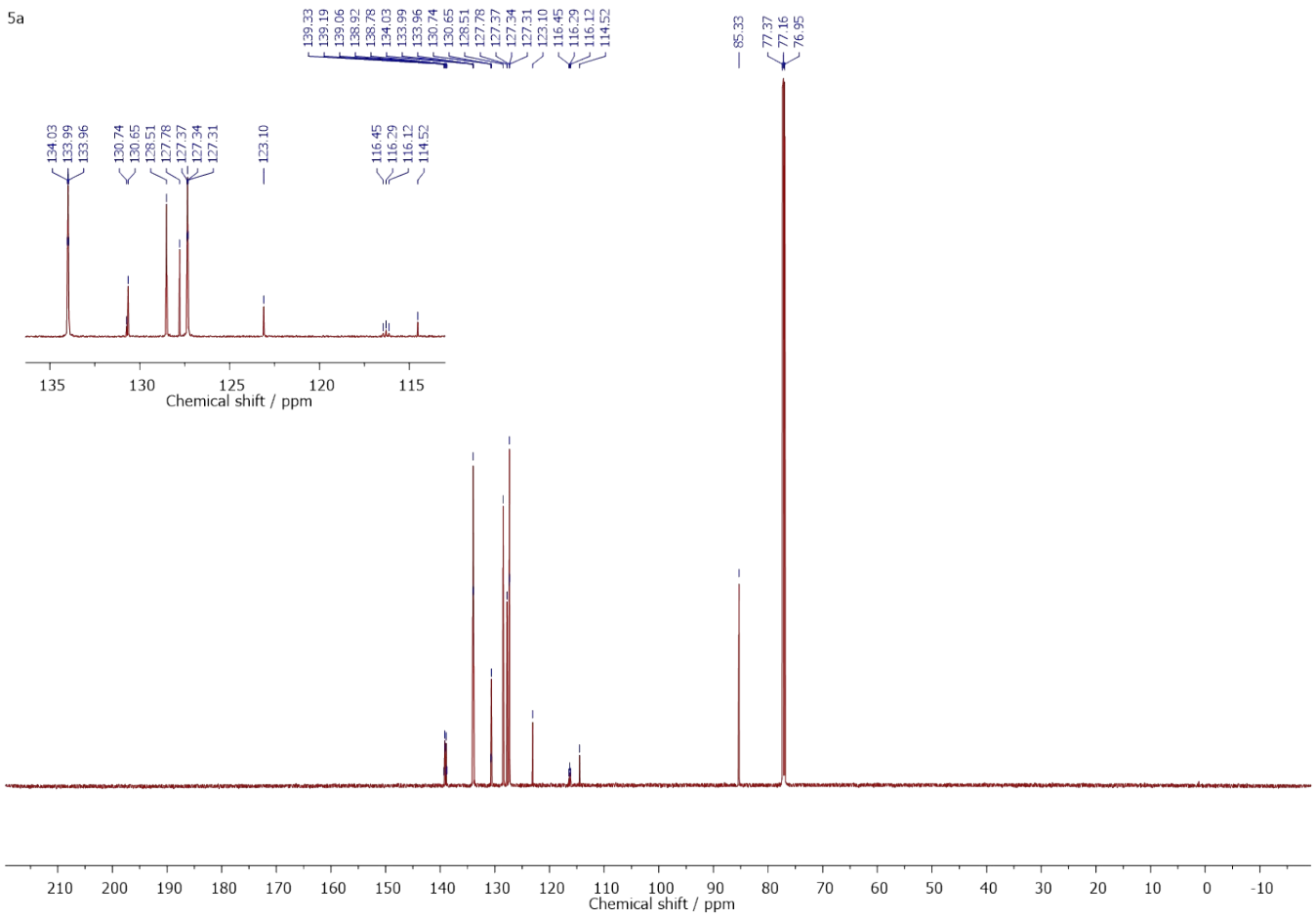

Figure S69. The $^{13}C\{^{1}H\}$ NMR spectrum of [**5a**]. The inset shows an expansion of the aromatic region for clarity.

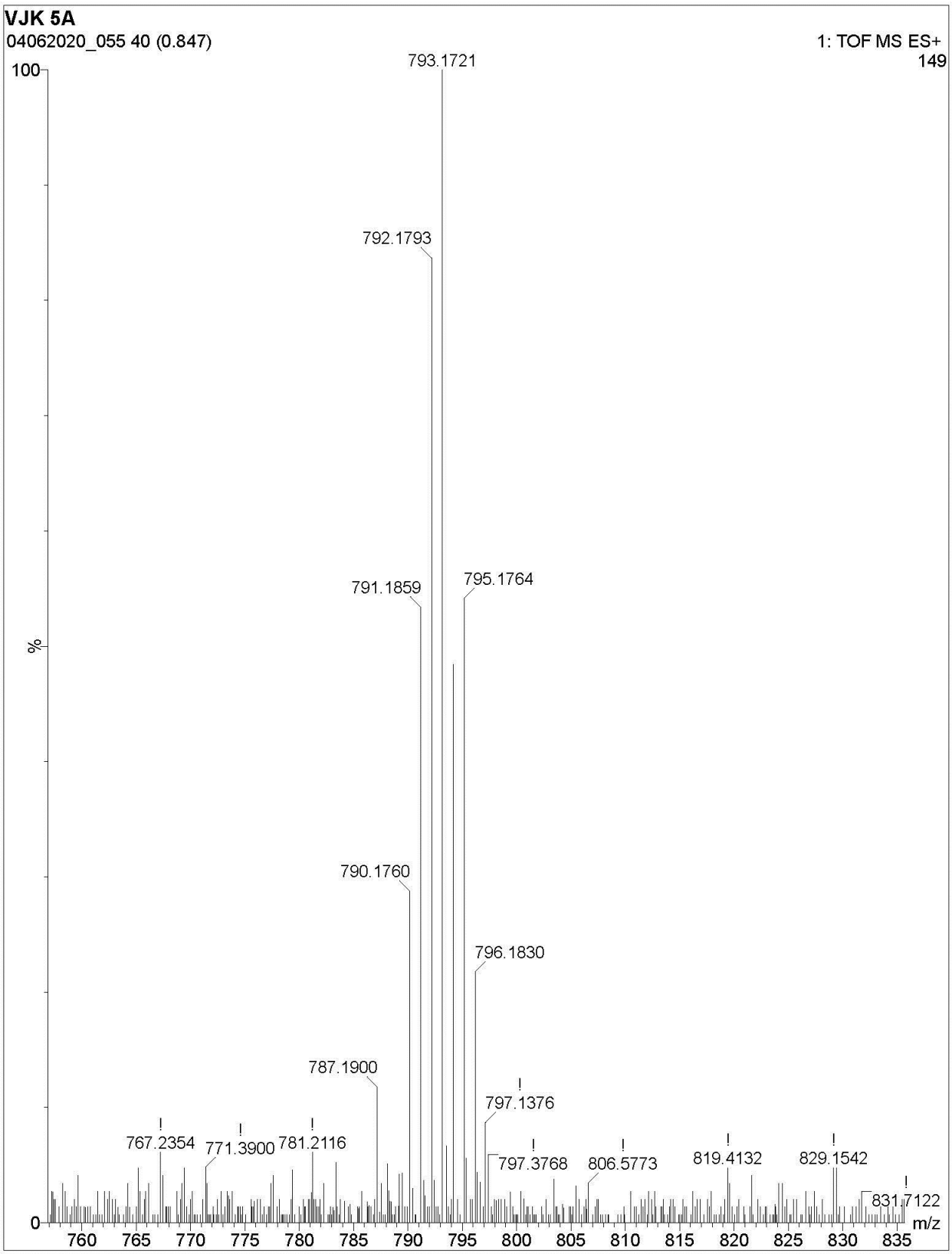

Figure S70. The ESI(+) mass spectrum of [**5a**].

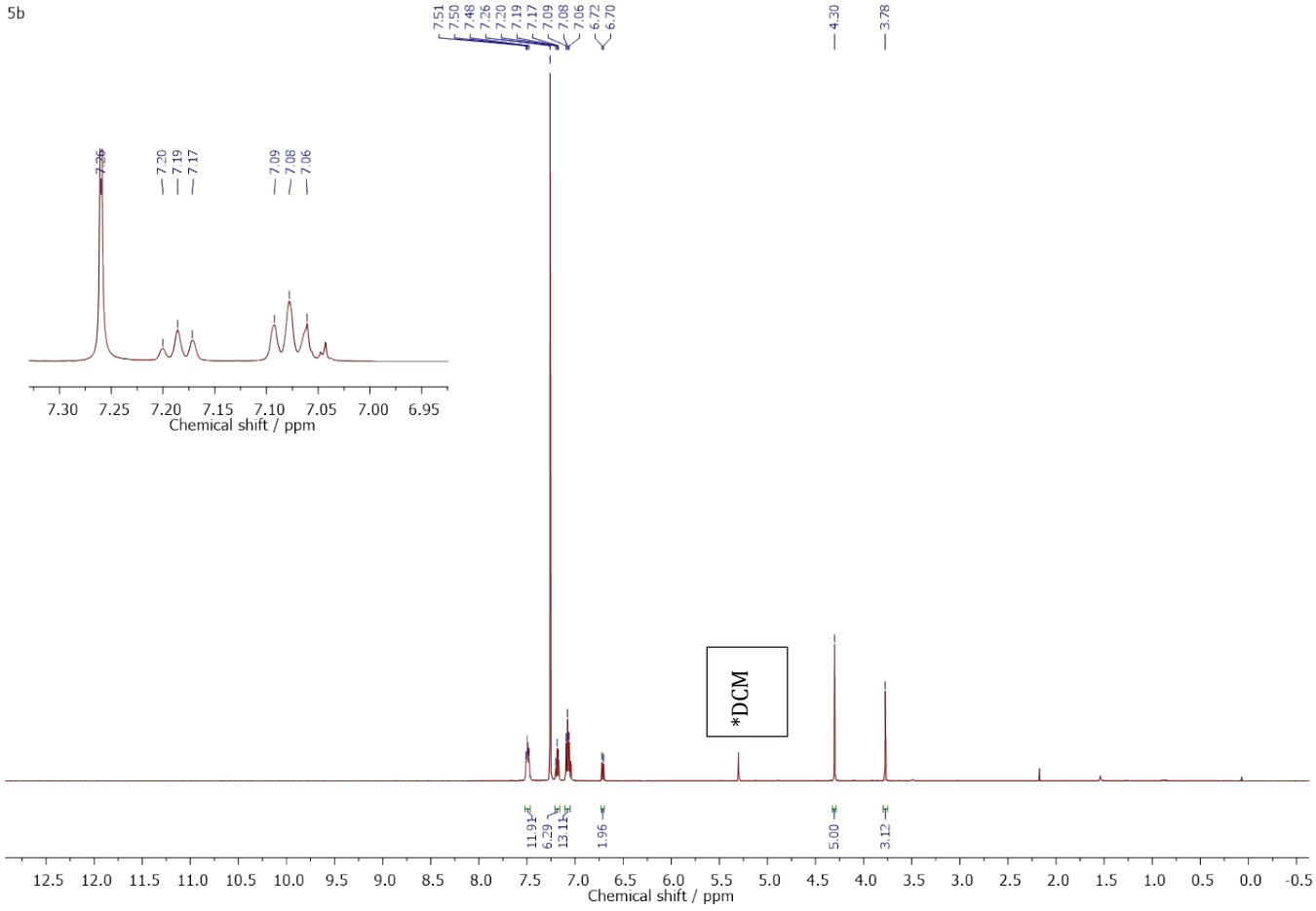

Figure S71. The ^{1}H NMR spectrum of [**5b**]. The inset shows an expansion of the aromatic region for clarity.

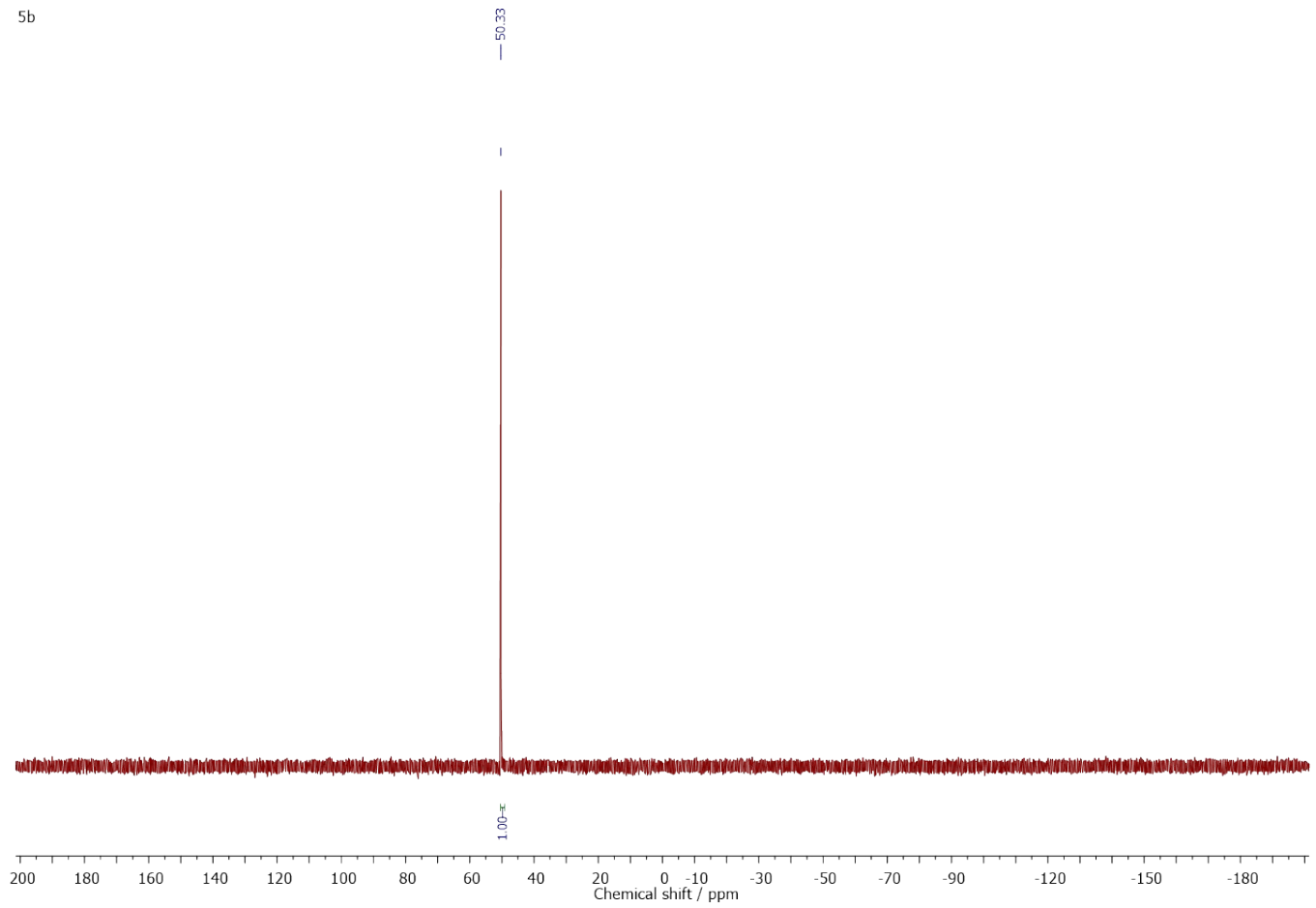

Figure S72. The ^{31}P NMR spectrum of [**5b**].

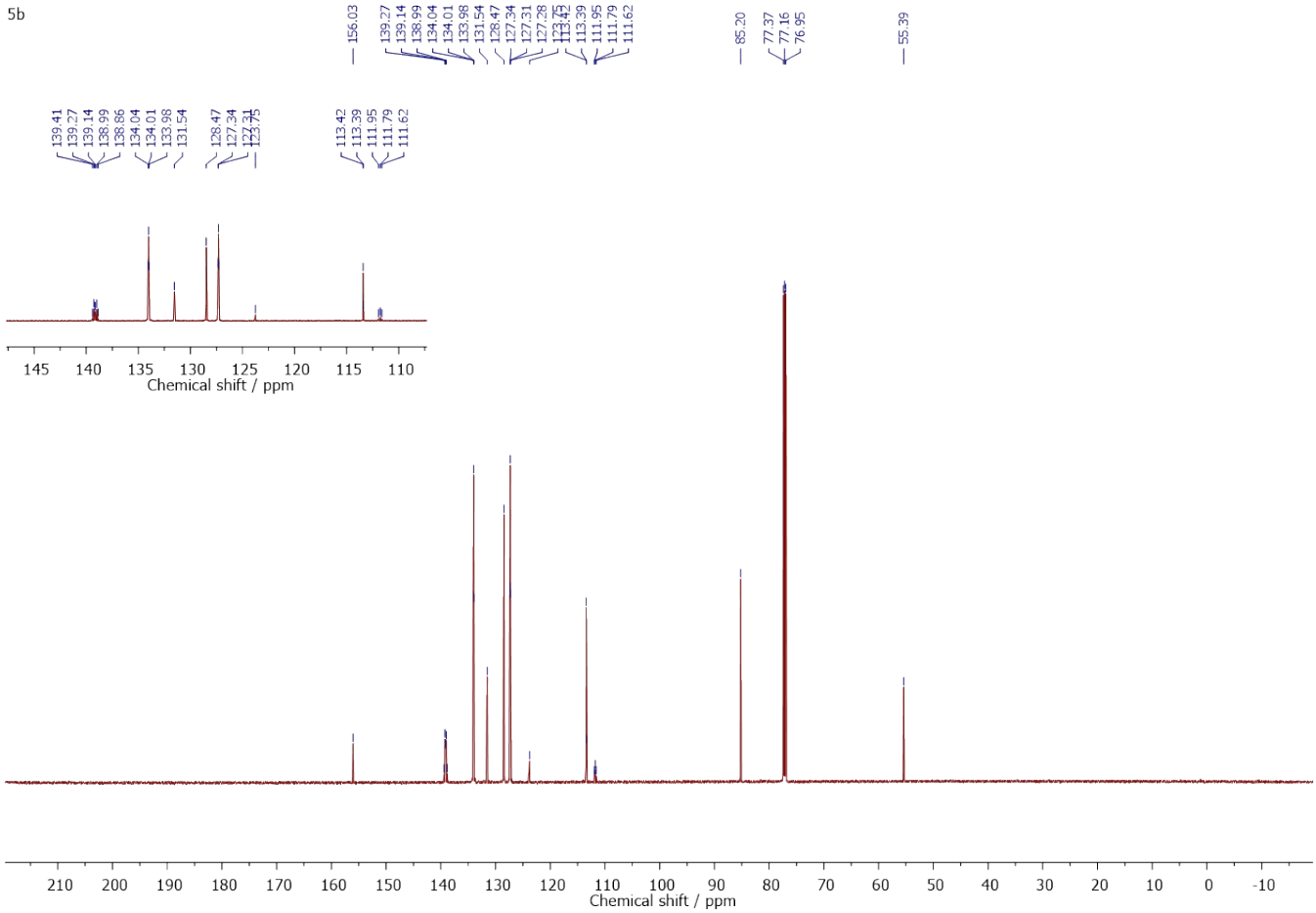

Figure S73. The $^{13}C\{^{1}H\}$ NMR spectrum of [**5b**]. The inset shows an expansion of the aromatic region for clarity.

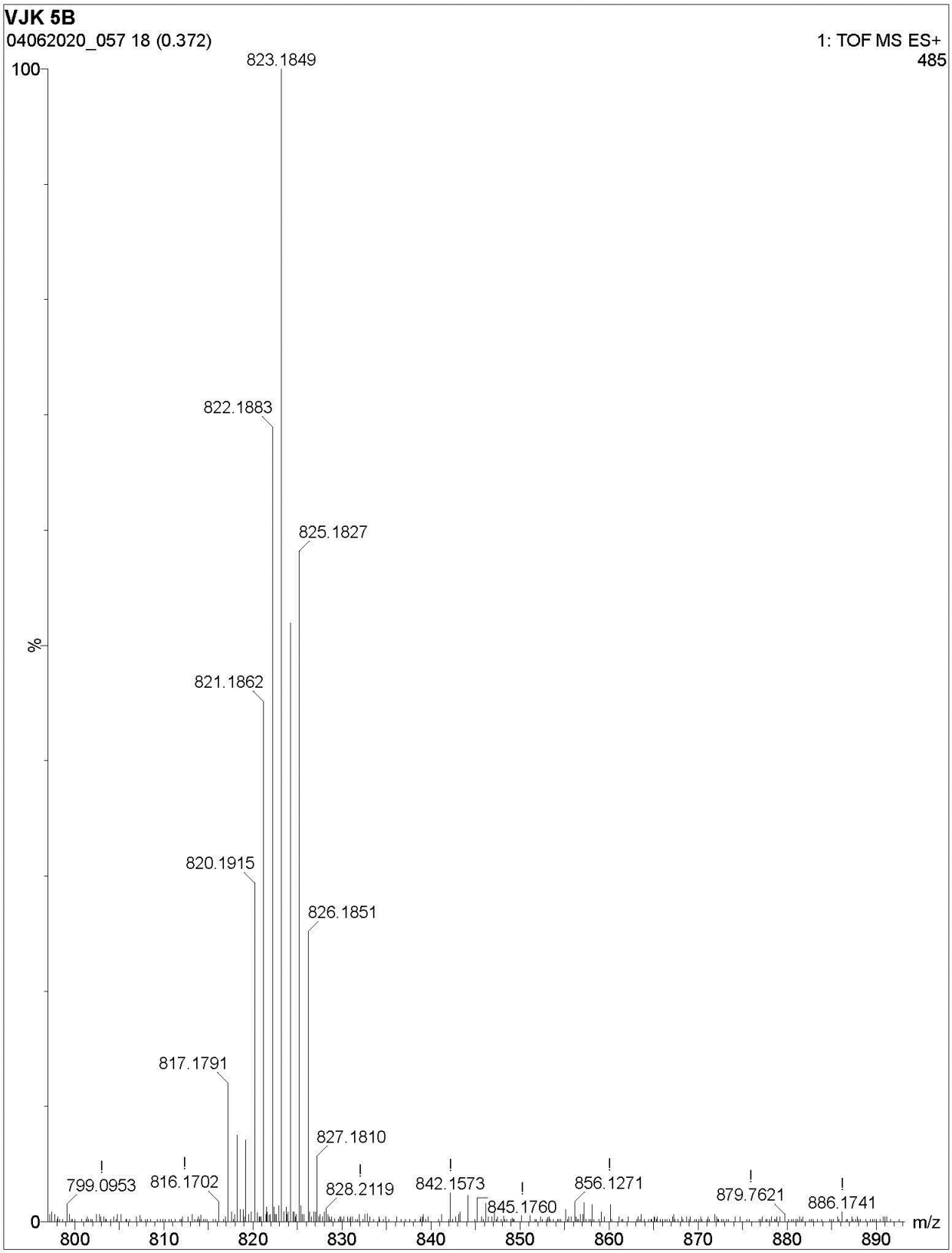

Figure S74. The ESI(+) mass spectrum of [**5b**].

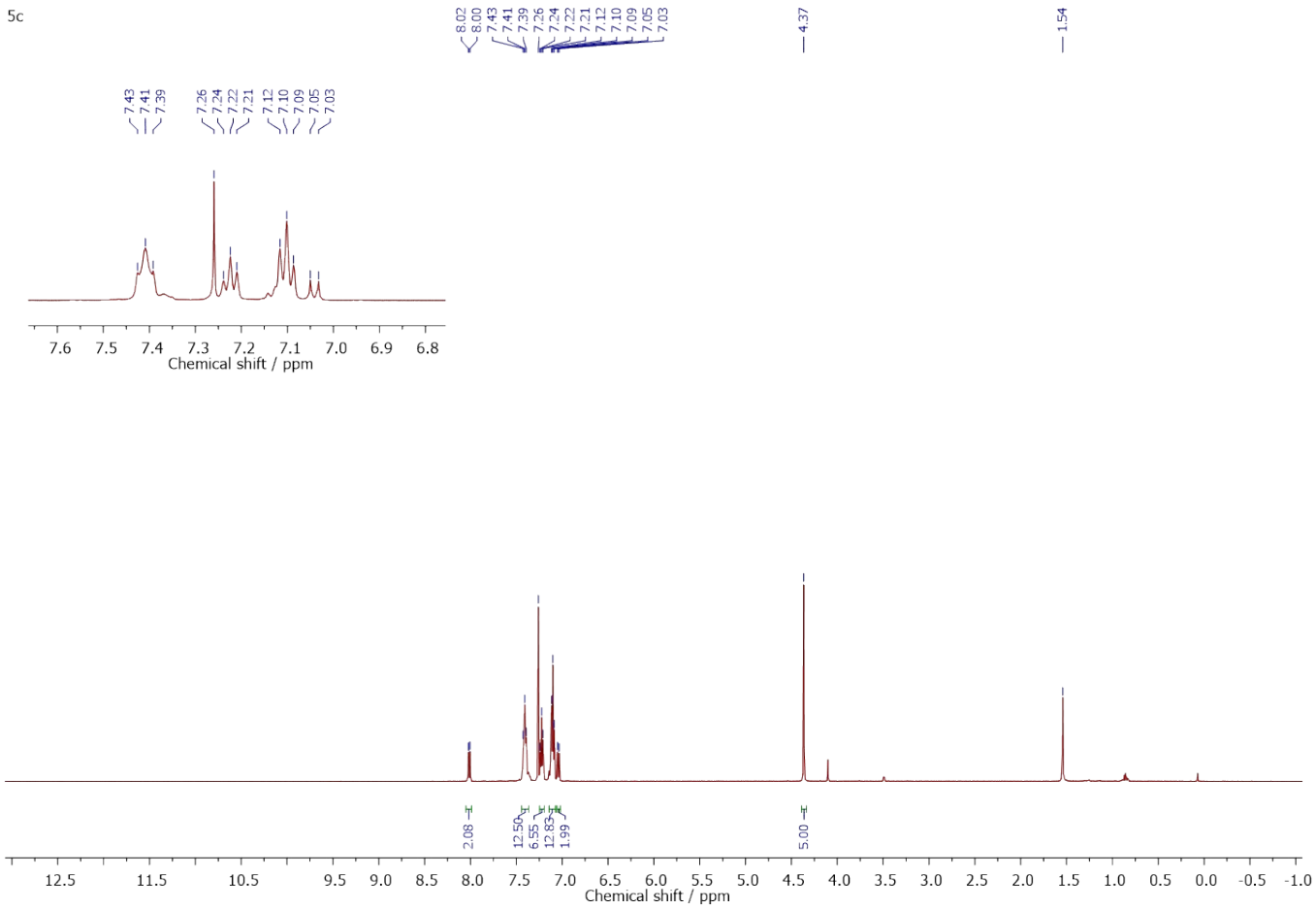

Figure S75. The ^{1}H NMR spectrum of [**5c**]. The inset shows an expansion of the aromatic region for clarity.

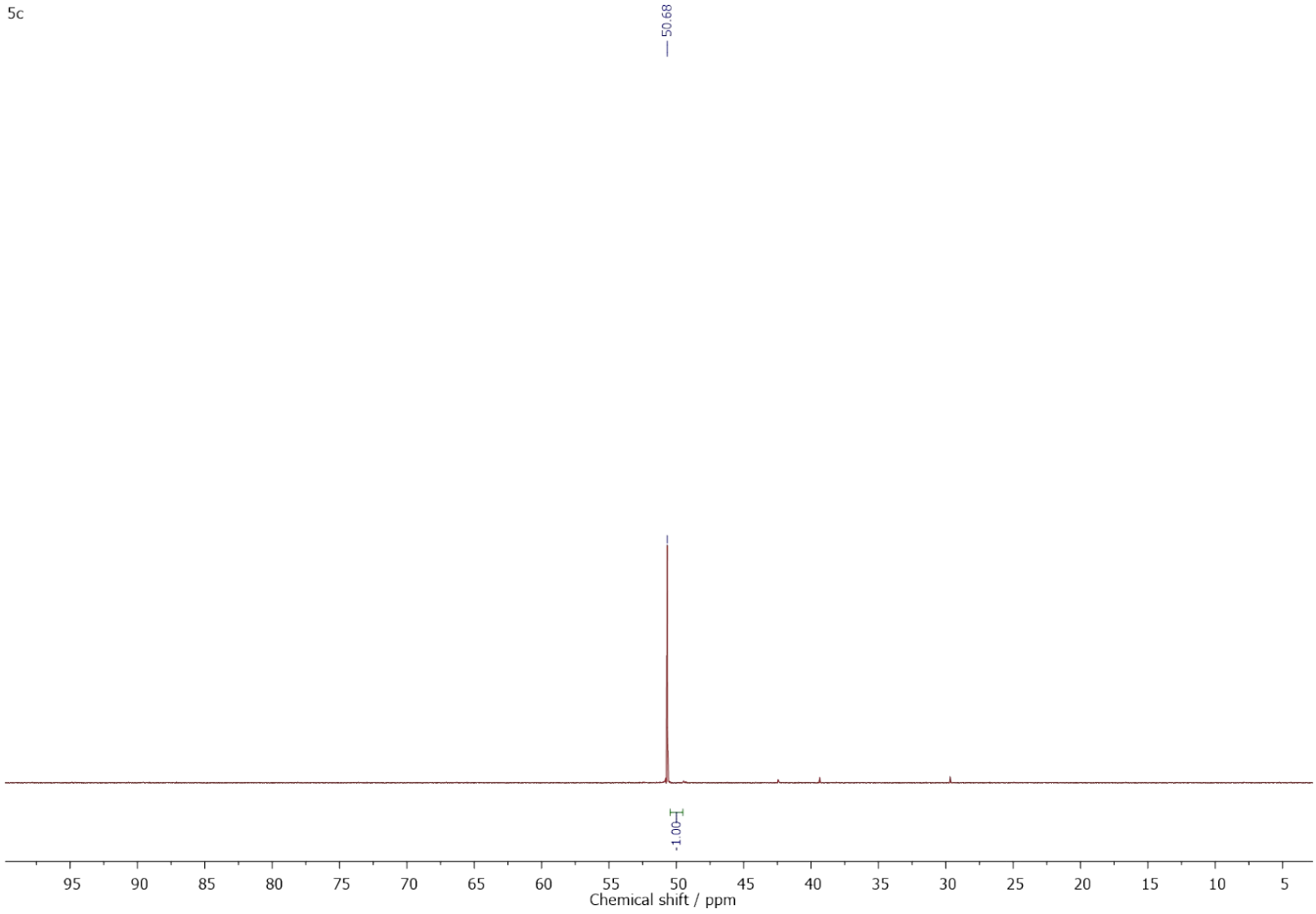

Figure S76. The ^{31}P NMR spectrum of [**5c**].

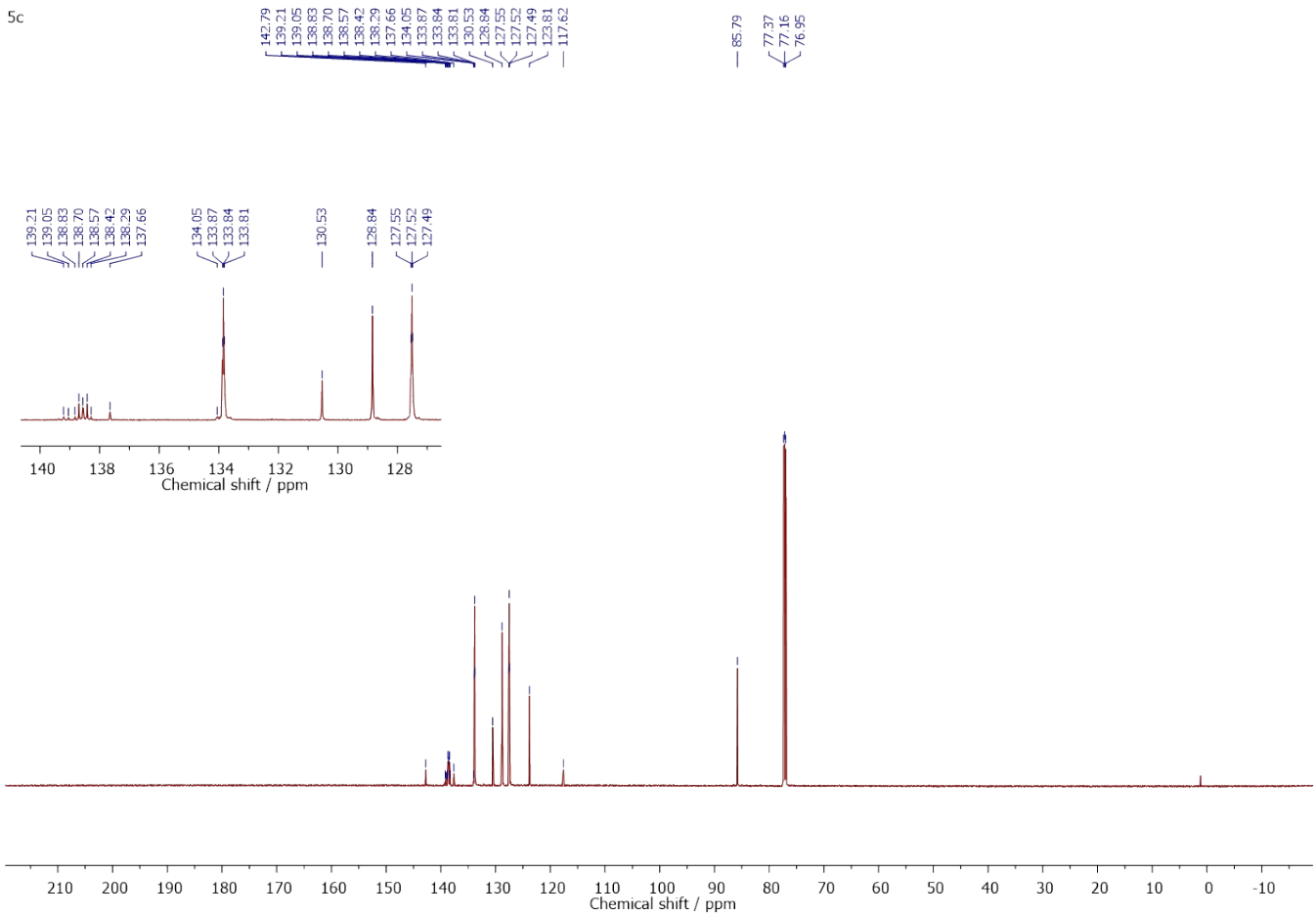

Figure S77. The $^{13}C\{^{1}H\}$ NMR spectrum of [**5c**]. The inset shows an expansion of the aromatic region for clarity.

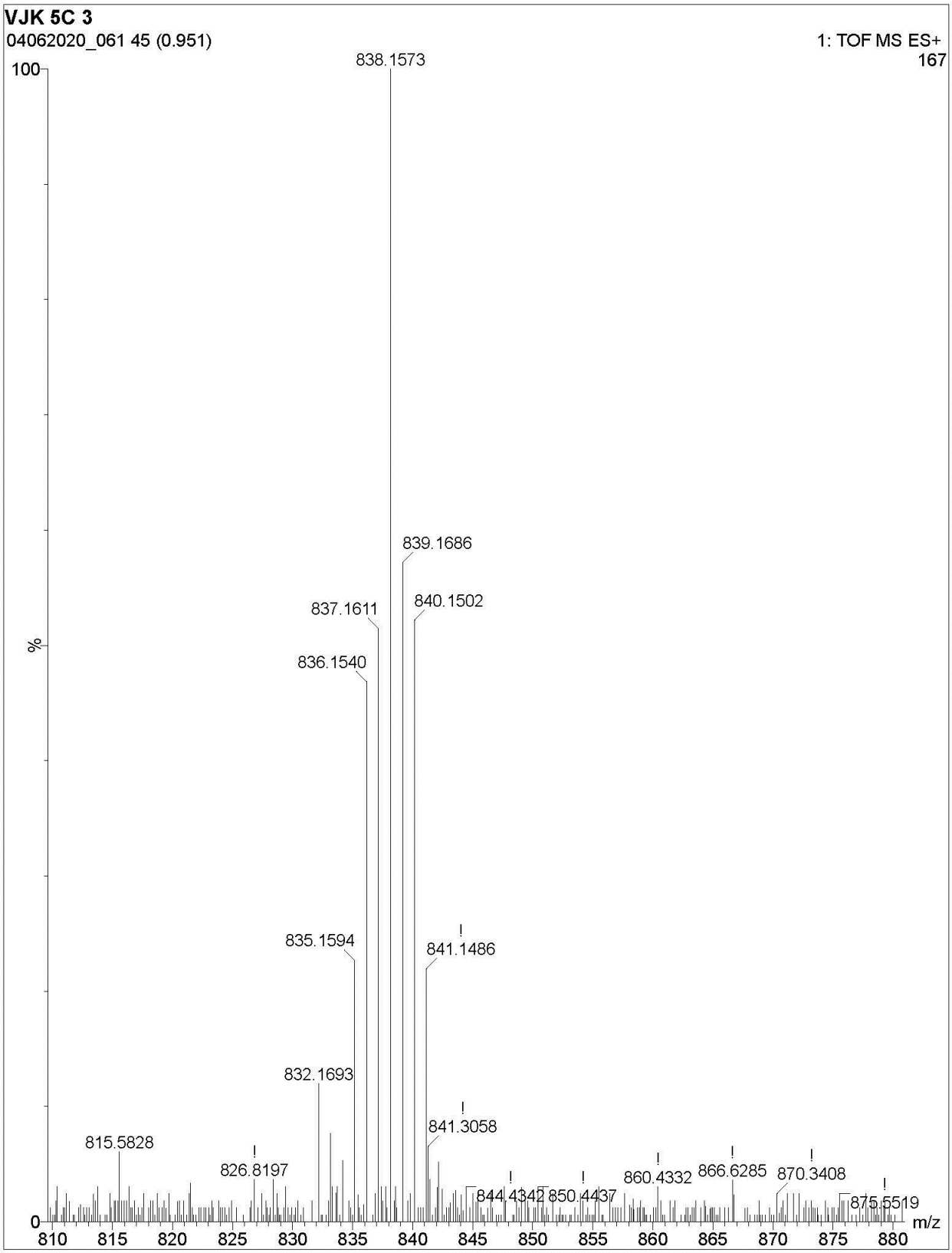

Figure S78. The ESI(+) mass spectrum of [**5c**].

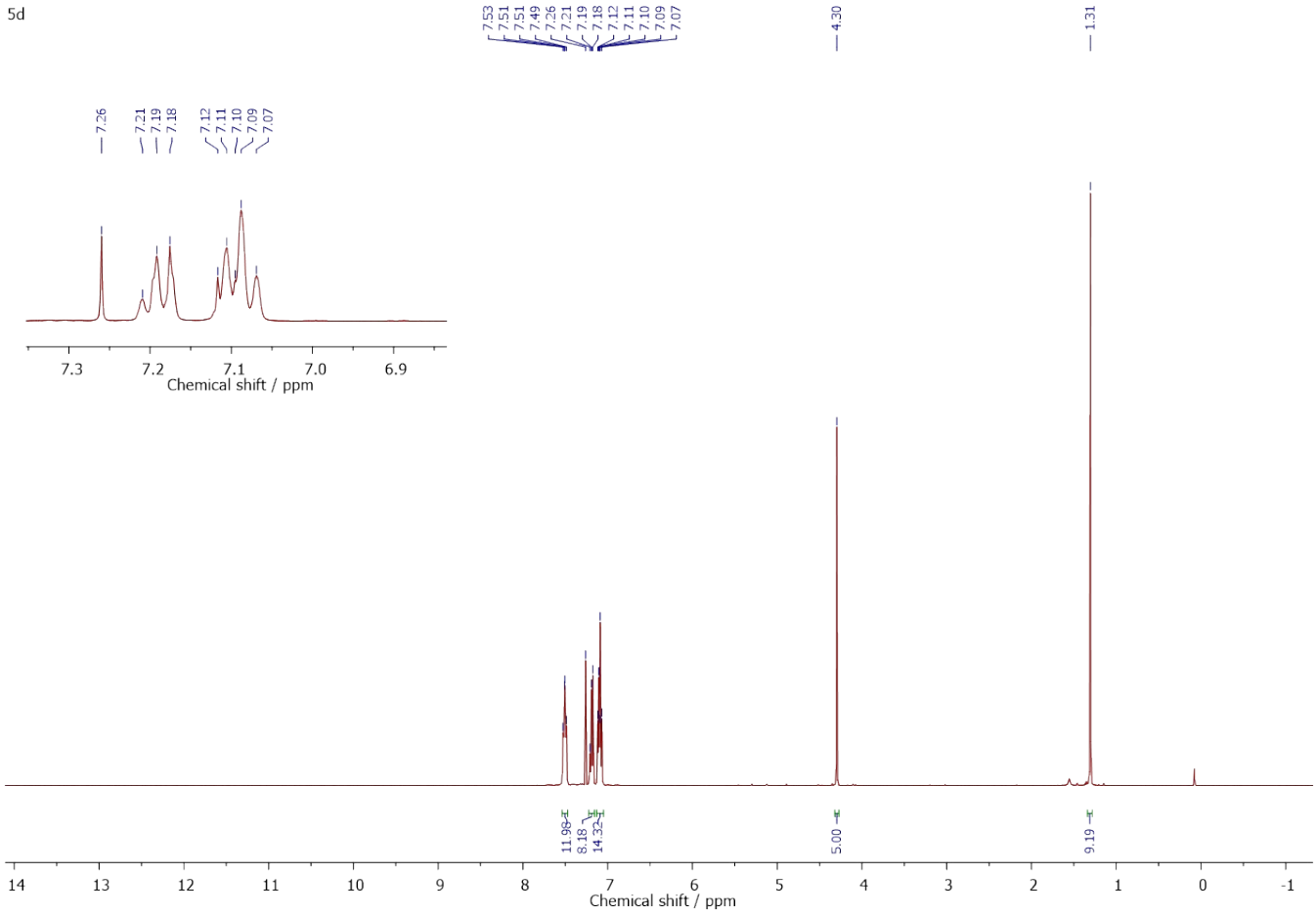

Figure S79. The ^{1}H NMR spectrum of [**5d**]. The inset shows an expansion of the aromatic region for clarity.

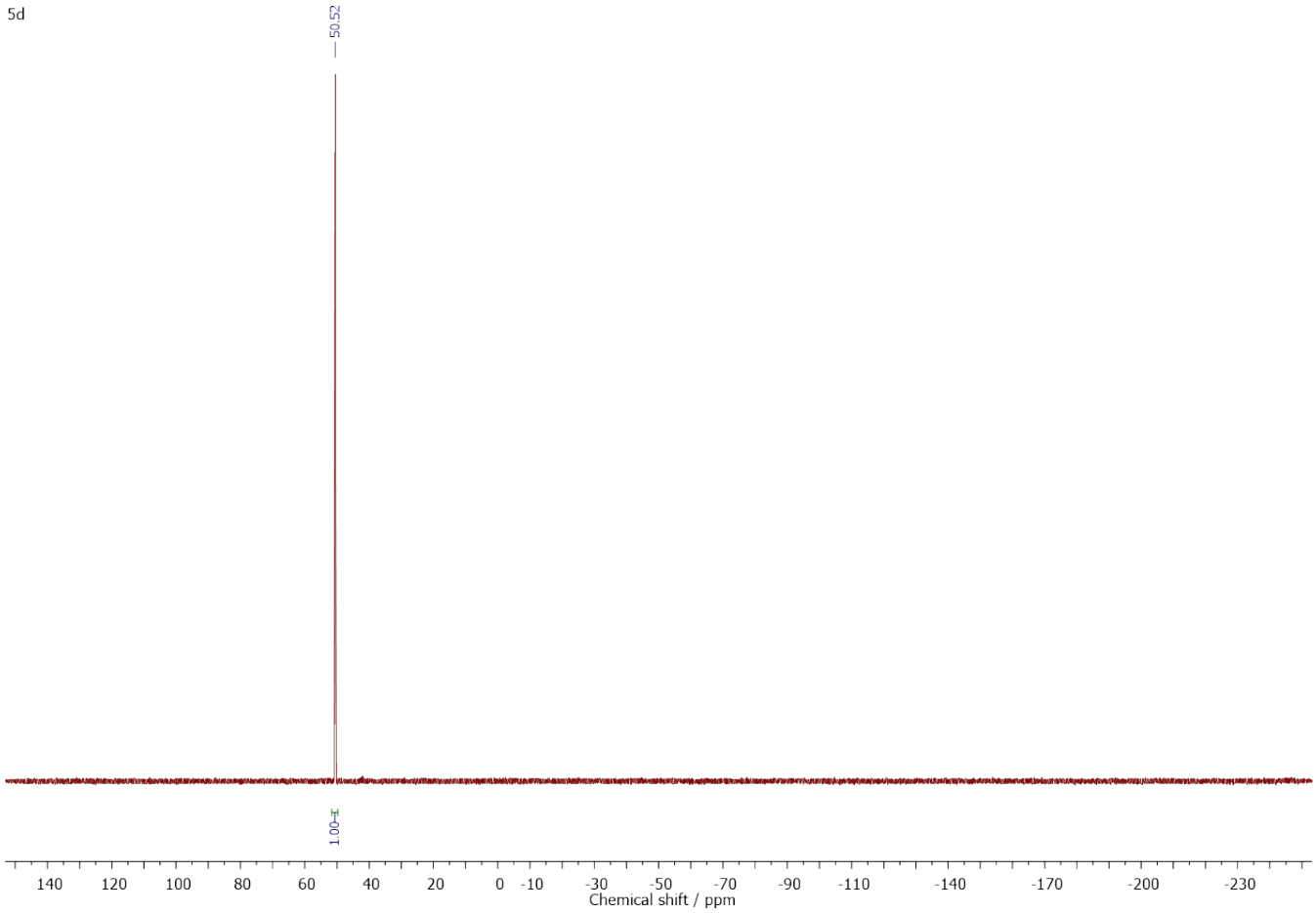

Figure S80. The ^{31}P NMR spectrum of [**5d**].

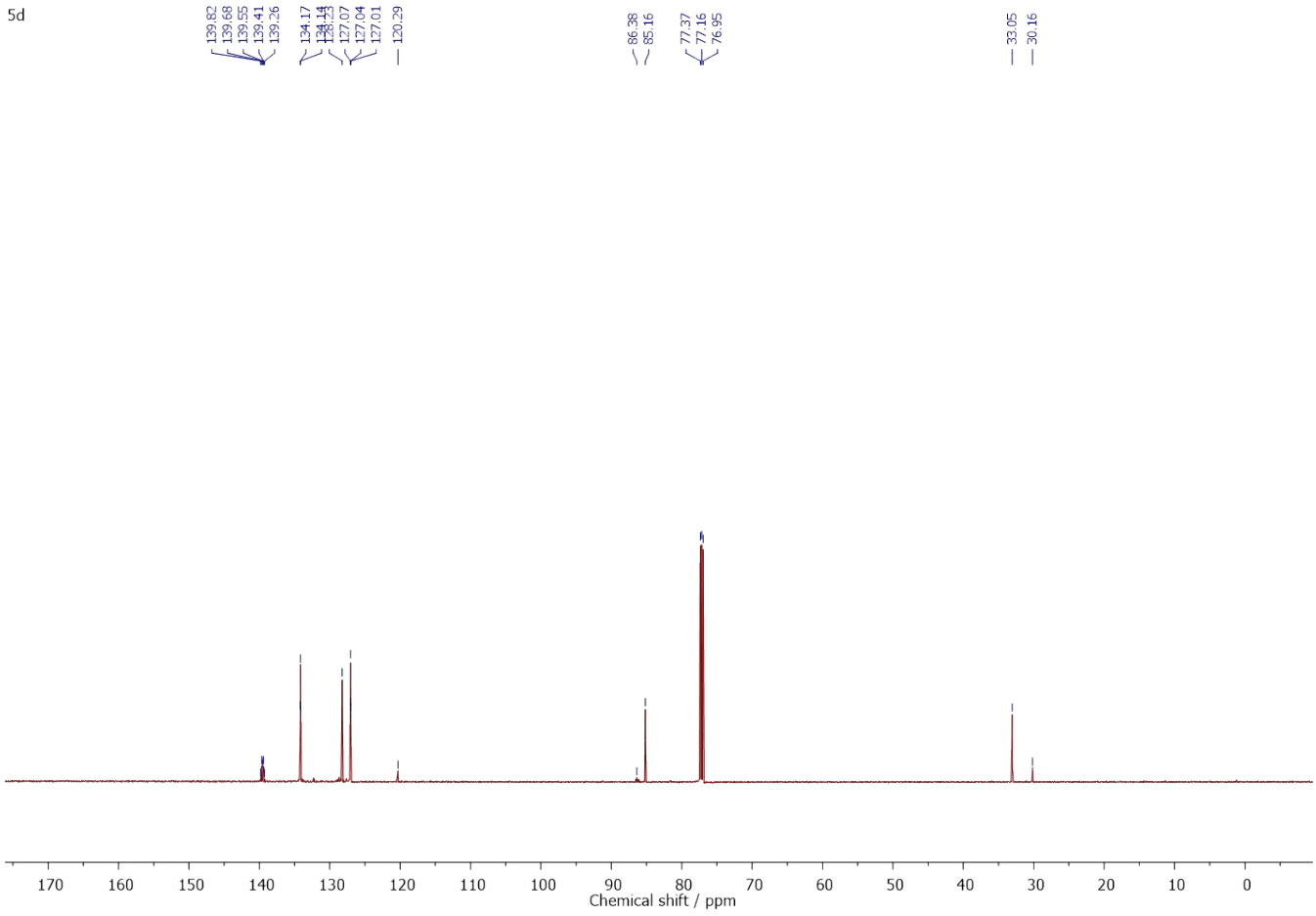

Figure S81. The $^{13}C\{^{1}H\}$ NMR spectrum of [**5d**].

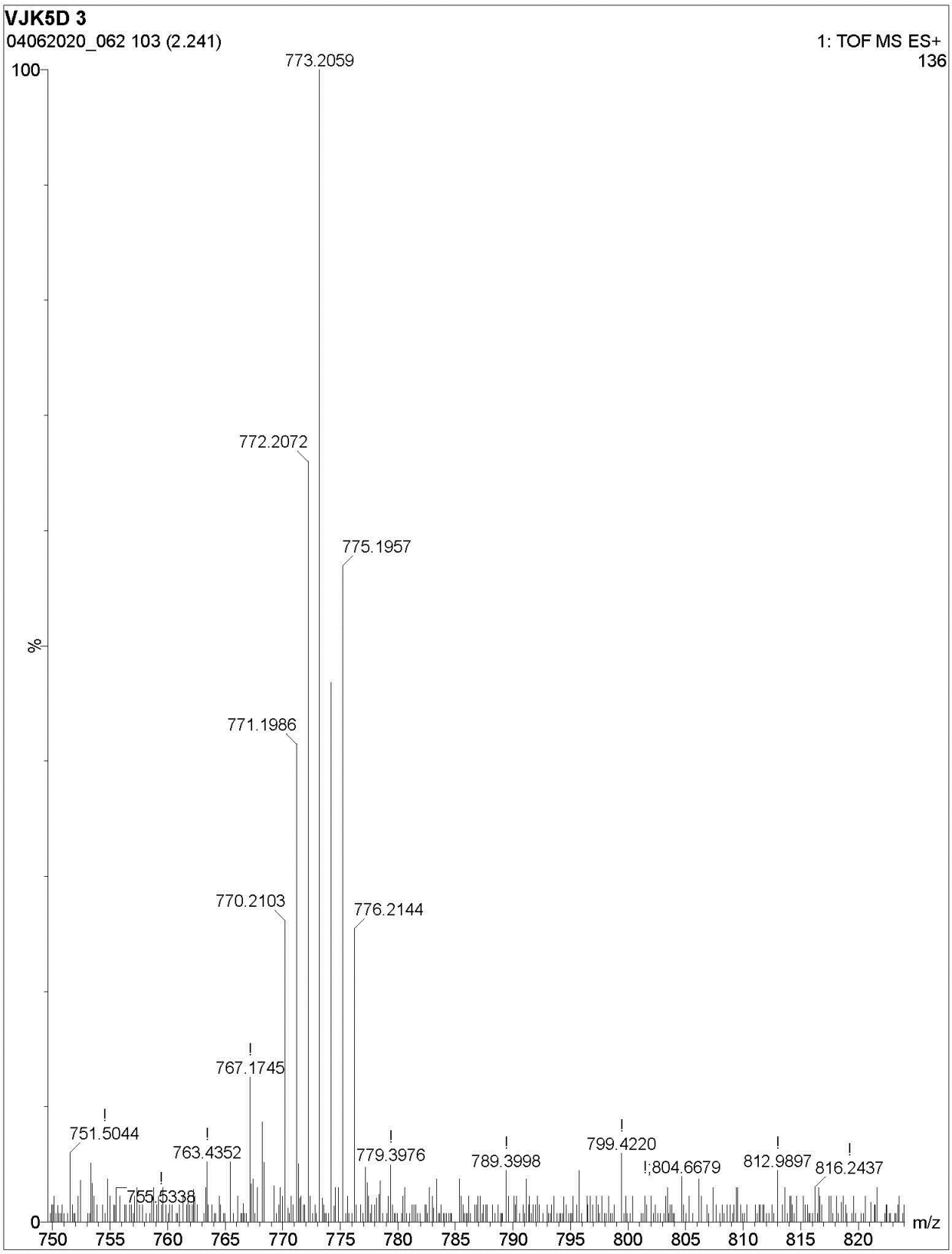

Figure S82. The ESI(+) mass spectrum of [**5d**].

Table S2. X-ray Single-Crystal Experimental Details.

Structure code	**1d**	**2d**	**3d**	**4d**	**5d**
Crystal data					
Chemical formula	$C_{42}H_{48}FeP_2$	$C_{37}H_{38}FeP_2$	$C_{42}H_{48}P_2Ru$	$C_{37}H_{38}P_2Ru$	$C_{47}H_{44}P_2Ru$
M_r	670.59	600.46	715.81	645.68	771.83
Crystal system, space group	Monoclinic, *Cc*	Triclinic, $P\bar{1}$	Monoclinic, $P2_1$	Monoclinic, $P2_1/c$	Monoclinic, $P2_1/c$
Temperature (K)	100	100	99	120	100
a, *b*, *c* (Å)	8.3802 (1), 22.2533 (3), 19.4016 (3)	9.9070 (2), 12.3781 (3), 25.5901 (7)	8.7348 (2), 19.3206 (4), 10.6426 (2)	8.6680 (1), 18.5220 (2), 20.3518 (2)	10.7560 (1), 16.9328 (2), 20.8157 (2)
α, β, γ (°)	90, 90.318 (1), 90	91.779 (2), 91.683 (2), 101.312 (2)	90, 96.473 (2), 90	90, 98.041 (1), 90	90, 93.991 (1), 90
V (Å^3)	3618.09 (9)	3073.65 (13)	1784.61 (6)	3235.33 (6)	3781.95 (7)
Z	4	4	2	4	4
Radiation type	Cu *K*α	Mo *K*α	Mo *K*α	Cu *K*α	Mo *K*α
μ (mm^{-1})	4.37	0.62	0.56	5.02	0.53
Crystal size (mm)	0.15 × 0.04 × 0.02	0.17 × 0.12 × 0.09	0.36 × 0.15 × 0.08	0.22 × 0.18 × 0.10	0.26 × 0.19 × 0.18
Data collection					
Diffractometer	Oxford Diffraction Gemini-R Ultra	Oxford Diffraction Xcalibur-S	Xcalibur, Ruby, Gemini ultra	XtaLAB Synergy, Single source at home/near, HyPix	Oxford Diffraction Xcalibur-S
Absorption correction	Multi-scan *CrysAlis PRO* 1.171.39.46 (Rigaku Oxford Diffraction, 2018)	Multi-scan *CrysAlis PRO* 1.171.39.46 (Rigaku Oxford Diffraction, 2018)	Multi-scan *CrysAlis PRO* 1.171.40.53 (Rigaku Oxford Diffraction, 2019)	Analytical *CrysAlis PRO* 1.171.40.53 (Rigaku Oxford Diffraction, 2019)	Multi-scan *CrysAlis PRO* 1.171.39.46 (Rigaku Oxford Diffraction, 2018)
T_{min}, T_{max}	0.915, 1.0	0.926, 1.0	0.945, 1.000	0.822, 0.912	0.949, 1.0
No. of measured, independent and observed [$I > 2\sigma(I)$] reflections	15913, 4949, 4455	65673, 20231, 12908	55220, 8148, 7175	160066, 6916, 6215	43512, 12511, 10287
R_{int}	0.060	0.075	0.066	0.092	0.037
$(\sin\theta/\lambda)_{max}$ (Å^{-1})	0.599	0.753	0.665	0.637	0.753
Refinement					
$R[F^2 > 2\sigma(F^2)]$, $wR(F^2)$, *S*	0.045, 0.110, 1.00	0.057, 0.129, 1.00	0.037, 0.066, 1.08	0.038, 0.106, 1.09	0.036, 0.092, 1.00
No. of reflections	4949	20231	8148	6916	12511
No. of parameters	414	727	390	339	454
No. of restraints	2	0	1	15	0
$\Delta\rangle_{max}$, $\Delta\rangle_{min}$ (e Å^{-3})	0.45, -0.34	0.81, -0.49	1.16, -0.48	0.56, -0.90	0.88, -0.58

Structure code	**2a**	**2b**	**3c**	**4b**
Crystal data				
Chemical formula	$C_{39}H_{34}FeP_2$	$C_{40}H_{36}FeOP_2$	$C_{44}H_{43}NO_2P_2Ru$	$C_{40}H_{36}OP_2Ru$
M_r	620.45	650.48	780.80	695.70
Crystal system, space group	Monoclinic, *P*2/*c*	Orthorhombic, *Pbca*	Monoclinic, $P2_1/c$	Orthorhombic, *Pbca*
Temperature (K)	100	100	100	102
a, *b*, *c* (Å)	39.5527 (15), 9.5048 (4), 33.7838 (16)	9.4107 (1), 17.3043 (3), 39.0246 (6)	12.8214 (1), 22.3082 (1), 14.6199 (1)	9.3194 (2), 17.5662 (4), 39.2393 (13)
α, β, γ (°)	90, 100.680 (4), 90	90, 90, 90	90, 113.563 (1), 90	90, 90, 90
V (Å^3)	12480.7 (9)	6354.98 (16)	3832.96 (5)	6423.7 (3)
Z	16	8	4	8
Radiation type	Cu *K*α	Cu *K*α	Cu *K*α	Cu *K*α
μ (mm^{-1})	5.04	5.00	4.39	5.13
Crystal size (mm)	0.18 × 0.03 × 0.02	0.24 × 0.04 × 0.03	0.33 × 0.05 × 0.05	0.26 × 0.09 × 0.03
Data collection				
Diffractometer	Oxford Diffraction Gemini-R Ultra	Oxford Diffraction Gemini-R Ultra	Oxford Diffraction Gemini-R Ultra	Xcalibur, Ruby, Gemini ultra
Absorption correction	Multi-scan *CrysAlis PRO* 1.171.39.46 (Rigaku Oxford Diffraction, 2018)	Multi-scan *CrysAlis PRO* 1.171.39.46 (Rigaku Oxford Diffraction, 2018)	Multi-scan *CrysAlis PRO* 1.171.39.46 (Rigaku Oxford Diffraction, 2018)	Multi-scan *CrysAlis PRO* 1.171.39.46 (Rigaku Oxford Diffraction, 2018)
T_{min}, T_{max}	0.942, 1.0	0.705, 1.0	0.650, 1.0	0.871, 1.000
No. of measured, independent and observed [$I > 2\sigma(I)$] reflections	64691, 22211, 12161	29925, 5666, 4162	38371, 6847, 5985	30269, 5711, 3779
R_{int}	0.153	0.103	0.039	0.119
$(\sin\theta/\lambda)_{max}$ (Å^{-1})	0.599	0.598	0.598	0.598
Refinement				
$R[F^2 > 2\sigma(F^2)]$, $wR(F^2)$, *S*	0.065, 0.151, 0.96	0.055, 0.144, 1.00	0.032, 0.089, 1.00	0.045, 0.091, 1.06
No. of reflections	22211	5666	6847	5711
No. of parameters	1513	398	456	398
No. of restraints	0	0	0	0
$\Delta\rangle_{max}$, $\Delta\rangle_{min}$ (e Å^{-3})	0.43, -0.45	0.90, -0.42	0.90, -0.33	0.69, -0.38

Computer programs employed for crystallographic work: *CrysAlis PRO* 1.171.39.46 (Rigaku Oxford Diffraction, 2018), *CrysAlis PRO* 1.171.40.53 (Rigaku Oxford Diffraction, 2019), *SHELXT2015*/1,[12] *Olex2.solve* 1.3,[13] *SHELXL2018*/3 (Sheldrick, 2015), *SHELXL* 2018/3,[14] *X-SEED* v. 4.0,[15] *Olex2* 1.3[16]

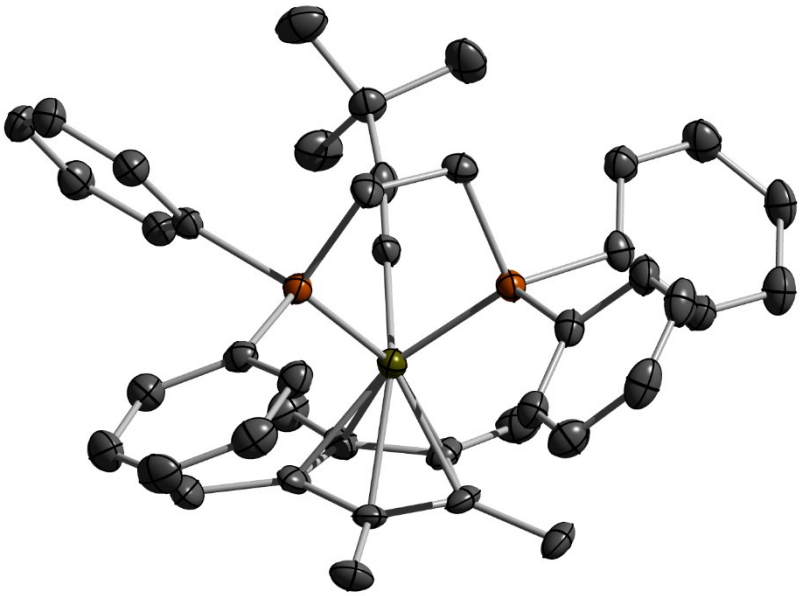

Figure S83. Structure of **1d** with anisotropic displacement parameters drawn at 50% probability. Colour scheme is grey: Carbon, orange: Phosphorous and yellow: Iron. H-atoms have been removed for clarity.

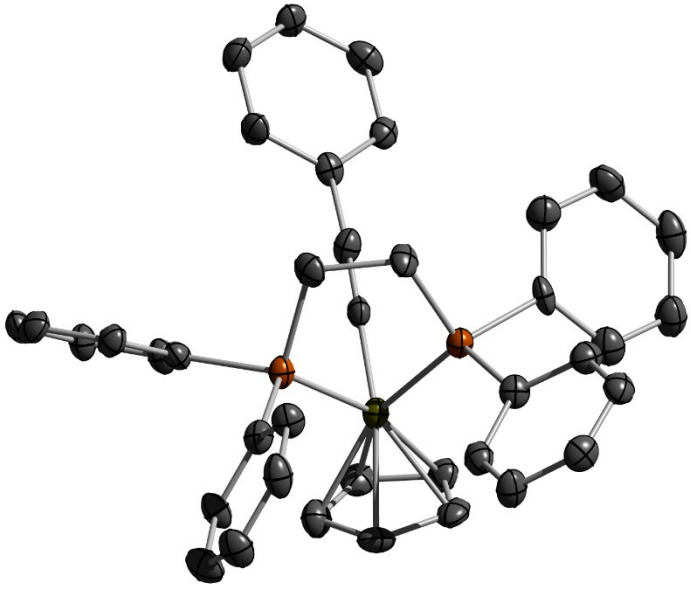

Figure S84. Structure of **2a** with anisotropic displacement parameters drawn at 50% probability. Colour scheme is grey: Carbon, orange: Phosphorous and yellow: Iron. H-atoms have been removed for clarity.

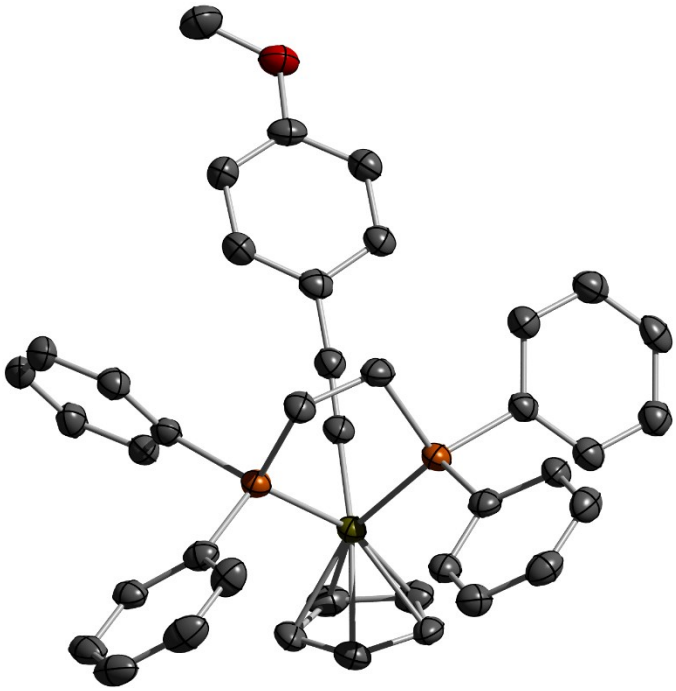

Figure S85. Structure of **2b** with anisotropic displacement parameters drawn at 50% probability. Colour scheme is red: Oxygen, grey: Carbon, orange: Phosphorous and Teal: Ruthenium. H-atoms have been removed for clarity.

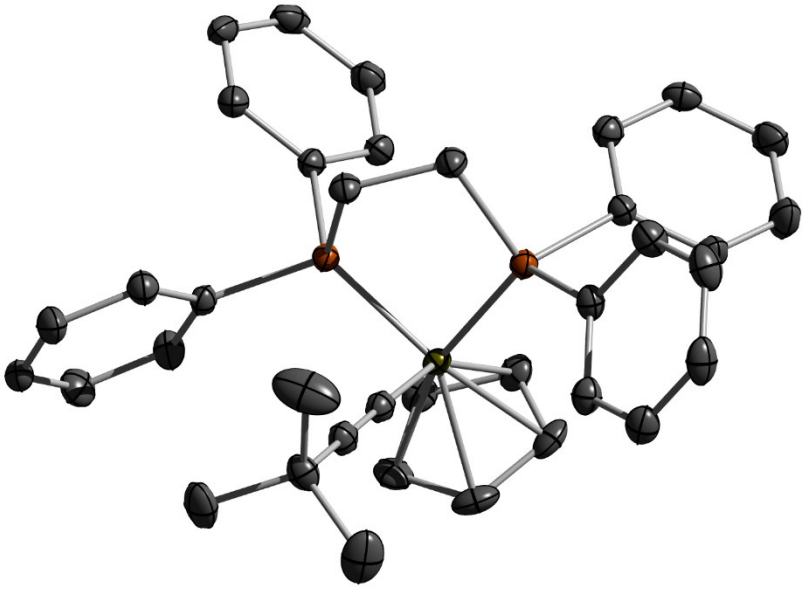

Figure S86. Structure of **2d** with anisotropic displacement parameters drawn at 50% probability. Colour scheme is grey: Carbon, orange: Phosphorous and yellow: Iron. H-atoms have been removed for clarity.

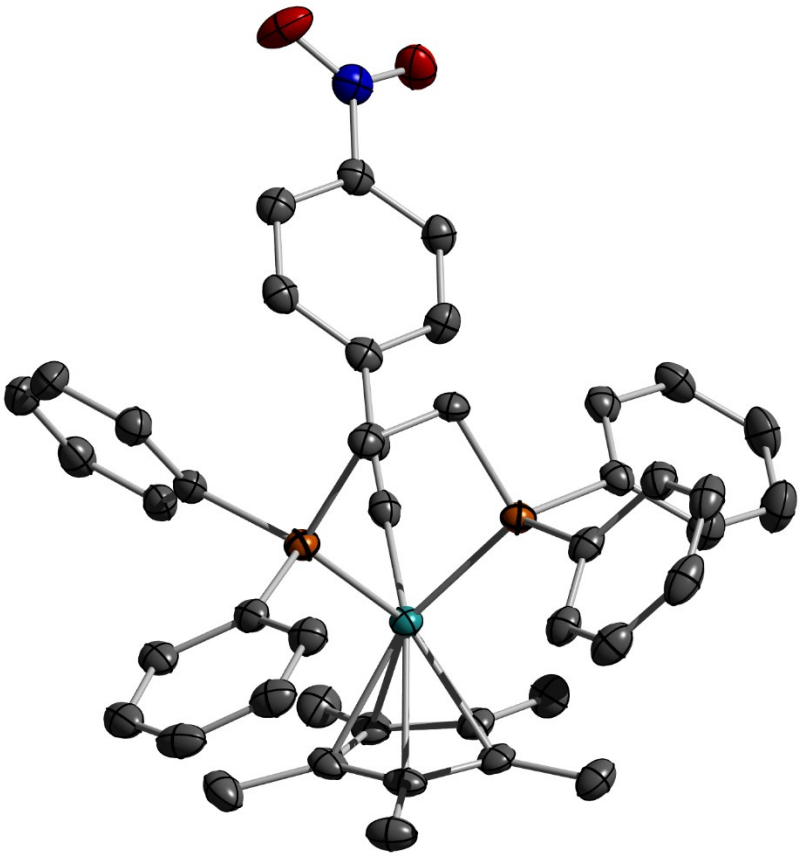

Figure S87. Structure of **3c** with anisotropic displacement parameters drawn at 50% probability. Colour scheme is red: Oxygen, blue: Nitrogen, grey: Carbon, orange: Phosphorous and Teal: Ruthenium. H-atoms have been removed for clarity.

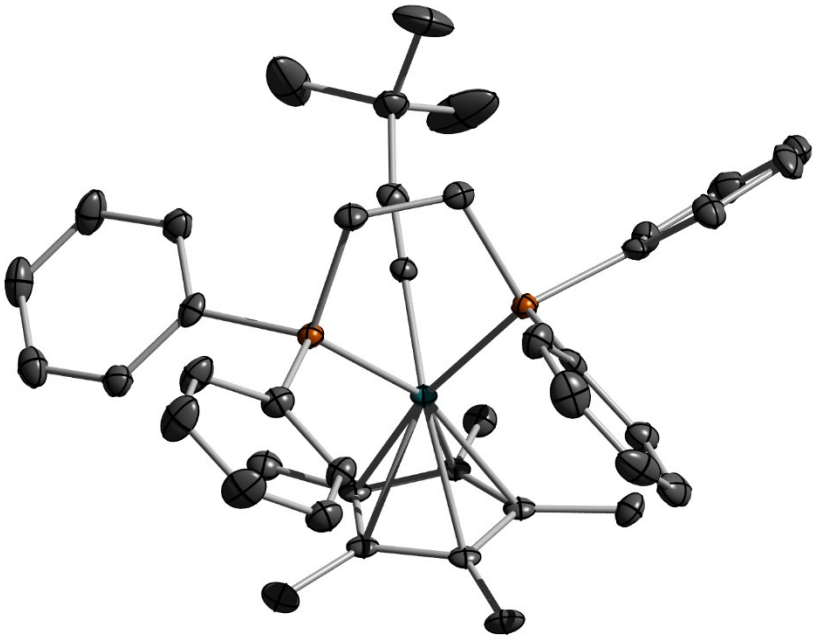

Figure S88. Structure of **3d** with anisotropic displacement parameters drawn at 50% probability. Colour scheme is grey: Carbon, orange: Phosphorous and teal: Ruthenium. H-atoms have been removed for clarity.

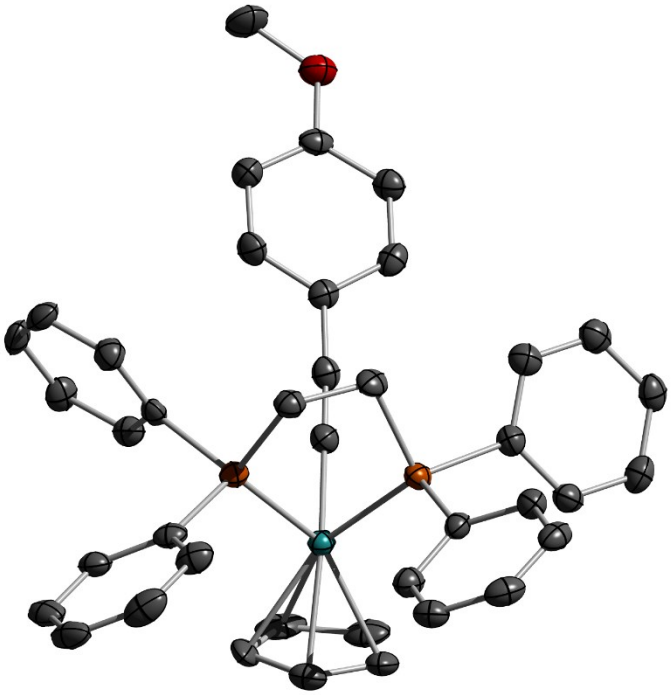

Figure S89. Structure of **4b** with anisotropic displacement parameters drawn at 50% probability. Colour scheme is red: Oxygen, grey: Carbon, orange: Phosphorous and Teal: Ruthenium. H-atoms have been removed for clarity.

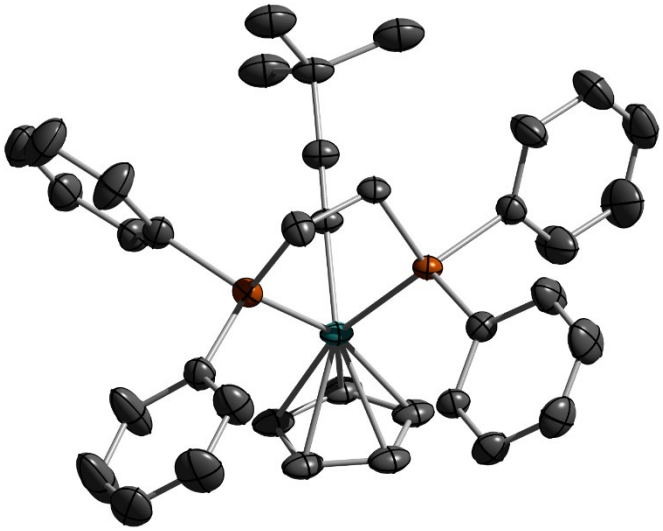

Figure S90. Structure of **4d** with anisotropic displacement parameters drawn at 50% probability. Colour scheme grey: Carbon, orange: Phosphorous and Teal: Ruthenium. H-atoms and the disorder on the tert-butyl and Cp ligand have been removed for clarity.

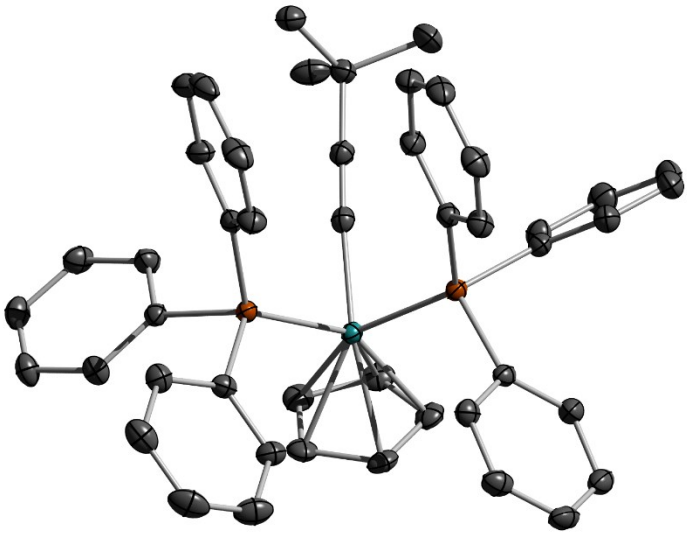

Figure S91. Structure of **5d** with anisotropic displacement parameters drawn at 50% probability. Colour scheme is grey: Carbon, orange: Phosphorous and Teal: Ruthenium. H-atoms have been removed for clarity.

References

1. N. G. Connelly, M. P. Gamasa, J. Gimeno, C. Lapinte, E. Lastra, J. P. Maher, N. Lenarvor, A. L. Rieger and P. H. Rieger, *J. Chem. Soc. Dalton Trans.*, 1993, 2575-2578.
2. R. Denis, L. Toupet, F. Paul and C. Lapinte, *Organometallics*, 2000, **19**, 4240-4251.
3. W. M. Khairul, M. A. Fox, N. N. Zaitseva, M. Gaudio, D. S. Yufit, B. W. Skelton, A. H. White, J. A. K. Howard, M. I. Bruce and P. J. Low, *Dalton Trans.*, 2009, 610-620.
4. M. H. Garcia, M. P. Robalo, A. R. Dias, M. T. Duarte, W. Wenseleers, G. Aerts, E. Goovaerts, M. P. Cifuentes, S. Hurst, M. G. Humphrey, M. Samoc and B. Luther-Davies, *Organometallics*, 2002, **21**, 2107-2118.
5. C. Bitcon and M. W. Whiteley, *J. Organomet. Chem.*, 1987, **336**, 385-392.
6. F. Paul, B. G. Ellis, M. I. Bruce, L. Toupet, T. Roisnel, K. Costuas, J. F. Halet and C. Lapinte, *Organometallics*, 2006, **25**, 649-665.
7. C. W. Chang, M. C. Cheng, G. H. Lee and S. M. Peng, *Dalton Trans.*, 2019, **48**, 11732-11742.
8. C. E. Powell, M. P. Cifuentes, A. M. McDonagh, S. K. Hurst, N. T. Lucas, C. D. Delfs, R. Stranger, M. G. Humphrey, S. Houbrechts, I. Asselberghs, A. Persoons and D. C. R. Hockless, *Inorg. Chim. Acta*, 2003, **352**, 9-18.
9. M. A. Fox, R. L. Roberts, W. M. Khairul, F. Hartl and P. J. Low, *J. Organomet. Chem.*, 2007, **692**, 3277-3290.
10. E. M. Long, N. J. Brown, W. Y. Man, M. A. Fox, D. S. Yufit, J. A. K. Howard and P. J. Low, *Inorg. Chim. Acta*, 2012, **380**, 358-371.
11. I. R. Whittall, M. G. Humphrey, D. C. R. Hockless, B. W. Skelton and A. H. White, *Organometallics*, 1995, **14**, 3970-3979.
12. G. M. Sheldrick, *Acta Crystallogr. A*, 2015, **71**, 3-8.
13. L. J. Bourhis, O. V. Dolomanov, R. J. Gildea, J. A. K. Howard and H. Puschmann, *Acta Crystallogr. A*, 2015, **71**, 59-75.
14. G. M. Sheldrick, *Acta Crystallogr. C*, 2015, **71**, 3-8.
15. L. J. Barbour, *J. Supramol. Chem.*, 2001, **1**, 189 - 191.
16. O. V. Dolomanov, L. J. Bourhis, R. J. Gildea, J. A. K. Howard and H. Puschmann, *J. Appl. Crystallogr.*, 2009, **42**, 339-341.